UFL/COEL-92/018

THE ROLE OF WAVE AND CURRENT FORCING IN THE PROCESS OF BARRIER ISLAND OVERWASH

by

Mark A. Pirrello

Thesis

1992

THE ROLE OF WAVE AND CURRENT FORCING IN THE PROCESS OF BARRIER ISLAND OVERWASH

By

MARK A. PIRRELLO

A THESIS PRESENTED TO THE GRADUATE SCHOOL
OF THE UNIVERSITY OF FLORIDA IN
PARTIAL FULFILLMENT OF THE REQUIREMENTS
FOR THE DEGREE OF MASTER OF ENGINEERING

UNIVERSITY OF FLORIDA

1992

ACKNOWLEDGEMENTS

To begin, I would like to express my thanks to my advisor and supervisory committee chairman, Dr. Robert J. Thieke, for his insight, guidance, and support throughout my study at the University of Florida. It has been an honor to work with someone so dedicated to teaching students. Appreciation is also extended to Dr. Robert G. Dean and Dr. Ashish J. Mehta for their advice and encouragement while serving on my committee.

I would like to sincerely thank the Florida Department of Natural Resources, Shore and Beach Division, for funding the project this thesis is based on.

I am indebted to Sidney Schofield for his technical and personal assistance with the laboratory experiments and to Jim Joiner for keeping the wave tank operating while performing them. My thanks is also extend to Rajesh Srinivas and Dr. Parchure for their invaluable help.

Words can not express the appreciation felt for the assistance of the Coastal Engineering staff, especially Sandra Bivins and Becky Hudson for their humor and to Helen Twedell and Connie Burgess for their personal assistance.

I would like to extend heartfelt thanks to my friends and fellow students, Phil Harris, Jon Grant, Phil Dompe, Eric Thosteson, and Steve Peene, for instilling in me that "beach bum spirit" and to Max Ramos (Muscles), Mike DelCharco, Tim Mason, Chris Jette, Paul Work, and Jei Choi for their personal support during my stay.

Finally, I wish to thank my parents for their love, support, and understanding throughout my education. They have instilled in me the values of hard work, perseverance and responsibility, and for this I am forever grateful.

TABLE OF CONTENTS

LIST OF TABLES

LIST OF FIGURES

LIST OF SYMBOLS

l	=	Length
d	=	Depth
t	=	Time
v	=	Longshore Velocity Component
u	=	Cross-Shore Velocity Component
g	=	Gravitational Acceleration
h	=	Water Depth to Still Water Line
d_{tr}	=	Depth of Water from Bottom to Trough Level
D	=	Sediment Grain Diameter
H	=	Wave Height
T	=	Wave Period
W	=	Sediment Fall Velocity
Q	=	Volumetric Flow Rate
A	=	Area of Surface Roller
C	=	Wave Propagation Speed (Wave Celerity)
γ	=	Fluid Specific Weight
ν	=	Fluid Kinematic Viscosity
X	=	Horizontal Distance
Z	=	Elevation
η	=	Setup of Mean Water Level

Abstract of Thesis Presented to the Graduate School
of the University of Florida in Partial Fulfillment of the
Requirements for the Degree of Master of Engineering

THE ROLE OF WAVE AND CURRENT FORCING IN THE PROCESS OF BARRIER ISLAND OVERWASH

By

MARK A. PIRRELLO

December 1992

Chairman: Dr. Robert J. Thieke
Major Department: Coastal and Oceanographic Engineering

With the rapid growth and development of barrier islands, understanding the long-term stability of these islands is an integral part of future coastal planning. The overwash process is the largest influence on the long-term stability of these islands and thus a corresponding understanding is of major importance. A laboratory experiment was undertaken to physically model the wave and current forcing as they pertain to the overwash process. The physical model was subjected to various storm conditions common to the occurrence of the overwash. Combinations of wave height, wave period, and overwash depth were tested in an attempt to isolate the significant parameters. Water surface gradients were also applied to observe their influence on the overwash process. Wave height, current, and bed profile measurements were taken at different locations throughout the tank. In addition, wave height transformation modeling and mean current prediction were performed and compared to the laboratory results in an attempt to model the overwash process through computer simulations.

The experimental results demonstrate that the water surface gradient is the mechanism

that has the greatest influence in producing "significant" overwash and is most likely responsible for transporting large quantities of sand on to and over barrier islands. In addition, two other conclusions were drawn about the overwash process: 1) the overwash depth plays an important role in determining the overwash velocity and hence the amount of sand deposited on the barrier island. 2) There seems to exist a correlation between the strength of the return flow and bar formation.

It was also determined that modeling the wave height transformation during the overwash process is possible if the model is expressly written for the overwash process and not for non-overwashing cases. The method utilized to predict the mean currents during overwash was not able to predict their strength but was able to substantiate the correlation between return flow and bar formation. As a result of overwash, the increased shoreward mass transport and reduced return flow in the water column are able to initiate and sustain a shoreward sediment transport. Finally, it was concluded that in all likelihood only "significant" overwash events affect the long-term stability of the barrier islands.

CHAPTER 1
INTRODUCTION

1.1 Reason for Study

The past several decades have seen a tremendous and rapid growth of population and development in the coastal areas along the Eastern and Gulf coasts of the United States. It has been estimated that 36% of the population in the United States lives within 100 miles of the coast (World Almanac, 1992). Barrier islands have taken a significant measure of this development because they offer both residential and recreational opportunities within close proximity to the water. The onslaught of development has placed the barrier island in a precarious situation. These islands are dynamic in nature, shifting position due to tide, wave, and wind forcing. In many instances, they afford the mainland protection from the harsh conditions that are brought forth by storms and hurricanes. Growing development conflicts with this dynamic nature. Striking a balance between development and protection of the barrier island has raised questions about determining ways to maintain the long term stability of these islands.

With the increased awareness surrounding barrier island stability, it is essential for long term coastal planning that an understanding of the sediment transport processes related to island stability be thoroughly examined. More specifically, a detailed analysis is needed of the overwash process that controls the island's dynamic nature. The overwash process is the most effective mechanism for shaping long term island stability and thus is an important aspect of future planning for barrier island development. But understanding the overwash process itself does not give a complete picture of barrier island stability. Cross-shore processes along with

morphological changes on the barrier island created by the tidal range and wave regime are an integral part of understanding the total overwash condition.

1.2 Barrier Islands: Background

Barrier islands are narrow, sandy, low lying islands that primarily occur on coastal plains located on shallow continental shelves. In most instances, these islands are separated by tidal inlets and are occasionally connected to the mainland. They are native to 30% of the world's coastlines but are most prevalent in areas of low to moderate tidal action (< 4 meters) (Hayes and Kana; 1980). According to Leatherman (1979), barrier islands along with bay barriers and barrier spits are a sub-category of barrier beaches. Barrier beaches consist of an entire system that includes the beach, foredunes, backdune flats and the associated bays or estuaries. These features are shown in Figure 1.1 and Figure 1.2. It is these areas that respond to the actions of wind, waves, tides, storms, and sediment supply. In fact, tide and wave conditions are the important factors influencing the morphology of the islands (W. Price; 1955). Areas with a strong tidal influence will produce short, drumstick shape islands that are separated by many inlets. These islands frequently accrete on the updrift side from stored sand at the ebb-tidal shoals. In contrast, islands dominated by wave energy are flat with few inlets, and are susceptible to overwashing during storms. These islands tend to erode and accrete depending on wave climate and sediment supply.

Changing wave and tide conditions induce short term changes in barrier island dynamics. However, they are only a contributing factor in long term changes. Factors that affect future barrier island stability include the global rise in sea level, migrating inlets, and large storms. Studies concerning the rising sea-level have taken precedence in recent years. It is this trend that has heightened the debate over the continued development of the barrier beaches. The barrier beach is not without means to retard or stop the effects of the rising sea. Aeolian transport,

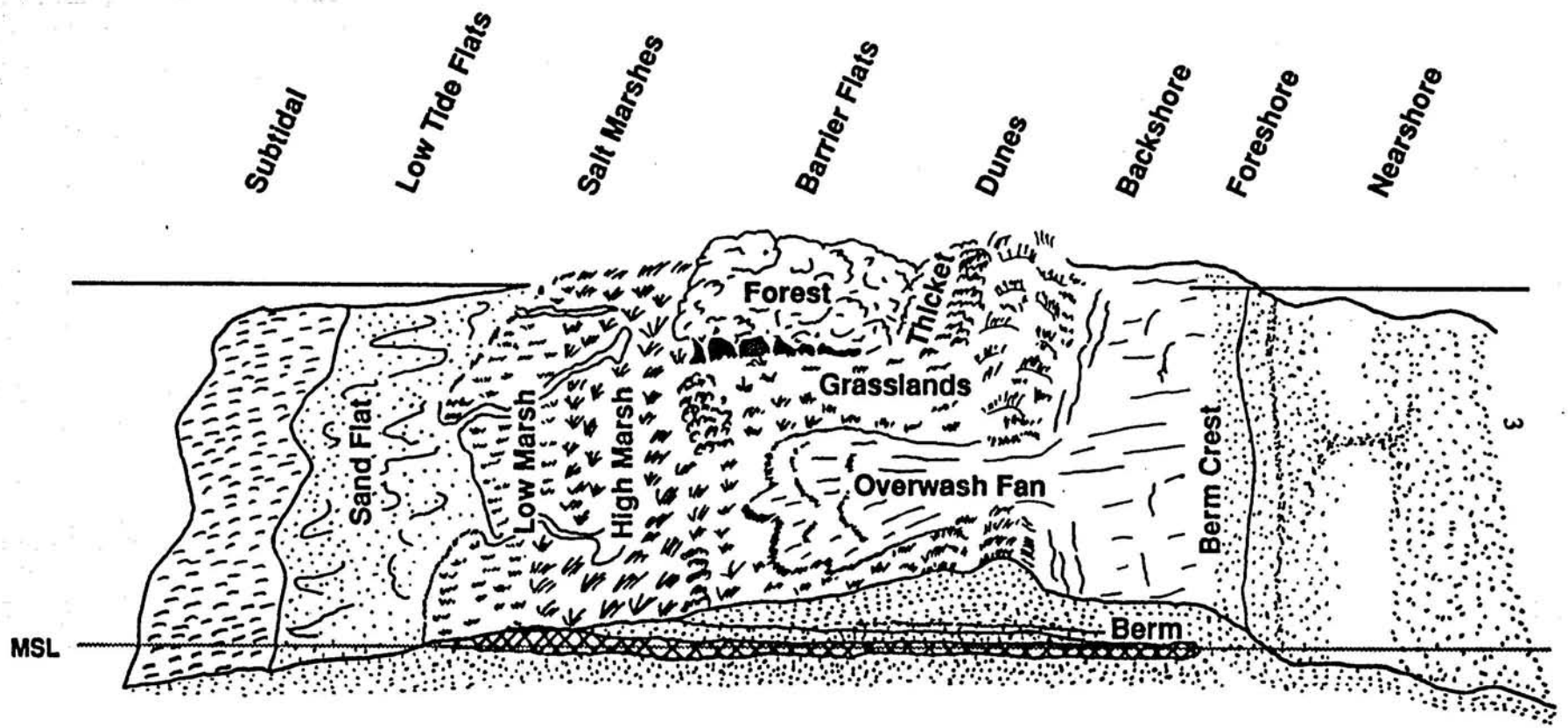

Figure 1.1 A Typical Overview of Morphological Features that Comprise a Barrier Beach System (Godfrey, 1970)

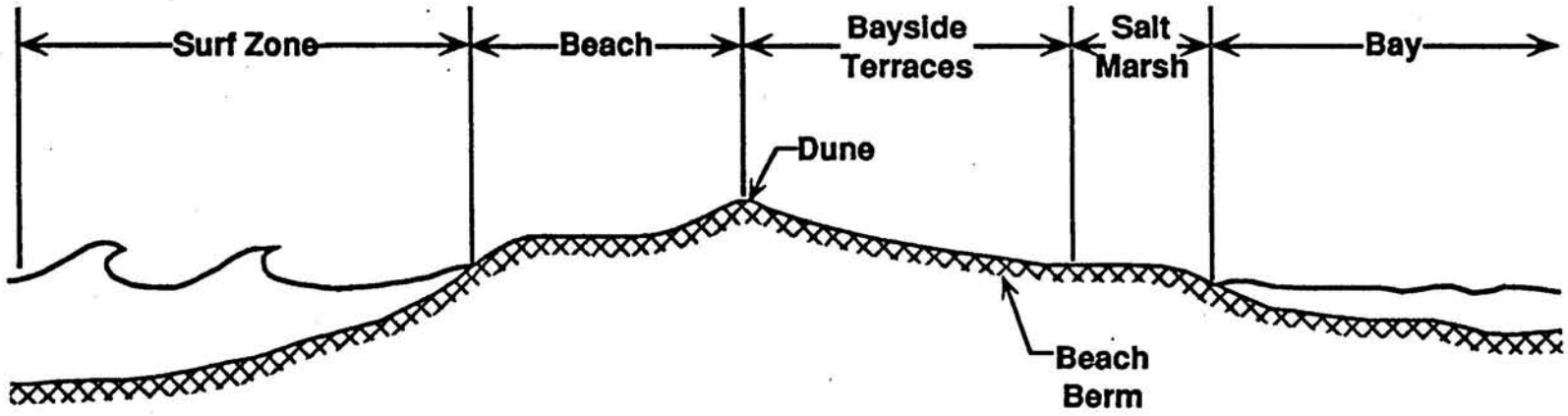

Figure 1.2 The Typical Cross Sectional View of a Barrier Beach System Showing the Three Major Dynamic Areas (Williams, 1978)

overwash, long shore currents, and even tidal inlets have the ability to transport sand shorewards. Overwashing of the barrier island has the greatest impact on counteracting the sea level rise. Washover deposits help the island to build and maintain its width from the encroaching sea. Comprehending the changes that overwash contributes to the barrier island in a morphological sense is important. However, it is only one part of the total equation.

1.3 Cross-shore Processes

In non-overwashing conditions, cross-shore and longshore processes are instrumental in transporting sand. When the island is overwashed, the sediment transport characteristics change. Cross-shore processes are now more likely to be predominant in carrying the sand over the island. Analysis of the overwash process can thus be idealized in a two-dimensional manner. Within such a framework, a highly simplistic view of the cross-shore sediment transport may be formulated in terms of two flows, shoreward mass transport and seaward return flow. The mass transport, formed by incompletely closed particle orbits in the wave, produces a net drift velocity in the upper part of the water column that carries suspended sediment towards shore. Depending on wave conditions, some of this sand is transported offshore again due to a return flow, created by an imbalance between the radiation stress and the set-up pressure gradient, in the lower portion of the water column (See Figure 1.3). The formation of these flows depends on the dissipation of wave energy created by the breaking wave, and they can vary greatly in strength depending on the nature of the wave conditions. Storm conditions with large wave heights produce the largest flows and therefore the most intense sand transport. The direction of the flows or current and therefore transport is influenced by the height and steepness (H_o / L_o) of the wave. As the wave becomes higher and steeper, it creates a greater radiation stress gradient thereby enlarging the imbalance between the stress and the set-up pressure gradients. This results in the return flow increasing in magnitude. Sand will tend to flow in the offshore direction.

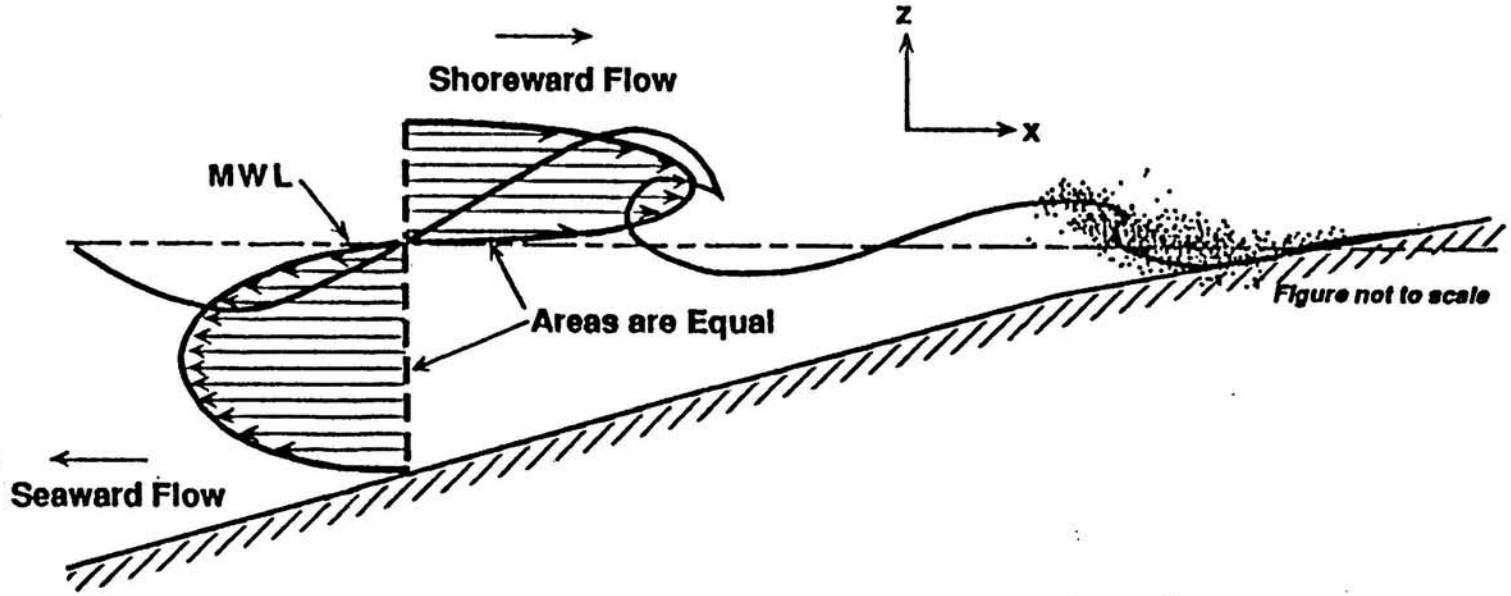

Figure 1.3: Schematic Representation of Mean Flow Profile in Surf Zone.

Longer wave periods create swell conditions (waves of low steepness). In this situation, the return flow is weaker, which, combined with the asymmetry of the orbital velocity, encourages onshore sediment motion.

Wave energy dissipation has the greatest effect on coastal morphology and sediment supply (Davis; 1981). The wave-induced currents developed by this dissipation of wave energy influence surf zone morphology. During severe weather, there is a marked increase in sand volumes transported offshore from the beach face. This sand is captured in the return flow and moved seaward. Often the excess sand transported offshore will form a bar in the general area of the breakpoint. As the bar continues to grow, the associated slope of the beach face becomes milder. After the passing of the storm, the profile will typically recover under swell conditions. Sediment stored at or near the breakpoint will gradually return shoreward and the associated beach face will become steeper.

How does this wave induced current interaction in the cross-shore relate to the overwash process? Cross-shore flow affects the sand transport during the overwash cycle. The return flow is weakened as a result of the mass transport of water over the island. Therefore, the increased shoreward mass transport carries more sediment onshore. Simultaneously, overwashing may also alter the bar formation offshore, since reducing the return flow undermines the ability for sand to be transported toward the break point. Any sand transported offshore is now more likely to remain in the surf zone. Finally, variations in wave height affect the speed of the current washing over the island which then determines the quantity of washover material.

1.4 Overwash Processes

Overwash is defined as the mass of water created by storm surge and waves that transports sand across the island from the beach and foredune areas. Washover is defined as the material deposited by the overwash process. Overwash occurs during storms, like northeasters

and hurricanes, when there are increased wave heights and storm surge created by the high winds. The frequency of overwash episodes is a function of storm frequency. Higher winds intensify the magnitude of both wave height and storm surge.

The process initiates when large wave heights coupled with an increased storm surge allow the wave runup to overtop the existing berm. Depending on the intensity of the storm, the water will completely overtop the island or will flow through low relief portions of the land, an example being the area between the foredunes. If the island is inundated, the sediment will be transported in a sheet flow. If the island has a higher relief, the runup will create a channel, called a trough, through which water and sediment can be transported. Once sand flows past the dune zone, it will either be transported to the back shore area or make its way to bay water. The distance that the washover travels depends on the flow velocity at the throat, which is a function of wave conditions, storm surge, and the topography of the island. The flow velocity could be enhanced by formation of a water surface gradient over the island. This water surface gradient occurs due to an imbalance between water levels in the bay and ocean created by the "storm tide". During the initial phase of overtopping, the bay water level is often lower than that of the ocean.

The sand deposits that are transported and overwashed originate from several sources. Schwartz (1981) found that the major source of the washover found in the overwash cycle originated from the nearshore and beach area. The increased shoreward mass transport generated by the overwash process brings sediment onshore from the surf zone. This sand is then carried by the currents over the island. Sand is also taken from the foredune area. As water either overtops these foredunes or cuts a channel through them, some sand is scoured away. The amount of washover moved and deposited is dependent on the storm surge, wave energy, slope of beach, and backshore-foreshore relief.

The morphology that the washover acquires is contingent only on the height of the storm surge and the topography of dune and back shore areas. The three different categories of washover morphology are fan-shape, coalescing, and sheet form. The fan-shape occurs on beaches with high relief dune forms. The high dunes channel the water through the low areas leaving an alluvial type fan on the bayside terraces. Moderate relief barrier islands promote coalescing of the fan while low relief, or no dunes, produce sheet-like deposits (Williams; 1978).

1.5 Objectives and Scope

Although there is a basic understanding of the overwash process, much of what is detailed in the preceding sections is qualitative in nature. In general, studies report the morphological changes and sediment volumes generated by the process. However, very few studies conducted relate these changes with the interaction of the wave and current forcing. And those that do discuss this interaction do not do so in a quantitative manner. The episodic nature of storms and the overwashing process make it difficult to study and obtain data from the actual event. One alternative is to model the process. The primary objective of this investigation is to physically model, in a laboratory environment, wave and current forcing as they pertain to the overwash process. A scale model of a cross-section of a barrier island will be utilized. Monochromatic waves will be generated and an elevated water level will be used to simulate the overwash condition. Wave height and current data will be measured at locations throughout the surf zone. Wave conditions and storm surge will be varied between the different experiments. Variation in storm surge depth is expected to be important in determining sand transport volumes throughout the beach and island profile. Water surface gradients resulting from an imbalance in bay and ocean water levels will also be investigated. This emphasis on waves and currents should give some insight into the various physical parameters and their respective contributions to the overwash process. The second objective is to model the wave and current patterns during

overwashing through computer simulations. Wave height evolution and current predictions will be compared to experimental data from the physical model in an attempt to isolate significant parameters. In addition, bed profiles and current data from the experimental data will be compared to data from non-overwashing cases to ascertain the changes in magnitude between the shoreward mass transport and the seaward return flow. By examining these various facets of the overwash process, an improved understanding of long term stability of barrier island will result.

This thesis will address the following topics. A literature review of past studies pertaining to overwashing will be discussed in Chapter 2. Distinctions will be made between the morphological changes discussed in the geological reports and the wave mechanics and sediment transport processes in the engineering investigations. In addition to these reports, a review of cross-shore modeling will be presented. Properties of waves and currents in the surf zone and profile evolution will be discussed. In addition, the effect of a water surface gradient on the profile will be examined. Chapter 3 will detail the conceptual design and criteria for the laboratory study. A brief explanation of the beach profile geometry, with references to equilibrium profiles, will be followed by similarity criteria for modeling waves and sediment. The experimental apparatus, procedure, and test conditions will be outlined in Chapter 4. Information on the data acquisition equipment and data acquisition program will be fully detailed in this chapter. The computed results from the test data and subsequent analysis will be presented in Chapter 5. Wave height decay relationships, including results obtained from a wave transformation model (Dally, Dean, and Dalrymple; 1985) will be compared to those found in the laboratory. In addition, the outcome from mean current predictions will be compared to laboratory measurements. Chapter 6 will comprise an investigative summary and conclusion based on the results of laboratory experiments and computer simulations.

CHAPTER 2
LITERATURE REVIEW

2.1 Overwash Research

Studies of the overwash process are limited in volume and nature. Most reports generally describe the overwash condition qualitatively, with little quantitative data. This is due to the time and cost of obtaining complete overwash data. This results in studies that mostly detail the morphological change and not the sediment transport processes.

Early reports of overwashing were written by geologists, who were the first to understand the significance of the washover and its role in the development of the barrier island. Wilby (1981) described the results of the great "New England Hurricane" of September 21, 1938, on Long Island, New York. This storm pushed through several gaps in the dune line and washed sediment from the beach onto streets and lawns, with the average depth of washover being four feet. Some of the sand was swept into the backbay and deposited. From an aerial vantage point on the south barrier shore of Long Island, he surmised that "the major geographical effect of the hurricane was to widen the [barrier] island." Lobeck (1939) continued the work of Wilby and others and concluded that "during storms, waves break over low portion of a bar and carry material back to the lagoon, depositing washover."

Price (1947) was the first to define specific terms associated with the overwash condition. In his report outlining the changes occurring on the coasts of Texas and Louisiana, he examined the various washover features. He stated that each washover feature had a throat, a diverging

channel, and formed broad fan-like deposits. It is these terms that are subsequently used today to describe the various features of washover.

Recently, several geologists have studied not only the morphological changes but also the mechanisms that drive the overwash. Hayes (1981) examined the washover deposits on the Texas barrier island chain from Hurricanes Carla (September, 1961) and Cindy (September, 1963). Using core samples from the island, he noted that most of the sand deposits originated from the near shore region and beach. The increased storm surge created a flood of water that passed over the island and transported the sand into the tidal marshes and bay. As the storm receded, an storm ebb flow was created that moved and deposited sediment from the tidal marshes back over the island and the offshore region. He suggested that the storm ebb flow was most responsible for depositing sand on the barrier flats and not the storm flood flow. He states that " ...the importance of catastrophic storms as sediment movers can not be overemphasized" (Page 93). Andrews (1970) expanded on Hayes' research by examining some washover deposits on St. Joseph Island, Texas. He concurred that most of the sand was taken from the nearshore zone, beach, and foredune ridge and carried onshore by the storm surge "flood tides." He points out that most of the sand was deposited on the barrier flats and bay waters.

Man's interference with the overwash process was documented by Dolan (1972). His research pertained to the Outer Banks of North Carolina. During the late 1930's and 1940's, the federal government tried to stabilize these barrier islands. They constructed a line of foredunes from Ocracoke to Nags Head. Dolan found that since the construction of these man-made dunes, the beach width had markedly decreased relative to the dune line. No new dunes were being formed due to a lack of overwashing on these islands. Dolan theorized that by taking away the overwashing condition, the island's ability to stabilize had been retarded. Godfrey (1970) also examined the impact of man-made stabilization on the Outer Banks. Using bench marks

established by the U.S. Army Corps of Engineers, Godfrey was able to see how much sand had accumulated over the island. He postulated that the primary source for marsh expansion and elevation increases in the bay bottom resulted from overwashing. Furthermore, he concluded that the growth of vegetation was important in keeping the newly deposited sand from being transported by the winds. If the overwash condition was eliminated by foredune construction, the sand normally transported over the island will tend to be moved offshore resulting in narrower beaches. Godfrey states that "Without this movement, and with a lack of sand supply, they", meaning the barrier islands, "could be overwhelmed by the rising sea level."

The rising sea level and its effect on the barrier island was the topic of research of Dillon (1981). Examining data from Charleston Harbor, Rhode Island, he concluded that the barrier island was transgressing landward due to overwashing and filling of the lagoon and bay. "This migration has resulted in the preservation of the lagoon during a period of rising sea level" (Page 26).

Research papers reviewed previously dealing with the subject of overwash were mainly detailed reports from observations conducted in the field. One of the first field studies conducted for the expressed purpose of obtaining pertinent data on the overwash process was Fisher (1974). The northern end of Assateague Island, Maryland, was the site chosen for the experiment because it experienced a high frequency of overwashing. A cross section of the island, including a washover fan and dune, was included in a rectangular grid. From this grid, monthly surveys, sand tracer studies and velocity data from the throat during overwashing conditions were taken. The first storm, a northeaster on March 22,1973, overtopped the island with six foot wave heights. An unknown amount of sand was eroded from the throat and deposited over the fan. Maximum surge velocity at the throat was 8 ft/sec (2.4 m/sec) at a depth of 1 ft (0.30 m) above the bottom. A second storm, Tropical Storm Gilda, occurring on October 26-27, 1973, deposited

considerably more sand on the washover fan. Using the data from these two storms, Fisher concluded that only severe cases of overwashing affect the stability of the islands. During smaller overwashing events, like those on Assateague Island, most of the sand transported remained on the beach and throat area. Sand that did deposit on the barrier flats from the storm did not significantly change the elevation of the flats because aeolian transport dispersed this sand throughout the island.

Fisher and Stauble (1978) continued field research on Assateague Island. Their data support previous claims by Fisher that most of the washover deposited during small overwashing events is brought back to the beach by aeolian transport. The beach width and the dune size that had been reduced by the storm returned to their original size or even grow. They concluded that overwash only affects the island's stability when it is of a large magnitude.

Schwartz (1981) conducted the first extensive U.S. Army Corps of Engineers field report on the overwash process. He studied a section of the Outer Banks, from Currituck to Cape Hatteras, and Presque Isle, on the Pennsylvania coast of Lake Erie. Both these areas were frequently overwashed due to either hurricanes or winter storms. The February 9-11, 1973 storm generated the overwash on the Outer Banks. A large frontal storm on the Great Lakes generated severe overwash on Presque Isle. The field research consisted of digging trenches to determine the depth and textural characteristics of the storm deposits. Schwartz found that the size and texture of the overwash deposits were horizontally layered throughout the washover fan. Furthermore, when surges entered the bay waters, the sediment deposited formed deltas at the inflow points. He concluded that the occurrence of overwashing has a two fold effect on the barrier island. It deposits coarser, subaerial sand which contributes to the landward and vertical accretion of the island. Second, overwash is important aspect of the littoral system in that it is a storage place for sand. As the beach width decreases, the washover will be acted upon by

storm events in the future. When this occurs, the sand will be released into the littoral system again.

Leatherman (1976) completed several more field experiments on Assateague Island, Maryland. His purpose was to quantify the short term impact of overwash on the sediment budget of the island and its relation to barrier island migration. Six sites were selected. Data were collected from the December 1, 1974 northeaster in the form of sediment volumes and surge velocities at the throat. Volumes of sand accreted for the six area ranged from 93 cubic feet (0.85 cubic meters) to 300 cubic feet(8.5 cubic meters). Overwash velocities were in the order of 5.2 ft/sec (1.6 m/sec). Leatherman speculated that washover fans in this area act as temporary reservoirs that later redistribute sand over the island and beach by aeolian transport. In addition, he suggested that there is a balance between the overwash process and aeolian transport with the wind transport being slightly dominant. Thus, wind transport provides sand to the island and beach area when severe storms have eroded sediment in these areas. He concluded that overwash contributes to the short term sand budget of the island thereby short term island stability is achieved. The following year Leatherman (1977) updated his research on this site. Using the same data from his previous report, he determined that fluvial mechanics pertaining to sand transport could be used to approximate the washover volumes within acceptable limits.

Although there is a growing number of field experiments, the time and money required for such experiments is beyond the means of many researchers. A different approach for studying overwash mechanics was taken by Williams (1978), who set up a laboratory experiment modeling the overwash process. His goal was to study the mechanisms of overwash and evaluate a predictive relationship for computing sediment transport rates. Using a wave tank 98 feet (30 meters) long, 8.2 feet (2.5 meters) wide, and 4.9 feet (1.5 meters) deep, monochromatic waves were generated. The hypothetical island consisted of 0.21 mm sand contoured into a 1:15 slope

seaward from the berm. Behind the berm, a 1:40 slope was used. Williams divided his experiment into three sections. The first section consisted of determining an initial equilibrium profile. The second section contained the methods for determining parameters for initiation of overwash. The last section consisted of overwashing the island until the process was terminated by the build-up of sediment. The completion of the first section required running the monochromatic waves at mean sea level over the planar beach. Equilibrium was reached when the seaward profile of the island remained in a steady state condition. This event took between six to ten hours. Water level was then raised until incipient overwashing conditions occurred. Incipient overwashing was defined as the point when runup of the waves initiated overtopping of the existing berm. The final overwash phase did not completely inundated the island but allowed the water to washover into portions of low elevation on the island. Each test was completed when overwash terminated due to the build-up of sediment. Upon completion of the experiment, the data were used to find a predictive relationship for washover volumes. This relationship was based on the idea that overwash sediment transport rates are a function of excess runup. A nonlinear least squares fit was employed to determine coefficients for the predicative relationship. For larger washover volumes, the relationship provided agreement to within $\pm 50\%$ between the measured and calculated volumes.

2.2 Cross-shore process and Bar formation

Except for the experiment by Williams, the engineering aspect of overwashing has not been fully researched. At present, there are no detailed reports of wave-current mechanics and bar formation for the overwash process. Since the overwash condition is an altered state of non-overwashing, the study of this area will be beneficial in understanding the implications to wave, current, and bar formation that overwashing incurs.

The overwash condition differs from non-overwashing in three major respects: 1) Bar formation and Profile Evolution, 2) Wave Height Evolution, 3) and Velocity profiles. Each of these topics will be examined from a hypothetical two dimensional viewpoint. During storm conditions, the beach profile will modify due to the changing wave and surge conditions. The increased steepness of the waves and the stronger return flow can result in sediment being carried offshore. If this event occurs, a milder profile from the berm to the break point will be created. The excess sand taken from the swash zone may then move to the general area of the break point. It is in this area that bar formation from the excess sediment is likely. This bar could remain until milder wave conditions return the sand shoreward. Initiation of overwash may alter this profile. The excess water brought in by the shoreward mass flux does not return to the surf zone, instead this water washes into the bay waters. That water brought in by mass transport is instrumental in creating the return flow. If the return flow should be weakened, then the resulting sediment transport will be affected. Bar creation could be suppressed, and the profile would then become milder throughout the entire surf zone.

Wave height distribution can also be modified by the overwash condition. Generally, when waves break, the wave decay associated with breaking depends on the amount of turbulence generated. The degree of turbulence can depend on the breaking wave height and the beach slope. Breaking wave height and beach slope change when overwashing occurs. When the island is overtopped, the increased mean sea level coupled with changes in mass transport and return flow can result in shifting the location of the break point. The breakpoint will typically move farther shorewards. If the breakpoint shifts shorewards, the beach slope becomes flatter. In most instances, the new topography will cause the breaking wave height to be smaller. The turbulence associated with breaking would be reduced. Wave decay would tend to be more gradual as it

continues across the island. In addition to wave decay, set-up associated with the incoming waves would also change.

Linked to the transformation of wave decay is the change in the cross-shore mean velocity profiles due to overwashing. In a strictly 2-dimensional view, the mean velocity profile may be represented schematically with a positive velocity value associated with the shoreward mass flux in the crest region while negative values indicate the return flow (seaward) in the lower region. When overtopping occurs, the velocity profile changes accordingly. The reduction in return flow and the increased presence of shoreward mass transport may result in profiles with little or no seaward velocity. In cases where a water surface gradient due to storm flood tide is evident, velocity profiles may be entirely positive (shoreward).

Research in cross shore processes for non-overwashing cases are numerous. There are many reports dealing with wave and current interaction. Since one of the objectives of this thesis is to model the overwash process, it is beneficial to review those works that have tried to model cross shore processes to provide a basis for the incorporation of the mechanics particular to overwash. Cross shore modeling will be divided in two sections: 1.) Wave Height Transformation, 2.) Cross shore currents.

LeMehaute (1962) described one of the first practical methods to model wave transformation in the surf zone. Using a steady-state equation for energy balance across the surf zone, he approximated the energy dissipation rate using the analogy between the turbulent front face of a breaking wave and a moving hydraulic jump. This method provided acceptable results for mild slopes only. Divoky, LeMehaute, and Lin (1970) modified the ideas of LeMehaute and modelled the rate of dissipation as a function of bed slope and the convergence of wave orthogonals. As before, this method was only applicable for mild slopes. Horkawa and Kuo (1966) used the same basic energy balance equation but modeled the rate of internal energy

dissipation in terms of turbulent velocity fluctuations. These velocity fluctuations were assumed to decay exponentially with distance from the breakpoint. Dally, Dean, and Dalrymple (1985) quantitaively modelled wave transformation by including various wave parameters found subsequent to wave breaking. Their approach to quantifying the energy dissipation rate was to approximate it as the difference between the energy flux computed by linear theory and the energy flux associated with an empirically determined "stable" wave condition. Solving the energy and momentum equations numerically, the transformation of wave height was modeled. In making this model as realistic as possible, the effects of bottom friction, wave-induced setup, and beach profiles of arbitrary shape were included.

There has been much research in the field of cross shore current modeling. The basis for each model is similar in scope. They are based on the equations of mass, momentum, and energy conservation. An exception between any one model is how the return flow is represented. I.A. Svendsen (1984b) used the qualitative ideas of Dyhr-Nielsen and Sorensen (1970) to quantitatively represent the mechanisms responsible for return flow. In his paper, he defined the driving force behind return flow as the local difference between the radiation stress and the set-up pressure gradient. Using Svendsen's (1984a) roller assumption for waves and particle velocities, an equation for the return flow was determined. In order to produce a steady state solution of the equation, turbulent shear stresses were required to balance out the inequality in the gradients of the radiation stress and the set-up. Boundary conditions consisted of satisfying continuity and using the Eulerian streaming condition at the bottom boundary layer to model the mean velocity. Svendsen found acceptable agreement between model and experimental data.

Stive and Wind (1986) continued work on cross shore modeling but modified Svendsen choices for the return flow boundary conditions. Both papers utilized the boundary condition that continuity had to be satisfied. The difference is in the second boundary condition. Svendsen

relied on a bottom boundary condition specifying the mean flow velocity. Stive and Wind, however, stated that a shear stress at the trough level would be more beneficial in determining the internal mean flow distribution. Using measured data from various laboratory experiments, a comparison with the computed values produced results that better represented the strength and direction of the return flow.

Svendsen and Hansen (1988) discuss the problem of incorporating cross shore circulation into a numerical model that predicts wave height and set-up. Two obstacles associated with this are determing the proper boundary conditions for the return flow and solving the mean bottom shear stress. For the return flow, Svendsen and Hansen counter Stive and Wind on the use of Eulerian streaming as the bottom boundary condition. They "suggest that the problem can be solved by satisfying the no-slip condition but assume a much smaller eddy viscosity in the bottom boundary layer than outside" (Page 1588). This idea is also applied in finding the bottom shear stress. The shear stress is a combination of the return flow and the mean oscillatory motion in the bottom boundary layer. Solving for this quantity is accomplished by simply applying the definition for the bottom shear stress at the point in the velocity profile where the transition occurs between the return flow and the bottom boundary layer. Employing their methods to the cross shore circulation model, Svendsen and Hansen believed that this method predicted circulation patterns more accurately.

Although these circulation models differ in detail, in each case the overall magnitude of below-trough seaward flow is largely determined by the chosen representation of the shoreward mass flux (mass conservation). Therefore, a viable simple alternative to detailed circulation modeling is to estimate the mass flux in the surf zone and then approximate a return flow from this shoreward mass flux.

CHAPTER 3
DESIGN OF EXPERIMENT

3.1 Introduction

Clearly, the amount of laboratory research pertaining to the study of overwash is limited. From the preceding chapter, only one of the experiments mentioned was a laboratory experiment. With little background in modeling this process, the design of this project is important. Wave and sediment processes and the beach profile geometry must be addressed in the same manner in the model as in the real situation. For the wave and sediment processes, this means that certain similarity criteria must be met. The beach profile must be designed so that the bed form will allow overwashing to occur. In this chapter, similarity criteria will be selected along with a beach profile geometry suitable for studying the overwash condition.

3.2 Beach Profile Geometry

Barrier islands that are frequently overwashed vary in topography, though low-relief islands are inclined to be overwashed more readily. In designing an appropriate beach profile geometry certain factors must be taken into account. First, the topography should be such that the island will be able to be overwashed during increased storm surge. Second, the slope of the profile, from the berm to the offshore region, should be chosen to represent a slope typically found in barrier island environments. Last, the type of sand used to represent the island and offshore profile should be consistent with similitude criteria.

Finding an actual barrier island to model that meets the above requirements is improbable. For this project, a hypothetical island was constructed that would satisfy the conditions. The

island, in prototype scale of 1:16, consists of a 400 foot (122 m) crest width and a 1:18 beach slope (Figure 3.1). The 400 foot (122 m) crest width is flat. This flat topography allows washover sediments to be transported across the entire island, thereby permitting simulation of the case of complete inundation, in contrast to the experiments of Williams (1978). At the far side of the island, there is a catch area for the sand that would normally flow into the bay waters during overwashing. Although vegetation does tend to affect the amount of washover and where it is deposited, this factor will not be studied. As for the beach slope, 1:18 represents a fairly steep slope but one that can be found in a typical barrier island environment and is readily accommodated in a wave flume. If the slope was considerably steeper than the one chosen, a large part of the incoming wave energy would be reflected, whereas a significantly flatter slope would be highly dissipative. Finally, a 0.18 mm sand grain was used in the model to represent sand from an actual situation. Details about determining this grain size will be summarized later in this chapter.

Although the hypothetical barrier island is suitable in studying the overwash condition, it does not give a totally accurate picture of the real situation. Although a 1:18 slope depicts a slope that is sometimes found in an actual situation, the shape of that slope is perhaps unrealistic. In this experiment, a planar slope is used from the berm to the point of closure offshore. Finding a completely planar slope in nature is possible but highly unlikely. Nevertheless, planar slopes are a good initial point from which to judge changes in the profile. They react quickly to existing wave conditions and tend to form the "correct" equilibrium profile. The amount of change that occurs depends on the initial planar slope. Planar profiles are classified into five different types according to decreasing beach slope steepness (Dean, 1991). Of the five types, the first three types are recessional, the last two accretional. A diagram depicting all five types can be seen in Figure 3.2. Recessional planar profiles are steeper than equilibrium conditions permit. Sand is

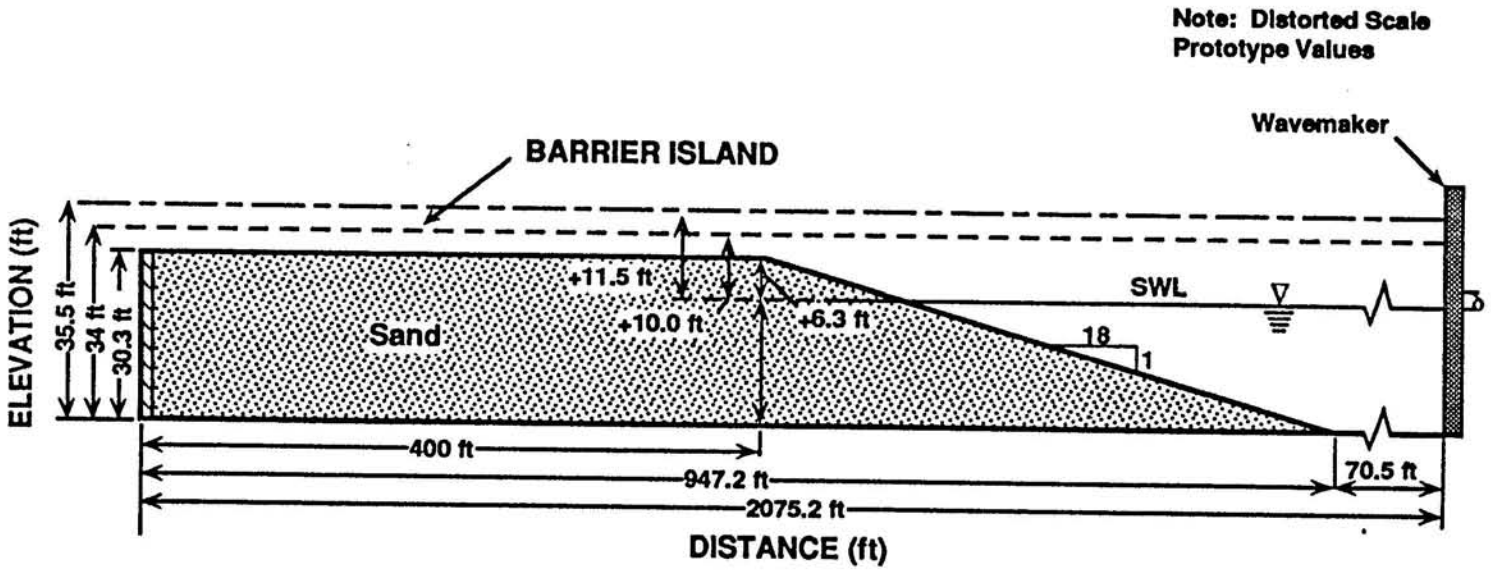

Figure 3.1 A Schematic Diagram Detailing the Hypothetical Barrier Island

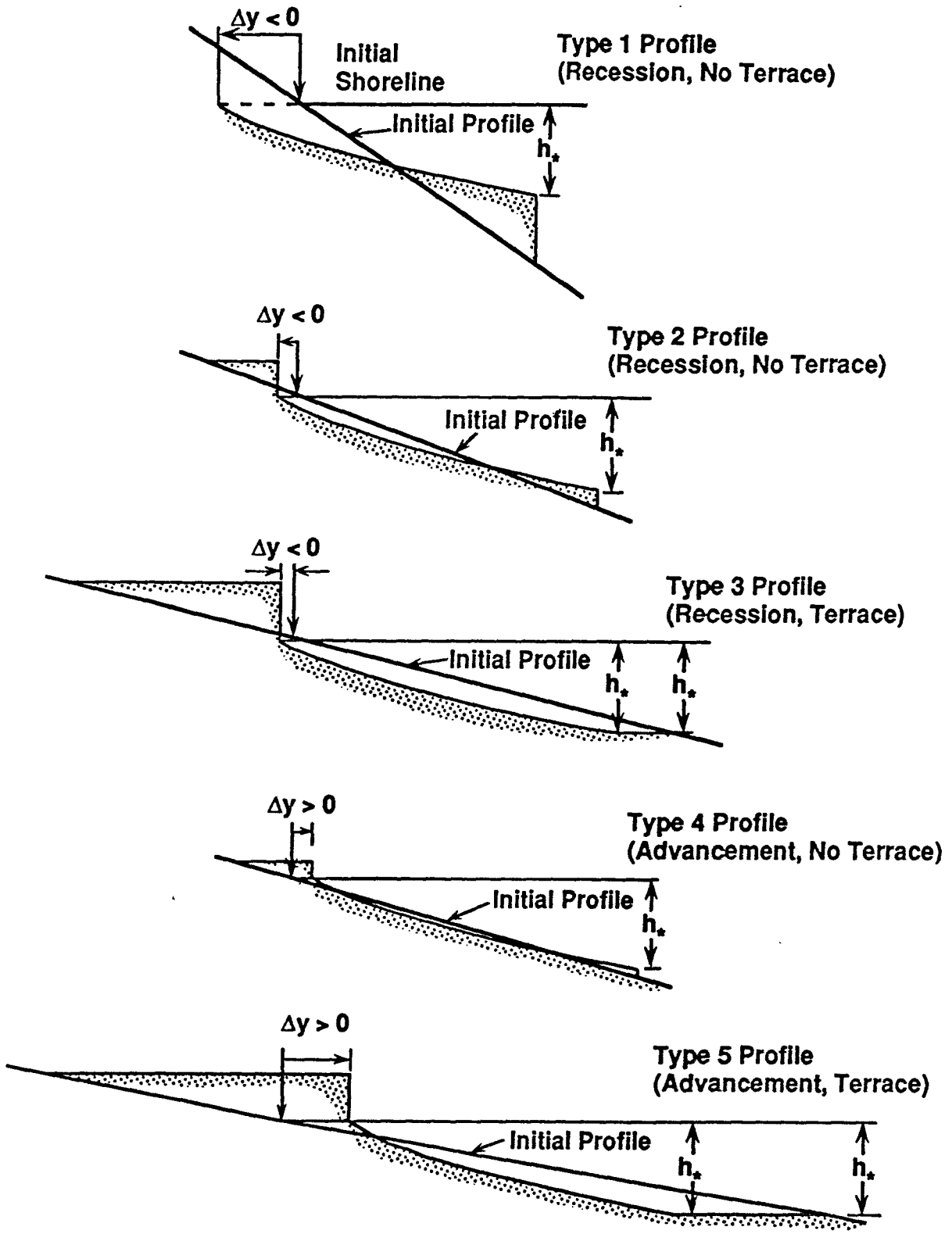

Figure 3.2 The Five Types of Planar Beach Profiles (Dean, 1991)

taken offshore to adjust the profile. The amount of sand taken offshore depends on the steepness of the slope. Accretional planar profiles are characterized by mild slopes. Equilibrium is reached in these cases when sand is brought onshore. In this experiment, a Type I planar slope is used. In the Type I case for typical (non-overwashing) conditions, no sand is brought onshore, the extra sand in the initial profile is taken offshore and forms a bar. This is evident in Figure 3.3.

3.3 Similarity Criteria

A model study is designed to simulate natural processes (prototype conditions) in a laboratory environment. Based on the ideas of the U.S. Army Corps of Engineers (1979), a model should: 1) reproduce the natural phenomena with sufficient exactness; 2) be consistent; 3) be sensitive; and 4) be economical to use. In order to provide for all these constraints, there must be similarity between the model and the prototype conditions. This means two requirements must be satisfied. One requirement is that there be geometric similarity; the other requires similitude between the predominant forces. Geometric similarity implies that the ratio between the unit lengths of all space coordinates must be equal in both the model and prototype. Similitude between the predominant forces requires that the ratio of the forces that govern the process be a constant.

In general, models cannot reproduce all the events that occur in the prototype. Limitations on tank size, bed material, and the degree of accuracy needed result in discrepancies. These discrepancies result in scaling effects which produce deviations between the model and the prototype. To minimize these scale effects, models usually will represent only the forces that are essential to the process under study.

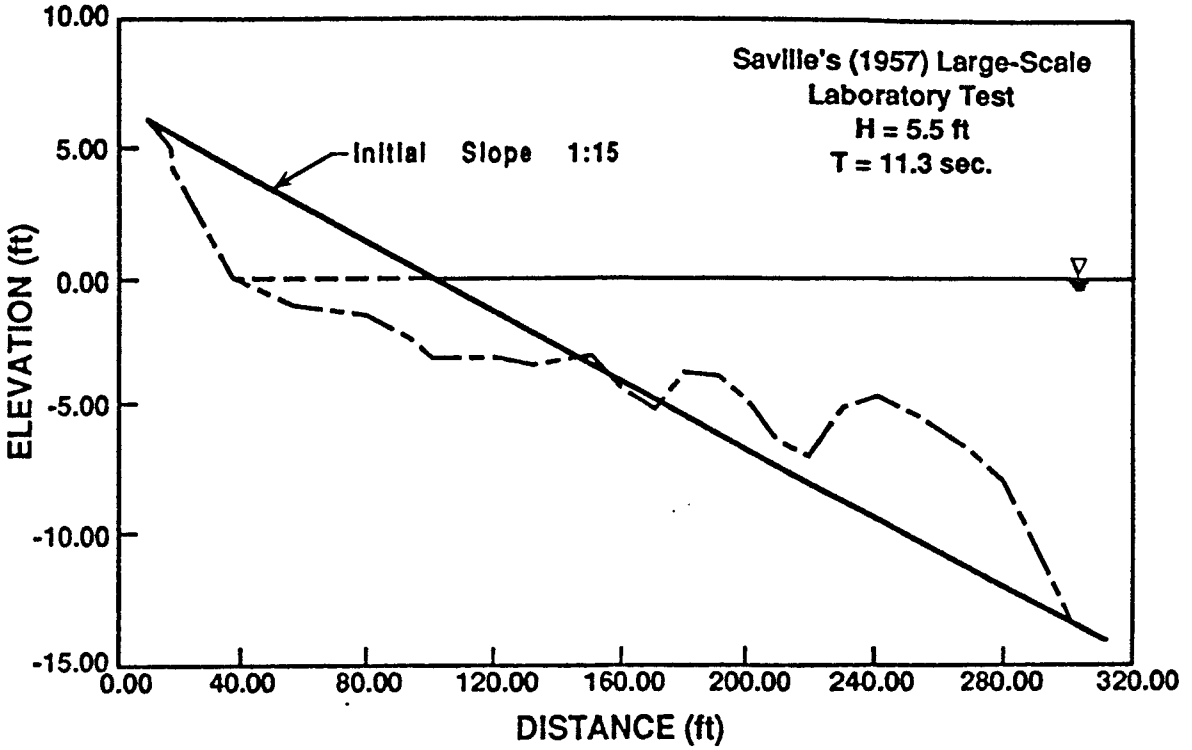

Figure 3.3 The Initial and Final Stages of a Type I Planar Beach Profile (Saville, 1957)

Similarity Criteria in Coastal Engineering

Coastal engineering physical models are divided into two categories: 1) Movable bed models; and 2) Non-movable bed models. Fluid flow mechanics are the only forces examined in non-movable bed models. Typically, similarity criteria utilized in these models revolve around the Reynolds's Number and the Froude Number. When the bed is able to move, it adds complications. Now, sediment flow processes as well as fluid flow mechanics of the prototype have to be reproduced. Deciding the appropriate similarity criteria for a movable model is dependent upon the physical phenomena studied and the predominant forces at play. In our case, the similarity criteria will center around the overwash condition.

To reproduce the overwash condition, two criteria must be chosen to represent the fluid flow mechanics and the sediment transport processes. Both the Reynold's Number and the Froude

Number can represent the fluid mechanics. However, these two criteria cannot be simultaneously satisfied on a small scale. The Froude Number is essential because it incorporates gravity. Gravity is the dominant restoring force for wave motion, thus it is better suited for this application. Similarity criterion representing the sediment transport processes of overwash is more difficult to determine. There are many criteria that can be used but criteria based on beach profile erosion are considered to best represent this event. Utilizing beach profile erosion criteria requires that five parameters be included. These are: the horizontal scale; the vertical scale; the median diameter of the sediment; the fall velocity; and the specific weight of the sediment. These four parameters work in conjunction to give the movable bed model its ability to simulate prototype conditions. The U.S. Army Corps of Engineers (May 1979) conducted an intensive review of similitude criteria for beach profile erosion. A summary of their findings is given in Table 3.1. Each of the criteria is significant for an appropriate case.

Noda (1972) combined the results of earlier studies and suggested a relationship for movable bed models based on ratios of length, depth, sediment diameter, and specific weight. For similitude to occur, the following relationship must be satisfied:

$$\frac{n_l}{n_d} = (n_d)^{0.32} (n_\gamma)^{-0.386} \tag{3.1}$$

and

$$n_D = (n_\gamma)^{1.85} = (n_d)^{0.55} \tag{3.2}$$

- n_l = model length / prototype length
- n_d = model depth / prototype depth
- n_D = (sediment diameter) model / (sediment diameter) prototype
- n_γ = ratio of specific weight of sediment in model to prototype

Table 3.1 Parameters for Beach Profile Erosion

Source	Basic Relations	Method of Derivation
Goddet and Jaffry (1960)	$n_D = \mu^{\frac{17}{20}} \Omega^{\frac{8}{5}}$ $n_{\gamma'} = \mu^{\frac{3}{20}} \Omega^{-\frac{3}{5}}$	Sediment motion due to combined action of waves and current
Valembois (1960)	$\Omega = n_{\gamma'}^{-1}$ $n_{\gamma'} n_D^3 = 1$ $\mu = n_{\gamma'} n_D \left(\frac{n_H}{\mu}\right)^4$	Kinematics of motion of suspended sediments Similitude of D_* Modified relation of initiation of sediment motion: $D_* = KR_*^{8/9}$
Yalin (1963)	$n_D = \mu^{\frac{3}{4}} \lambda^{\frac{1}{2}}$ $n_{\gamma'} n_D^3 = 1$	Dimensional Analysis
Bijker (1967)	$n_{\gamma'} n_D \Omega^{-1} = \mu n_{\mu r}$ $\Omega \leftarrow$ equilibrium beach profile	Similitude of F_* This basic relationship is incorrect
Fan and LeMehaute (1969)	$n_{\gamma'} n_D^3 = 1$ $n_{\gamma'} = \mu^3 \lambda^{-\frac{3}{2}}$ or $n_D = \lambda^{\frac{1}{2}} \mu^{-1}$ $\Omega \leftarrow$ equilibrium beach profile	Similitude of sediment transport characteristics, i.e., F_* and R_*
Noda (1971)	$n_D n_{\gamma'}^{1.84} = \mu^{0.55}$ $\lambda = \mu^{1.32} n_{\gamma'}^{-0.386}$ $\Omega \leftarrow$ equilibrium beach profile	Similitude of sediment transport characteristics, i.e., F_* and R_*

Dean (1973) identified the importance of a dimensionless fall velocity parameter in evaluating the directional nature of sediment transport in beach profile modeling. The basis of his development revolves around the idea that suspended sediment from breaking wave action will flow either onshore or offshore depending on how fast the sediment falls compared to the wave period. If the sand falls relatively fast in comparison to the wave period, then the net transport is onshore. If the fall time is longer relative to the wave period, then the sediment is directed onshore. Expanding on Dean's concept, Dalrymple and Thompson (1976) conducted a series of laboratory tests evaluating this parameter on beach profile modeling. They confirmed that for similitude to occur:

$$n\left(\frac{H}{TW}\right) = 1 \tag{3.3}$$

- n = ratio of model to prototype
- H = wave height
- T = period
- W = fall velocity

Their findings suggest that this parameter is best suited for modeling beach profile response in the laboratory. Additional laboratory experiments conducted by Graff (1977) and Vellinga (1978) provided reasonable results when the fall velocity parameter was used for movable bed models.

From the various sources cited above, it would appear that the non-dimensional fall velocity criterion is well suited for modeling beach profile response and hence the overwash condition. Thus, for this experiment, the dimensionless fall velocity parameter will be adopted to represent the sediment transport processes.

Now that the Froude Number and the dimensionless fall velocity have been chosen for this experiment, similitude between model and prototype for these two parameters must be met. For

this to occur, both the model and the prototype values for each dimensionless parameter must be the same. For the Froude Number, Equation 3.4 must be satisfied at all times.

$$\frac{V_m}{\sqrt{g\,d_m}} = \frac{V_p}{\sqrt{g\,d_p}} \tag{3.4}$$

- V = velocity
- g = gravity
- d = depth

When Equation 3.4 is solved for a time relationship between the model and the prototype, it provides a geometric scale between the two.

$$\frac{\frac{L_m}{T_m}}{\sqrt{g\,L_m}} = \frac{\frac{L_p}{T_p}}{\sqrt{g\,L_p}} \tag{3.5}$$

$$\sqrt{g\,L_p}\cdot\frac{L_m}{T_m} = \sqrt{g\,L_m}\cdot\frac{L_p}{T_p} \tag{3.6}$$

$$(L_p)^{\frac{1}{2}}\cdot\frac{L_m}{T_m} = (L_m)^{\frac{1}{2}}\cdot\frac{L_p}{T_p} \tag{3.7}$$

$$\frac{T_m}{T_p} = \sqrt{\frac{L_m}{L_p}} \tag{3.8}$$

- L = length scale
- V = velocity scale
- T = time scale

From the basic relationship V= L/T, an equation relating velocity to the geometric scale between model and prototype is determined.

$$\frac{V_m}{V_p} = \sqrt{\frac{L_m}{L_p}} \tag{3.9}$$

Equation 3.8 will later be used in conjunction with the dimensionless fall velocity parameter. Before similitude can occur between model and prototype in regards to the dimensionless fall velocity parameter, values for the fall velocity have to be calculated for the model and prototype condition. Stokes derived a formula for calculating the fall velocity from the Navier-Stokes equation. He solved this equation by assuming a falling particle in water has two forces acting on it, i.e weight and the force of drag. Using this basis, there are three basic steps in solving the fall velocity. First, if the inertia and body forces terms are neglected, then the Navier-Stokes Equation in conjunction with continuity results in equation 3.10.

$$\nabla^2 p = 0 \tag{3.10}$$

Next, for steady state flow past a sphere, the boundary conditions utilized result in an equation for the force of drag on the particle (Equation 3.11).

$$F_D = 6\Pi R \mu U_\infty \tag{3.11}$$

Finally, equating the weight of the particle and the drag force and assuming a terminal velocity U_∞, so that $U_\infty = W$, results in equation 3.12.

$$F_D = W \tag{3.12}$$

Solving this equality, the fall velocity is defined as:

$$W = \frac{1}{18} \cdot \frac{D^2 g}{\nu} \cdot \left(\frac{\gamma_s - \gamma_f}{\gamma_f} \right) \tag{3.13}$$

- W = fall velocity
- D = diameter of sediment particle
- g = gravitational acceleration
- ν = kinematic viscosity of fluid
- γ_s = specific weight of sediment
- γ_f = specific weight of fluid

The following assumptions were made in the derivation of Stokes' Law:

1) Inertia forces are neglected (highly viscous flow)

2) Spherical grains were assumed

3) No slip between the fluid and the surface of the particle

4) The particle falls in an infinite and calm fluid

These assumptions limit the usefulness of the fall velocity equation. Since inertia forces are omitted, the equation will only predict the fall velocity correctly if the Reynold's Number, $R_e << 1$. Furthermore, most sand grains are not completely spherical. In addition, the last assumption is seldom found in real situations. Although Stokes' fall velocity equation does have limitations, for our purposes it gives a reasonable prediction of the fall velocity.

In order to solve the fall velocity equation, the sediment sizes for the prototype and model are required. The sand obtained for the model consisted of a mean diameter of 0.18 mm. A grain size distribution graph showing the median grain size for the model is seen in Figure 3.4. The prototype sediment size was 0.4 mm. This size was chosen because it is a typical size found in the field. In Leatherman (1979), the median grain size for Assateague Island, Maryland was approximately 0.3 mm and the median grain size for Nauset Spit, Massachusetts was approximately 0.4 mm. Applying these values to the fall velocity equation, the values for W_p and W_m are 0.51 ft/sec (0.16 m/sec) and 0.13 ft/sec (0.04 m/sec), respectively. For similitude

to occur between the fall velocities, the model value of the dimensionless fall velocity parameter must equal the prototype value. This relationship is seen in Equation 3.13.

$$\left(\frac{H}{TW}\right)_m = \left(\frac{H}{TW}\right)_p \tag{3.14}$$

Solving for W_m / W_p;

$$\frac{W_m}{W_p} = \frac{T_p}{T_m} \cdot \frac{H_m}{H_p} \tag{3.15}$$

Substituting in Equation 3.8 and replacing H and T with their equivalent length scale (according to Froude Similitude).

$$\frac{0.13}{0.51} = \frac{L_m}{L_p} \cdot \sqrt{\frac{L_p}{L_m}} \tag{3.16}$$

Gives the following result:

$$\frac{L_m}{L_p} = \frac{1}{16} \tag{3.17}$$

For this experiment, the geometric scale will be 1:16. From equation 3.8, the time relationship between model and prototype is therefore 1:4.

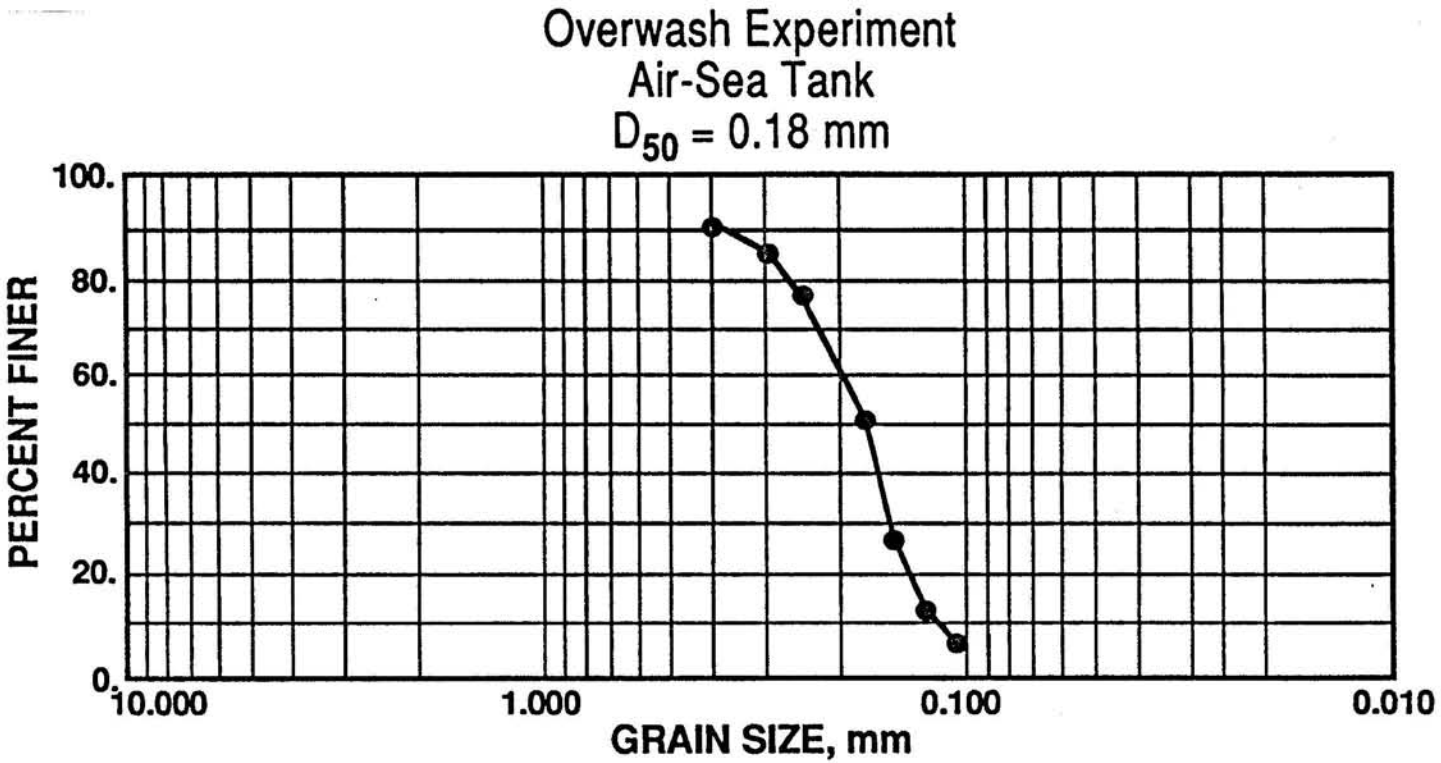

Figure 3.4 The Grain Size Distribution of Sand Utilized in the Model Barrier Island

CHAPTER 4
EXPERIMENTAL APPARATUS, PROCEDURE AND CONDITIONS

4.1 Introduction

The primary objective of this laboratory experiment was to investigate the wave evolution and the wave induced currents produced by the overwash process. This chapter outlines the apparatus, procedure, and test conditions employed in obtaining this objective. Emphasis will be placed the data collection methods and experimental procedures utilized.

Experimental Apparatus

The laboratory experiments were conducted in the "Air-Sea" Tank situated in the Coastal and Oceanographic Engineering Laboratory at the University of Florida. The tank is 150 ft (46 m) long, 6 ft (1.8 m) wide, and 6.5 ft (2 m) high. It is partitioned by a 6.5 ft (2 m) wall into two sections of equal width. One wall of one section is paneled with glass, facilitating construction and visualization of the changing beach profile. A sand beach is placed with the toe of the beach 70.5 ft (21.5 m) from the wave generator. A 1:18 slope travels a distance of 34 ft (10 m) from the toe to the crest of the berm. The last 25 ft (7.6 m) consist of a horizontal beach from the berm to the retaining wall. A 3 ft (0.9 m) catch basin is beyond the retaining wall for the purpose of holding washover deposits. Schematic drawings of the tank, detailing the dimensions, beach profile, and catch basin are shown in Figure 4.1.

Wave motion is supplied to the tank by means of a wave paddle and hydraulic power unit located at one end of the tank. The paddle is approximately 5.5 ft (1.7 m) from the beginning

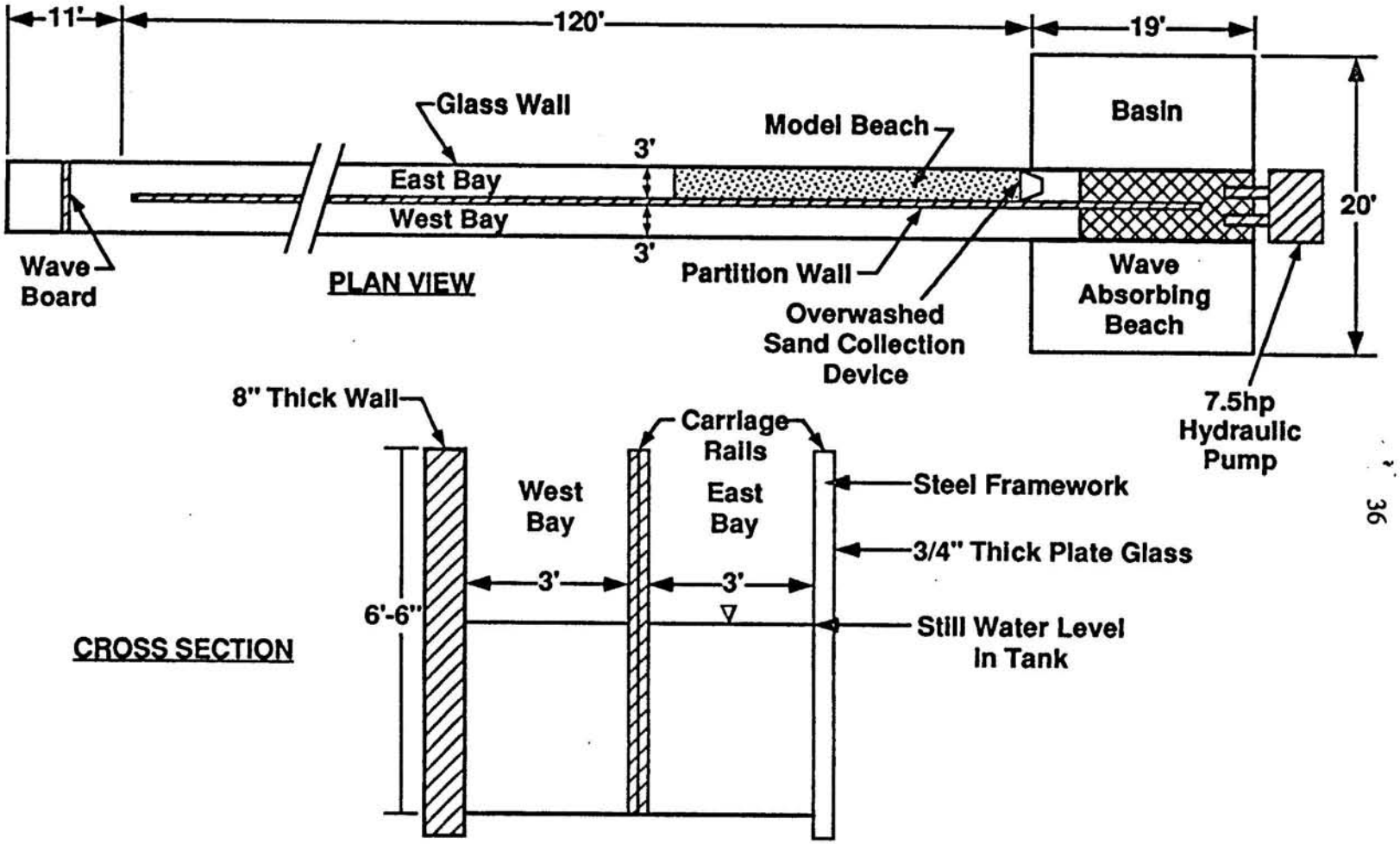

Figure 4.1 Schematic Drawings of the "Air-Sea" Tank Detailing the Location of the Equipment and Model Barrier Island Utilized in the Overwash Experiment

of the splitter wall which divides the tank. The wave paddle is constructed of wood and is driven by a two level rod and bearing system connected to the power unit. The paddle can either be operated in the flap or piston mode and produces regular or random waves. Wave signals for paddle operation are generated by a SeaSim Function generator and a Pegasus Servo Controller/Amplifier. To prevent cross tank wave action that might be generated by the wave paddle, wave screens were placed approximately at the start of the splitter wall. Additionally, horse hair and nylon bags filled with pebbles were placed behind the wave maker and beyond the catch basin to dampen any extemporaneous waves caused by reflection from the ends of the tank.

In several experiments, a water surface gradient was created over the island to test its effects on the overwash condition. This gradient was created by a 7.5 hp hydraulic pump situated at the downwave side of the tank. The pump intake was located behind the catch basin and discharged the water in the unused section of the tank. Variable flows were possible by adjusting the pump intake valve.

In Chapter 3, the beach profile geometry and sediment size were discussed. The beach profile was first laid out by drawing the profile on the glass panels. These outlines aided in construction of the profile. Afterwards, these marks were used as a reference point for future experiments. A scale representing the various water levels was placed on a glass panel located at the toe of the beach. This scale marked the mean sea levels and the overwash depths used in the experiment. In these sets of experiments, the prototype water depth at the toe of the beach was 24 feet (7 m) below the mean sea level. The crest of the berm was 6.3 feet (1.9 m) above this level.

As stated in the preceding chapter, the sediment size for the model was 0.18 mm. This sorted sand is found throughout the beach profile. To negate the compaction problems associated with the newly constructed profile, water was sprayed on the sand and compacted by hand. This

process was carried out before the start of each new test.

Data Acquisition Equipment

Studying the wave and current processes required equipment that would record these actions across the entire beach profile. The mobility of the equipment was paramount if wave and current profiles are to be modeled. A motorized trolley carriage was positioned atop the tank on a pair of rails.

A capacitance wave gauge was employed to measure the wave height and period. The wave gauge was positioned on the seaward side of the carriage. Incoming waves could be measured in deep water, the surf zone, and over the island, depending on the trolley position. The wave gauge was calibrated at the beginning of each test, eliminating error caused by changing water temperature, etc. Currents were measured by a electro-magnetic current meter mounted on the shoreward side of the carriage. This two channel current meter measured both "x" and "y" velocities, where the x direction is in the direction of wave propagation and the y direction is perpendicular to the wave direction. A capacitance sensing bottom profiler was also mounted on the trolley to measure the changing beach profile. As the carriage moves across the beach profile at a preset speed, the profiler's sensor follows the contours of the bed maintaining a gap of 0.2 cm between it and the bed.

Data Acquisition Program

Data signals acquired by the wave gauge, current meter, and bed profiler were converted and then stored by the data acquisition program GLOBAL LAB. For the wave gauge and current meter, GLOBAL LAB sampled the output from both the wave gauge and current meter at a rate of 10 MHz. The program then transformed this analog signal to a digital signal which was then transferred to the screen and the hard disk. The only modification needed for the program consisted of incorporating an amplifier to amplify the small signal generated by the current meter.

This amplifier enlarged the signal by a factor of ten. For the bed profiler, GLOBAL LAB converted the two signals generated into one combined signal. The horizontal signal from the instrument is based on the pulses created by equally spaced magnets mounted on one of the trolley's wheels. The vertical signal is based on the relationship between the position of the profiler arm as it moves across the profile and the number of turns on a potentiometer. Thus, the rate of data acquisition depends on the speed of the carriage and the rate of sampling by the data acquisition program. Finally, all data that were collected for each test were then downloaded from the hard disk to diskettes for future analysis.

4.2 Experimental Procedure

Each test that was carried out followed a detailed set of procedures. Initially, the bed was shaped into the beach geometry discussed earlier by means of a shovel, graders, and the human hand. Once completed, the sand was compacted by spraying water on it. The tank was then filled to the desired initial water level using a city water supply. This filling took approximately three hours to complete.

Before beginning a test, the bed profiler recorded the elevations across the entire profile length. Cross tank variations in the profile due to initial profile configurations and subsequent three dimensional effects (if any), were accounted for by recording profiles at three different locations. Location B1 was 10 inches (0.25 m) from the glass panel, B2 was 10 inches (0.25 m) from the splitter wall, and B3 coincided with the centerline of the profile.

The capacitance wave gauge was calibrated before the beginning of the test by moving the capacitance wire from its uppermost position to its lowest position through the still water level. The voltage from the gauge was recording at the corresponding height. After converting the analog signal to a digital one, a least squares fit was applied. The result was a relationship

between measured water levels and their associated voltages recorded from the wave gauge. This relationship is later used to determine the calibration constant for converting wave height signals.

Test Procedure

Generating monochromatic waves required a series of procedures. First, the Pegasus servo-controller and accompanying amplifier were turned on. The Seasim signal generator was switched on and the preprogrammed code for desired period waves was entered. The hydraulic motor was started and after a brief warm up time, the servo valves were opened. The generated pressure was increased to 1700 lb/ft (2322 N/m). Gain and amplitude buttons were rotated slowly until the correct deep water wave height was obtained (approximately) using a fixed measuring tape located on the deep water end of the tank.

If a test was to include the effects of a water surface gradient, the hydraulic pump was first primed with water. Once the wave maker was activated, the intake valve on the pump was turned slowly at the same time the start button was depressed. Once the pump started, the desired flow rate was adjusted by rotating the intake value.

Each test ran for 18 hours prototype time. This time was selected because: 1) typically, storms do not last longer than one day; 2) a quasi-equilibrium can be attained for the beach profile in this period of time. Based on similarity criteria for the time relationship, 18 hours prototype time corresponds to 4.5 hours model time. To analyze the rapid changes that occur in the profile, the bed profiler recorded the profile every 2 hours prototype time (30 minutes model time). During several 2 hour time intervals, both current and wave measurements were taken . The location of these measurements were as follows: 1) Deep water, beyond the toe of the profile, 2) On the beach profile, before wave breaking, 3) the break point, 4) after breaking, and 5) over the island. The sampling duration for each piece of equipment was 16 minutes prototype time. With the completion of the 2 hour interval, the bed profile was taken and the

whole process repeated. When the 18 hours were finished, bed observations were recorded and an estimate of the sediment volume in the catch basin noted. After completion of the trial, the bed was remolded to its initial planar form in preparation for the next test.

4.3 Test Condition

Wave height, wave period, and overwash depth have varying effects on the overwash process. As mentioned earlier, wave height and wave period tend to alter the volume of sand transported onshore or offshore. The overwash depth is important in that it is a critical factor in determining the sand volumes transported over the island. Therefore, adjusting all of these parameters more or less will influence the magnitude of overwashing.

Choosing the optimal values for each of the three parameters is based on typical overwash conditions apparent in field studies. For this experiment, 7.0 and 8.5 foot (2.1 and 2.6 m) monochromatic waves represent average prototype wave heights seen in storms where overwash is apparent. Wave periods vary between storms. During severe storms, periods of 6 to 10 seconds are not uncommon. In many instances, storms consist of a variety of wave periods, some long, some short. In this experiment, 8 and 10 second period waves were chosen as an average prototype period. Aside from adjusting the wave height and period, an appropriate value for the overwash depth needed to be determined. Previously, the dependence of the overwash depth on the storm surge was discussed. Hence, the greater the storm surge, the greater the overwash depth. In severe storms, the surge may create an overwash depth that completely inundates the island. The severity of this case enables one to see the impact that overwashing has across the entire island. For these sets of experiments, two depths were chosen that would completely inundate the island to various degrees. Thus, prototype overwash depths of +10.0 feet (3.0 m) above mean sea level (still water level in wave flume) and +11.5 feet

(3.5 m) above mean sea level were selected. These conditions correspond to water depths over the berm of +3.7 feet (1.1 m) and +5.2 feet (1.6 m) respectively.

Taking into consideration the various combinations between the three parameters, eight trials are listed in Table 4.1 in order of increasing overwash depth.

Table 4.1: Prototype Conditions for the Overwash Trials.

Trial Number	Overwash Depth (Ft)	Wave Height (Ft)	Wave Period (Sec)
1	+10.0	7.0	8.0
2	+10.0	7.0	10.0
3	+10.0	8.5	8.0
4	+10.0	8.5	10.0
5	+11.5	7.0	8.0
6	+11.5	7.0	10.0
7	+11.5	8.5	8.0
8	+11.5	8.5	10.0

In addition to the eight experiments completed above, four additional experiments were undertaken to include the effects of a water surface gradient formed by storm flood tides. The magnitude of the gradient will depend on the pump speed, which was alternated between full and half speed. To single out the effects of the gradient, wave height and period were kept at 8.5 ft and 8.0 sec, respectively. Only the overwash depth changed since depth changes are assumed most closely linked to the impact the water surface gradient has to the overwash process. The four trials are listed in Table 4.2.

Table 4.2: Prototype Conditions for the Overwash Trials with Superimposed Water Surface Gradient.

Trial Number	Overwash Depth (Ft)	Wave Height (Ft)	Wave Period (Sec)	Pump Speed
9	+10.0	8.5	8.0	Full
10	+10.0	8.5	8.0	Half
11	+11.5	8.5	8.0	Full
12	+11.5	8.5	8.0	Half

CHAPTER 5
ANALYSIS AND RESULTS

5.1 Test Results

In this section, the test results from the laboratory experiment are presented. The data obtained from the laboratory experiment will focus on the wave height evolution, mean current distribution, and the beach profile changes associated with the overwashing of the island. Actual measurements of wave height, mean current, and bed changes will be analyzed for the twelve trials completed. Pertinent features and characteristics of each of these measurements will be addressed and a comparison of these features with those of the non-overwashing cases will be discussed.

Wave Height Measurements

During overwashing, the magnitude of the wave height can influence the amount and direction of sediment transported. Thus, a record of wave height transformation across the surf zone was needed to examine its effects on wave-induced currents and sand volumes. For each trial, wave height measurements were made at five locations or more (except for trials 1 and 2). Although the five locations were not exactly the same for each trial, the measurements were taken in the following five general areas: 1) Deep Water; 2) Before Breakpoint; 3) Breakpoint; 4) Surf Zone; 5) Over island. At each location, the wave gauge measured the incoming waves for a period of 4 minutes model time. Once the sampling was completed, the voltage signal was converted to elevations using the calibration coefficient determined at the beginning of each trial. The result was a wave record for each location in model units. A sample of a wave record

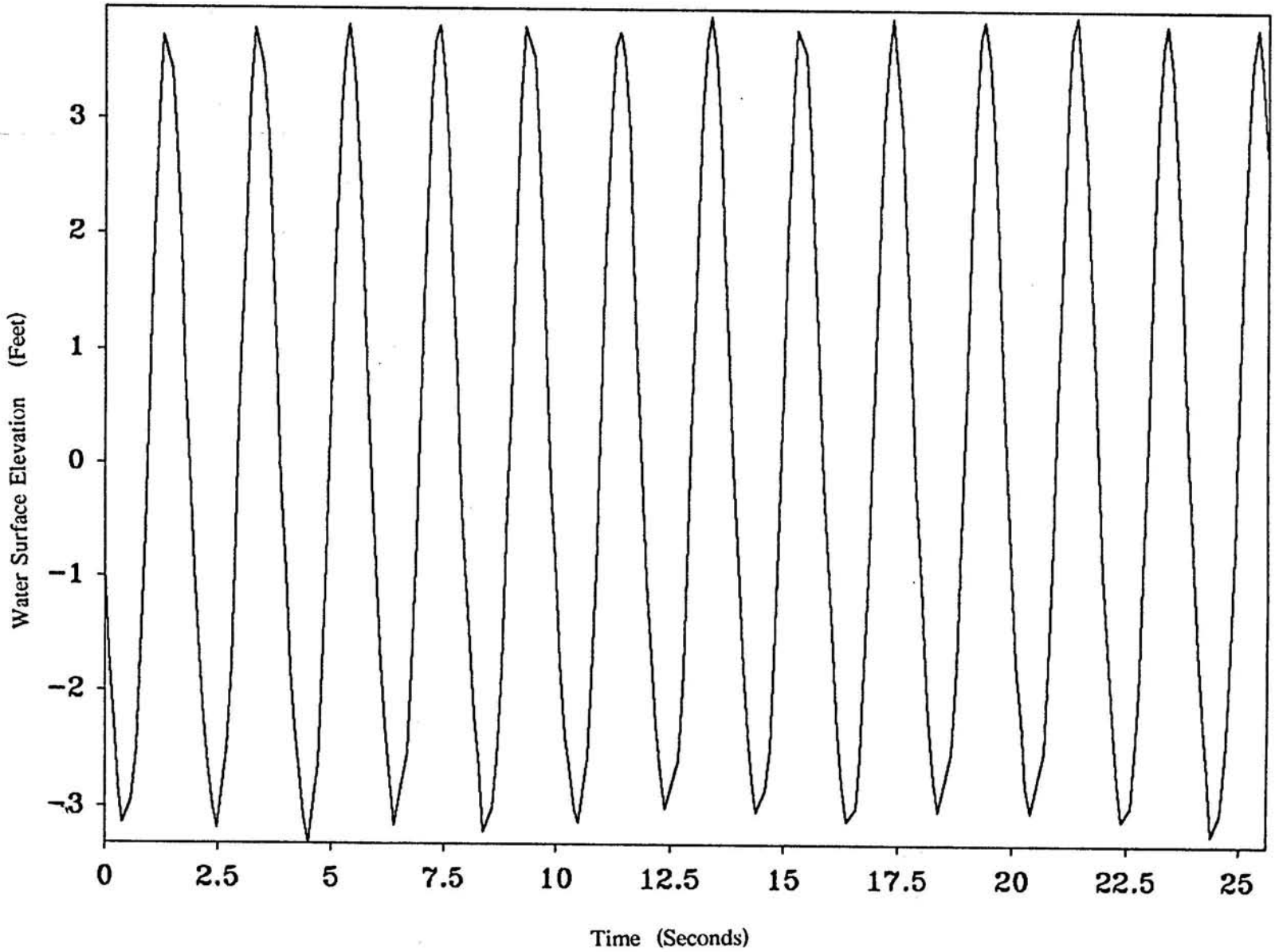

Figure 5.1 A Sample Deep Water Wave Record (Trial 1) Measured by the Wave Gauge

computed using the results for the deep water case of Trial 1 can be seen in Figure 5.1.

Once the wave record had been established, the units for each were changed to prototype conditions. A FORTRAN program was then written to compute the wave heights for each wave record. The program calculated both minimum and maximum wave heights for each wave record to account for wave reflection in the tank. The minimum and maximum of the wave record were averaged together to produce one single wave height. This procedure was done for all locations with the exception of those wave heights over the island. In this instance, the minimum wave height was typically spurious due to breaking-induced surface fluctuations, thus it was discounted and only the maximum value was used. The wave height results for each test are listed in the following tables. In order to keep the characteristics of each trial in proper perspective, the following notation will be utilized when trials are referred to by number. (+10.0, 7.0, 8.0) refers to the trial that has the following conditions: +10.0 Ft Overwash depth, 7.0 ft design deep water wave height, and a 8.0 second wave period.

Table 5.1: Trial 1 Wave Height Measurements for the Following Conditions: +10.0 Ft Overwash Depth, 7.0 Ft Design Deep Water Wave Height and 8.0 Second Monochromatic Wave Period.

Category	Location (Ft)	Wave Height (Ft)
Deep Water	1040	7.03
Before Breaking	672	8.59
After Breaking	548.8	6.65
Over Island	320	1.97

Table 5.2: Trial 2 Wave Height Measurements for the Following Conditions: +10.0 Ft Overwash Depth, 7.0 Ft Design Deep Water Wave Height and 10.0 Second Monochromatic Wave Period.

Category	Location (Ft)	Wave Height (Ft)
Deep Water	1024	5.90
Before Breaking	656	8.34
Break Point	600	9.77
After Breaking	512	2.25

Table 5.3: Trial 3 Wave Height Measurements for the Following Conditions: +10.0 Ft Overwash Depth, 8.5 Ft Design Deep Water Wave Height and 8.0 Second Monochromatic Wave Period.

Category	Location (Ft)	Wave Height (Ft)
Deep Water	1024	7.78
Break Point	672	10.13
After Breaking	576	6.53
Surf Zone	464	4.86
Over Island	360	2.29
Over Island	176	2.01

Table 5.4: Trial 4 Wave Height Measurements for the Following Conditions: +10.0 Ft Overwash Depth, 8.5 Ft Design Deep Water Wave Height, and 10.0 Second Monochromatic Wave Period.

Category	Location (Ft)	Wave Height (Ft)
Deep Water	1024	7.27
Break Point	624	10.67
After Breaking	528	4.97
Surf Zone	464	4.05
Over Island	368	1.54
Over Island	240	2.41

Table 5.5: Trial 5 Wave Height Measurements for the Following Conditions: +11.5 Ft Overwash Depth, 7.0 Ft Design Deep Water Wave Height, and 8.0 Second Monochromatic Wave Period.

Category	Location (Ft)	Wave Height (Ft)
Deep Water	1024	6.98
Before Breaking	736	7.75
Break Point	592	9.85
Surf Zone	464	6.61
Over Island	352	3.43
Over Island	272	2.02

Table 5.6: Trial 6 Wave Height Measurements for the Following Conditions: +11.5 Ft Overwash Depth, 7.0 Ft Design Deep Water Wave Height, and 10.0 Second Monochromatic Wave Period.

Category	Location (Ft)	Wave Height (Ft)
Deep Water	1024	5.88
Break Point	624	7.92
After Breaking	512	7.21
Surf Zone	416	4.51
Over Island	320	3.18
Over Island	176	2.77

Table 5.7: Trial 7 Wave Height Measurements for the Following Conditions: +11.5 Ft Overwash Depth, 8.5 Ft Design Deep Water Wave Height, and 8.0 Second Monochromatic Wave Period.

Category	Location (Ft)	Wave Height (Ft)
Deep Water	1024	8.66
Before Breaking	736	8.60
Break Point	648	10.34
After Breaking	520	8.32
Surf Zone	456	7.63
Over Island	352	3.68
Over Island	208	4.29

Table 5.8: Trial 8 Wave Height Measurements for the Following Conditions: +11.5 Ft Overwash Depth, 8.5 Ft Design Deep Water Wave Height, and 10.0 Second Monochromatic Wave Period.

Category	Location (Ft)	Wave Height (Ft)
Deep Water	1024	7.16
Break Point	688	10.32
After Breaking	592	10.22
Surf Zone	496	5.02
Surf Zone	416	3.96
Over Island	336	1.89

The wave height measurements provide an opportunity to examine how certain parameters of the overwash condition alter the wave transformation across the surf zone. For instance, the larger overwash depth, in combination with the period, can affect the location of the break point. Comparing cases with similar shorter periods and wave heights, the break point in cases of lower overwash depth and smaller periods tends to be farther offshore compared to its larger overwash cases. This is evident when comparing trials 1 (+10.0, 7.0, 8.0) and 5 (+11.5, 7.0, 8.0) and trials 3 (+10, 8.5, 8.0) and 7 (+11.5, 8.5, 8.0). However, this situation does not hold true when the period is increased. Comparison between trials 2 (+10, 7.0, 10) and 6 (+11.5, 7.0, 10) and trials 4 (+10, 8.5 ,10) and 8 (+11.5, 8.5, 10) show the opposite to happen. In this instance, the waves in larger overwash cases break farther offshore compared to the lower overwash condition. Wave period then can be considered an important factor in determining the location of the break point. If all these cases are compared to the non-overwashing case seen in Figure 5.2, it is apparent that overwashing will move the break point (evidenced by the bar location) shoreward regardless of the period or the depth of overwashing.

Besides altering the location of the break point, the wave height data collected gives credibility to observations that overwashing affects the wave decay across the surf zone. In cases without overwashing, wave heights decay rapidly across the surf zone until the wave energy is

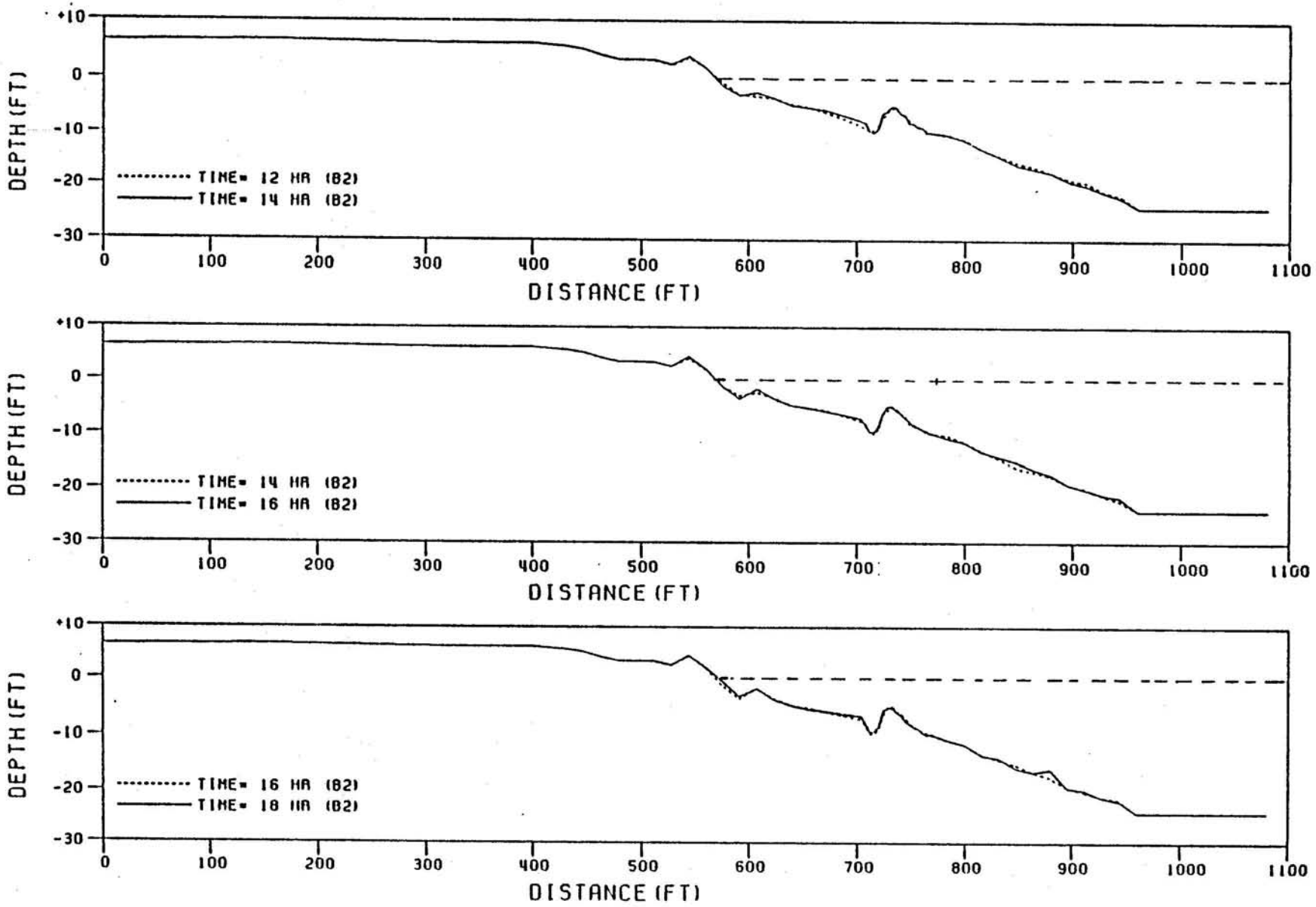

Figure 5.2 Sample Non-Overwashing Beach Profiles Showing the Location of the Breakpoint Bar (Parchure, Dean, and Srinivas, 1991)

finally dissipated. Since there is no "swash" when the island is completely inundated, wave height decay continues across the island and into the bay. In the eight trials, the rate of decay varies between the trials. In cases of the +10.0 Ft above MSL overwash depths, the wave heights decayed more rapidly after breaking compared to higher overwashing cases. However, after a certain distance over the island, the decay rate for both overwash depths were consistent.

Wave-Induced Currents

Although wave height measurements are important in the overwash process, it is the currents created by the waves that are especially significant in sediment transport. Depending on the strength of these currents, sand can either be transported over the island or taken offshore. If anything was to be learned about sediment transport during overwashing, measurements were needed to record the strength and direction of these currents. In this experiment, the wave-induced currents were measured at five or more locations across the beach profile and the island. Since the currents were measured at the same time as the wave heights, the five locations approximately correspond to those areas mentioned previously. The measurements do not completely correspond due to the 3 foot model (48 foot prototype) difference in mounting the current meter and the wave gauge. In addition to taking readings at various locations, some trials include current measurements taken at various heights at a given location. The current readings for each of the six trials are listed in Tables 5.9 to 5.15. It should be noted that each current reading is the mean value of the current record minus the offset value of the current meter. A failure with the current meter prevented measurements from being taken for trial 6 (+11.5, 7.0, 10) and only partial readings were recorded for trial 2 (+10, 7.0, 10). Beside each current reading listed below is the depth at which the reading was recorded. These depths are measured from the mean sea level. It should also be noted that a negative sign indicates the velocity is directed seaward; a positive sign indicates shoreward flow.

Some interesting trends arise when the data are non-dimensionalized and plotted as seen in Figures 5.3 and 5.4. The first trend evident is that all the trials exhibit similar flow patterns. Although each current measurement was taken at approximately mid-depth, it would be highly probable if variations in flow patterns existed due to changing conditions. Because this is not the case, it would appear that irrespective of the wave conditions, flow patterns remain the same. The plots, however, show that when the overwash depth is lower, there seems to be a

Table 5.9: Trial 1 Current Measurements for the following conditions: +10.0 Ft Overwash Depth, 7.0 Ft Design Deep Water Wave Height, and 8.0 Second Monochromatic Wave Period.

Category	Location (Ft)	Current (Ft/Sec)	$Y_{measured}$ Depth (Ft)
Deep Water	992	-0.172	15.80
Near Breaking	624	-0.446	11.47
After Breaking	500.8	-0.180	6.61
After Breaking	500.8	-0.320	3.93
Over Island	272	1.06	2.78
Over Island	272	1.17	1.21

Table 5.10: Trial 2 Current Measurements for the Following Conditions: +11.5 Ft Overwash Depth, 7.0 Ft Design Deep Water Wave Height, and 10.0 Second Monochromatic Wave Period.

Category	Location (Ft)	Current (Ft/Sec)	$Y_{measured}$ Depth (Ft)
Deep Water	976	0.032	19.47
Before Breaking	768	-0.192	19.47
Before Breaking	608	-0.540	11.6
After Breaking	552	-0.601	12.54
After Breaking	464	-0.359	5.04

* Note: This data set is not complete due to failure of current meter

Table 5.11: Trial 3 Current Measurements for the Following Conditions: +10.0 Ft Overwash Depth, 8.5 Ft Design Deep Water Wave Height, and 8.0 Second Monochromatic Wave Period.

Category	Location (Ft)	Current (Ft/Sec)	$Y_{measured}$ Depth (Ft)
Deep Water	976	-0.423	18.95
Before Breaking	784	-0.308	18.95
After Breaking	624	-1.35	9.50
After Breaking	528	-1.00	7.40
Surf Zone	416	0.074	3.83
Surf Zone	416	0.220	2.15
Over Island	312	0.538	2.41
Over Island	128	0.540	2.15

Table 5.12: Trial 4 Current Measurement for the Following Conditions: +10.0 Ft Overwash Depth, 8.5 Ft Design Deep Water Wave Height, and 10.0 Second Monochromatic Wave Period.

Category	Location (Ft)	Current (Ft/Sec)	$Y_{measured}$ Depth (Ft)
Deep Water	976	-0.632	19.47
Before Breaking	784	-0.568	19.47
After Breaking	576	-1.89	9.50
After Breaking	480	-0.656	6.09
Surf Zone	416	-0.398	3.99
Over Island	320	0.340	2.94
Over Island	192	0.684	2.68

Table 5.13: Trial 5 Current Measurements for the Following Conditions: +11.5 Overwash Depth, 7.0 Ft Design Deep Water Wave Heights, and 8.0 Second Monochromatic Wave Period.

Category	Location (Ft)	Current (Ft/Sec)	$Y_{measured}$ Depth (Ft)
Deep Water	976	0.596	15.80
Before Breaking	688	0.243	16.06
After Breaking	544	-0.587	10.55
Surf Zone	416	-0.525	4.25
Over Island	304	0.140	4.67
Over Island	304	0.600	1.89
Over Island	224	0.625	3.83

Table 5.14 Trial 7 Current Measurements for the Following Conditions: +11.5 Ft Overwash Depth, 8.5 Ft Design Deep Water Wave Height, and 8.0 Second Monochromatic Wave Period.

Category	Location (Ft)	Current (Ft/Sec)	$Y_{measured}$ Depth (Ft)
Deep Water	976	-0.428	13.70
Before Breaking	688	-0.522	16.06
After Breaking	600	-0.603	12.65
After Breaking	472	-0.298	8.19
After Breaking	472	0.031	3.99
Surf Zone	408	-0.710	5.67
Surf Zone	408	0.260	3.10
Over Island	304	0.305	3.86
Over Island	160	0.861	4.93

Table 5.15: Trial 8 Current Measurements for the Following Conditions: +11.5 Ft Overwash Depth, 8.5 Ft Design Deep Water Wave Height, and 10.0 Second Monochromatic Wave Period.

Category	Location (Ft)	Current (Ft/Sec)	$Y_{measured}$ Depth (Ft)
Deep Water	976	-0.125	21.0
Before Breaking	768	-0.218	21.0
After Breaking	640	-0.479	13.96
After Breaking	544	-0.698	10.55
Surf Zone	448	-0.528	5.30
Over Island	368	0.145	3.73
Over Island	368	0.508	1.63
Over Island	288	0.588	1.36

greater amount of return flow as seen by the greater negative velocities around the break point. Trials 3 (+10, 8.5, 8.0) and 4 (+10.0, 8.5, 10.0) show the greatest negative flows. This would suggest that the return flow is stronger in these two cases. Therefore, one would expect a larger amount of offshore sand transport associated with this flow.

Some of the salient differences between the trials are seen in Figures 5.5, 5.6 and 5.7. In Figure 5.5, there are few differences between trials 1 (+10, 7.0, 8.0) and 5 (+11.5, 7.0,

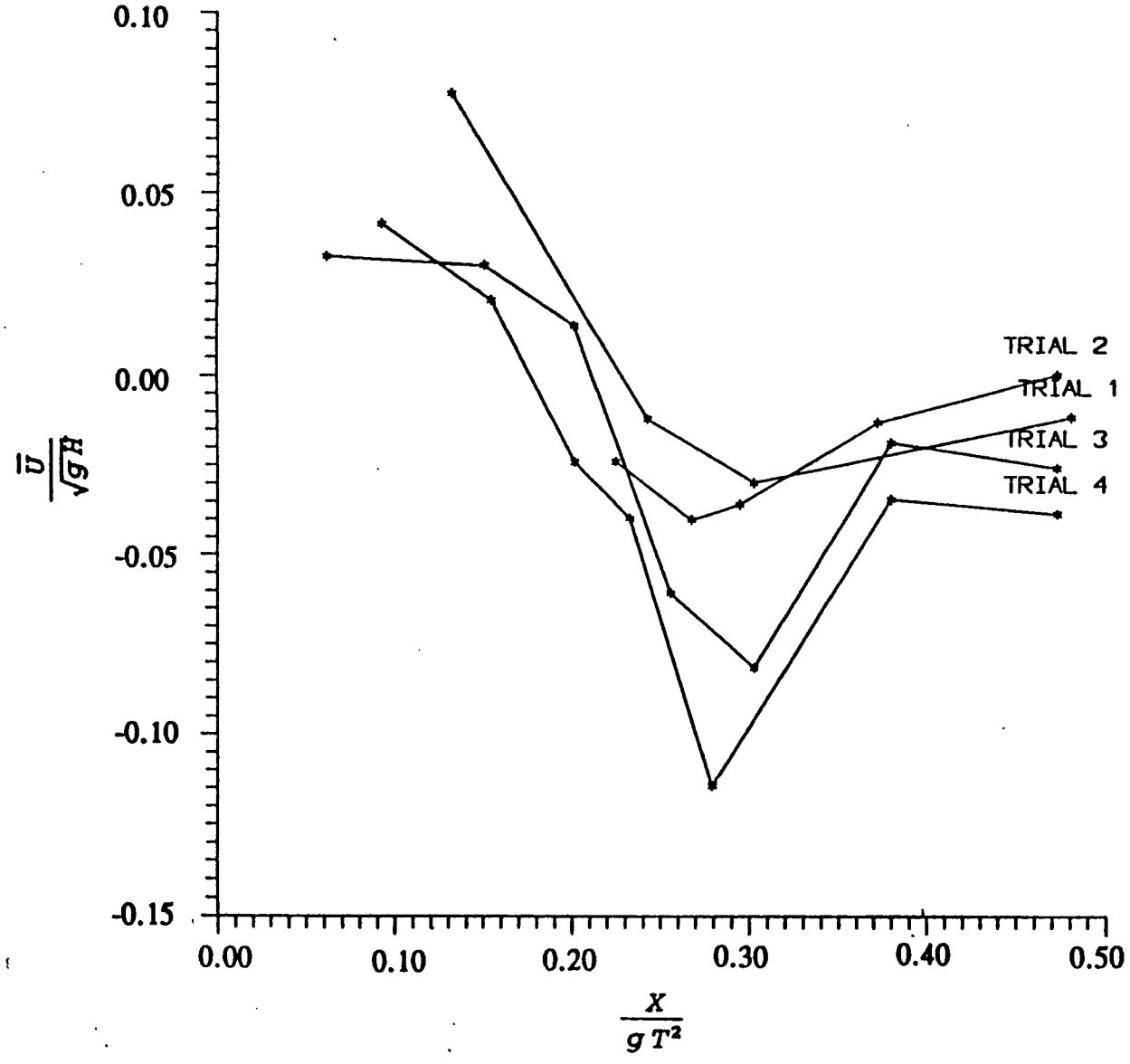

Figure 5.3 Distribution of Non-Dimensional Mean Cross-Shore Velocity for Trials 1-4 (+10.0 Ft Overwash Depth) (Measured at Mid-Depth)

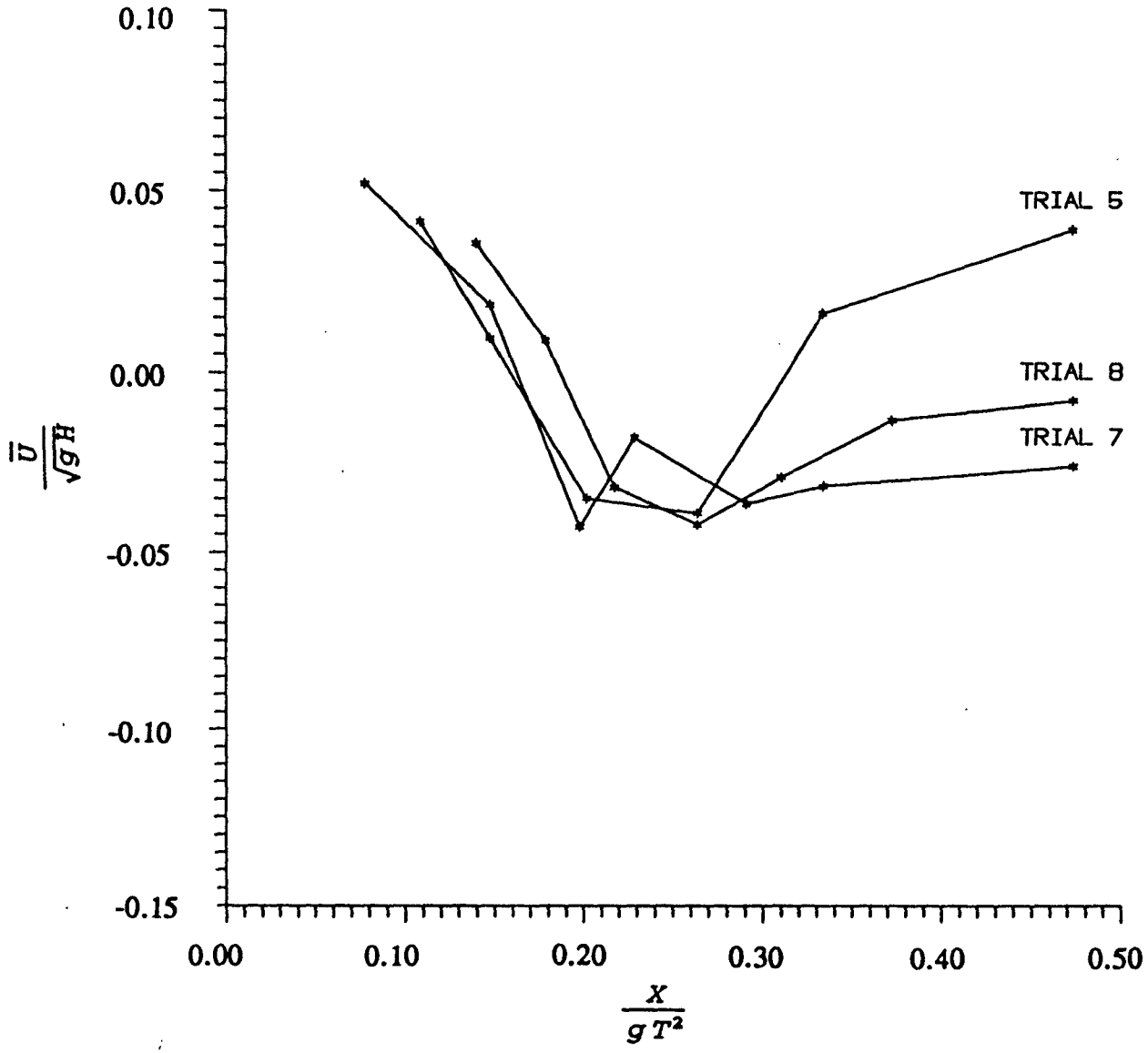

Figure 5.4 Distribution of Non-Dimensional Mean Cross-Shore Velocity for Trials 5, 7, and 8 (+11.5 Ft Overwash Depth) (Measured at Mid-Depth)

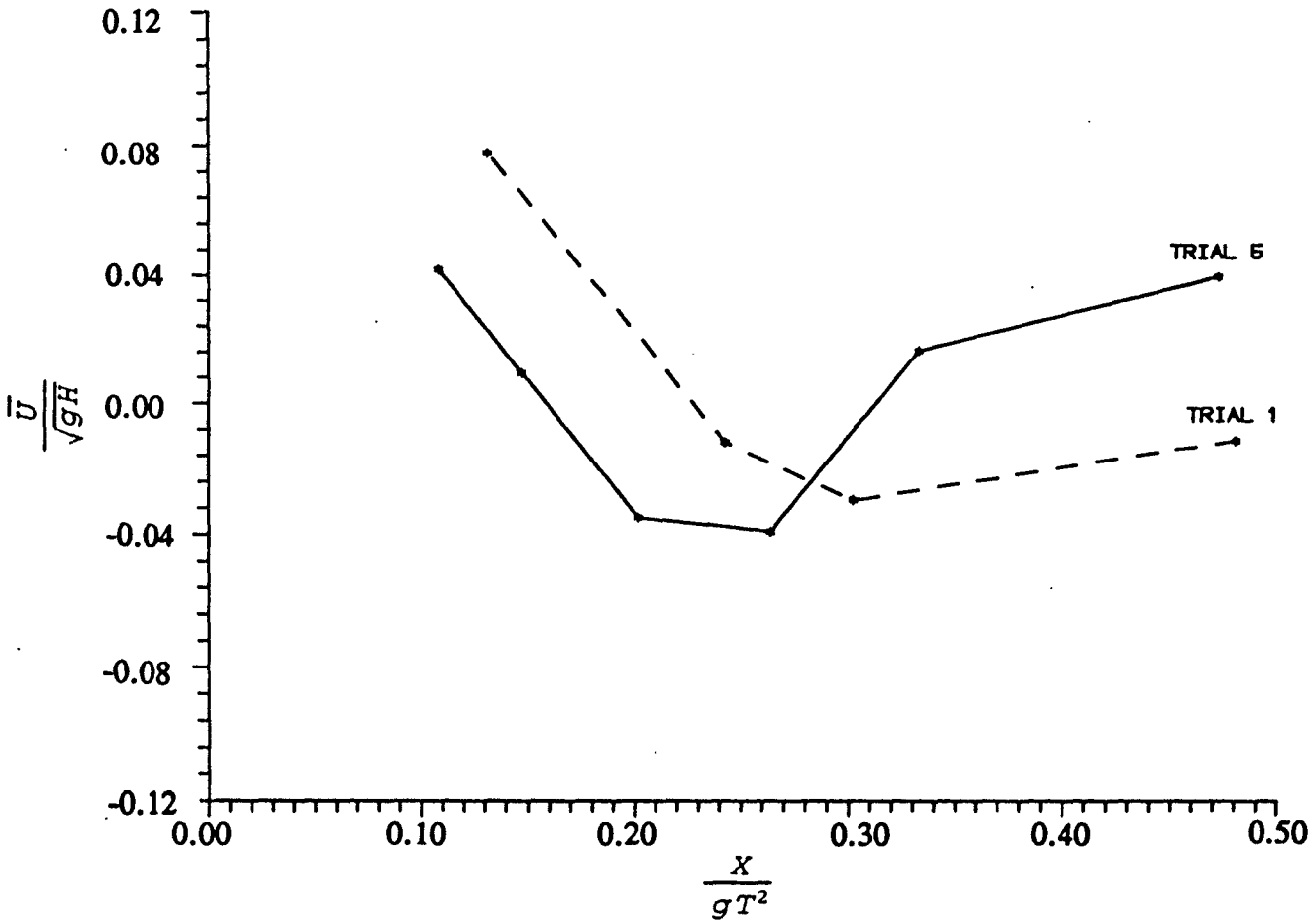

Figure 5.5 A Comparison of the Distribution of Non-Dimensional Mean Cross-Shore Velocity Between Trial 1 (+10, 7.0, 8.0) and Trial 5 (+11.5, 7.0, 8.0) (Measured at Mid-Depth)

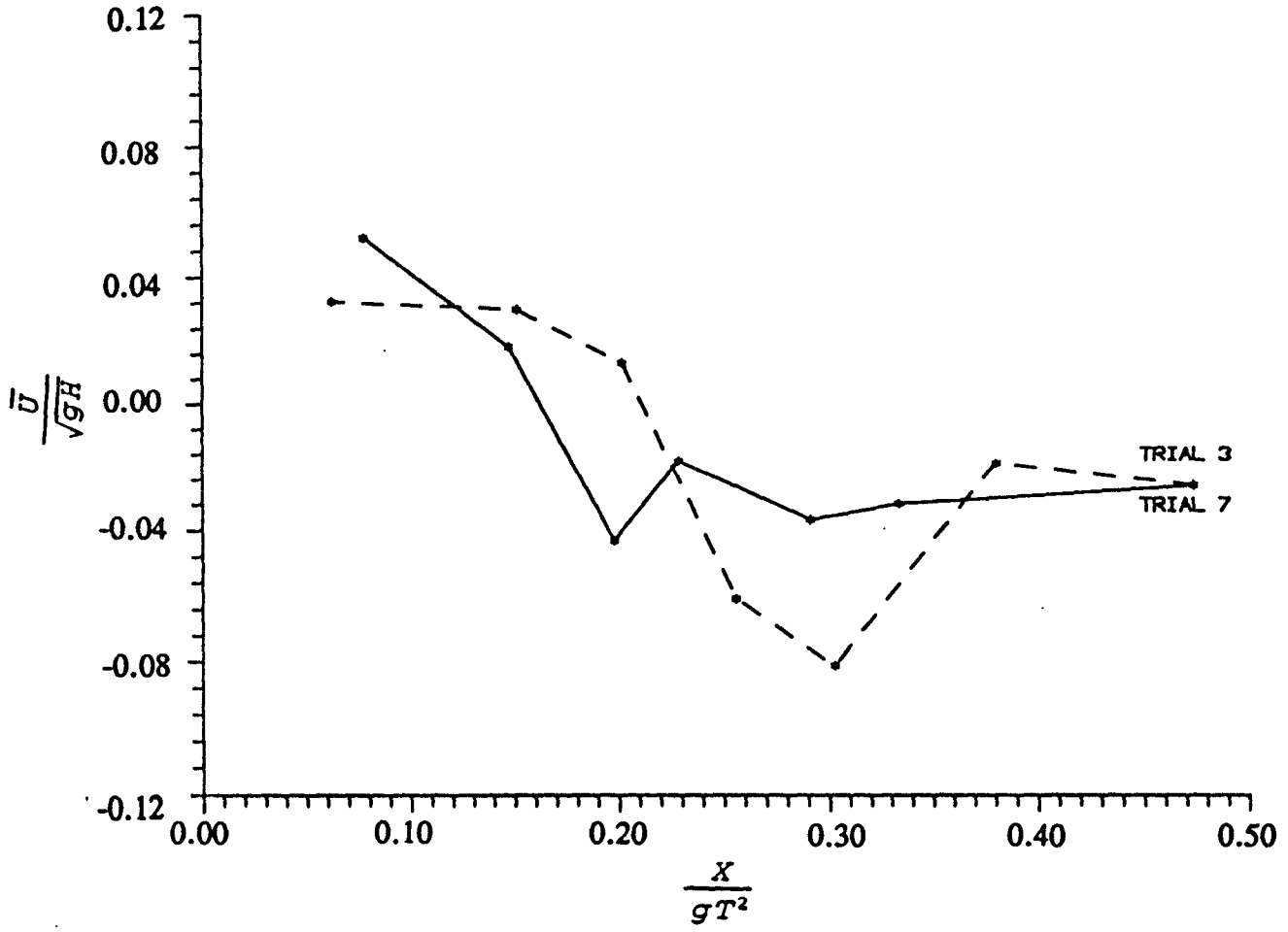

Figure 5.6 A Comparison of the Distribution of Non-Dimensional Mean Cross-Shore Velocity Between Trial 3 (+10, 8.5, 8.0) and Trial 7 (+11.5, 8.5, 8.0) (Measured at Mid-Depth)

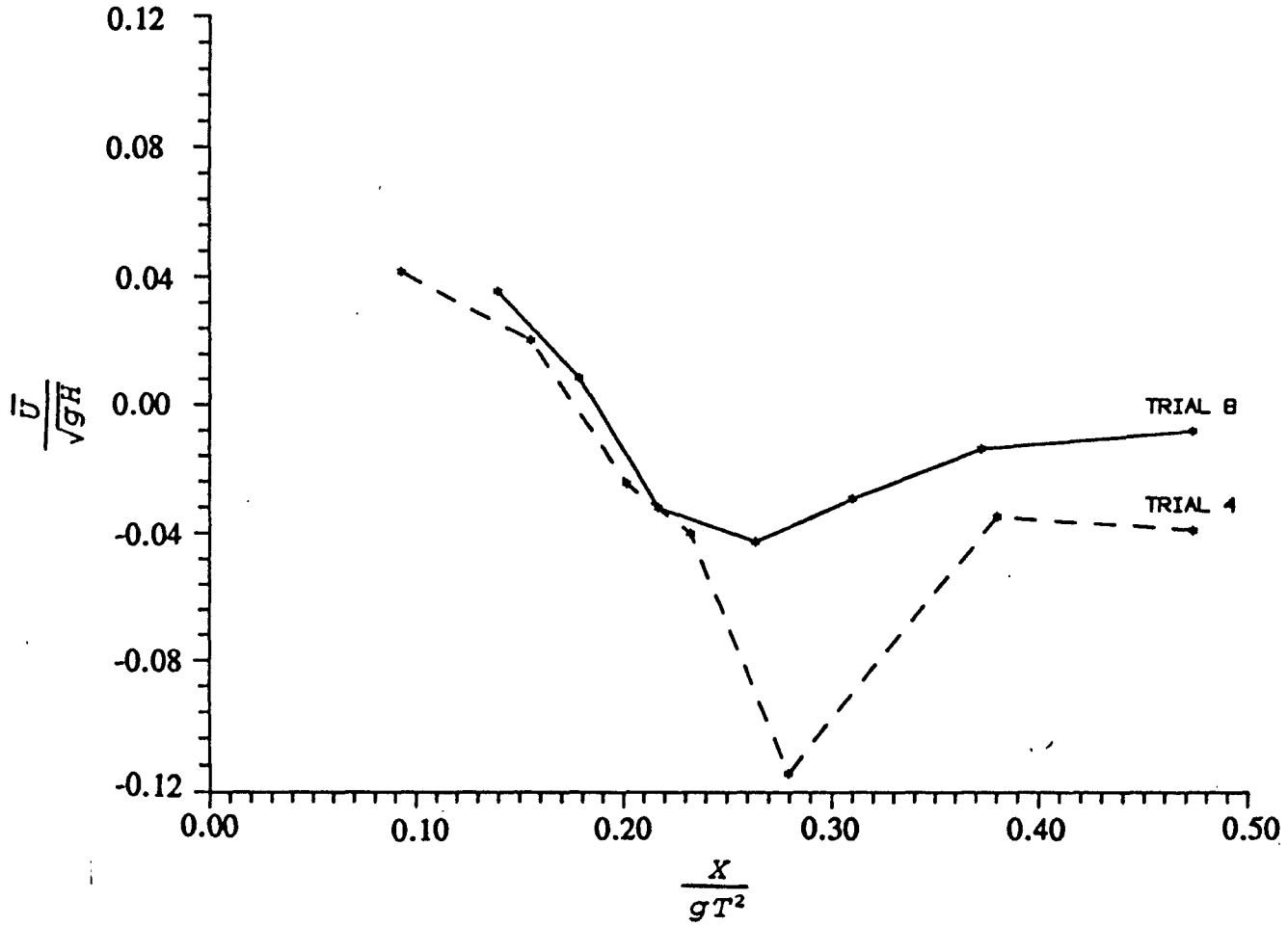

Figure 5.7 A Comparison of the Distribution of Non-Dimensional Mean Cross-Shore Velocity Between Trial 4 (+10, 8.5, 10) and Trial 8 (11.5, 8.5, 8.0) (Measured at Mid-Depth)

8.0). The shoreward movement of the largest negative velocity (ie. the breakpoint) in trial 5 is most likely due to the larger overwash depth. A comparison of trials 3 (+10, 8.5, 8.0) and trial 7 (+11.5, 8.5, 8.0) in Figure 5.6 displays more than overwash depth discrepancies. Trial 7 has an increase in velocity magnitude after the break point which is not evident in trial 3. The differences between trials 4 and 8 in Figure 5.7 is comparable to what is seen in trials 1 and 5 of Figure 5.5 in terms of a profile shift.

Examining the velocities over the island does not reveal clearly which overwash depth produces the fastest flows. It might seem logical to predict faster velocities with the higher overwash depth, an argument which is supported by the results of trials 3 (+10, 8.5, 8.0) and 7 (+11.5, 8.5, 8.0). In this case, the larger overwash depth of trial 7 produces the greater velocity over the island. But velocities over the island in trials 1 (+10, 7.0, 8.0) and 4 (+10, 8.5, 10) make this argument questionable. Comparing these two trials with their deeper overwash depth counterparts (Trials 5 and 8), trials 1 and 4 have the greater velocities. It is possible that the maximum velocities occur at some intermediate overwash depth and that the two overwash depths observed in this trial cannot reveal this. This is not the only anomaly in the velocities measured over the island. Although trial 1 (+10, 7.0, 8.0) has the greatest velocity, it is produced by a smaller wave height. This result is odd since larger wave heights tend to produce the greater velocities over the island.

Finally, there is some uncertainty in the deep water velocity direction for Trials 5 (+11.5, 7.0, 8.0) and 6 (+11.5, 7.0, 10). In deep water, there tends to be offshore flow in the lower part of the water column. This is evident in the remaining six trials. In trial 5, there is a large onshore directed velocity which would suggest that lower wave heights in combination with higher overwash depths produce little return flow and perhaps even layers of shoreward flow. The deep water velocity in trial 6 can support this explanation somewhat. The deep water

velocity is positive but very small. It is uncertain if another current reading would produce larger onshore velocities or that this value is due to fluctuations in velocity over the water column.

Beach Profile Response

The increased water level during the overwash process alters the quasi-equilibrium of the existing beach profile. In order to adjust to change, sediment will erode or accrete in certain areas. The location of erosion and deposition can relay information on the strength of wave-induced currents and flow rates over the island. In this experiment, beach profiles were measured every two hours prototype time. This time interval allowed visual observations of the sediment deposition and accretion. Figures 5.8 - 5.15 contain plots of the eight trials showing the initial and final profiles.

The degree of profile movement varied among the eight trials. In all instances, sand was moved offshore from the initial planar profile. The placement of this sand was spread throughout the profile. Except for trials 1 (+10, 7.0, 8.0), 5 (+11.5, 7.0, 8.0), and 7 (+11.5, 8.5, 8.0), bar formation near the break point was evident. In trial 1 (Figure 5.8), the profile did not dramatically change. Some sand was eroded shoreward of the break point and deposition occurred seaward of the break point and shoreward of the berm. Bar formation and erosion seaward of the break point characterized the bed profile of trial 2 (+10, 7.0 ,10) as shown in Figure 5.9. Trial 3 (+10, 8.5, 8.0) was typified by a large bar formation and severe erosion shoreward of the break point (Figure 5.10). It is apparent that this trial had the greatest bar formation. Trial 3 also had the one of the greatest return flow velocities near the break point (See figure 5.3). The results from this trial suggest that there is a correlation between the return flow and the creation of the bar. The large bar formation and the subsequent erosion seaward of the break point in Trial 4 (+10, 8.5, 10) (Figure 5.11) is similar to that of trial 2. But there is more deposition shoreward of the break point. The lack of a break point bar and severe erosion

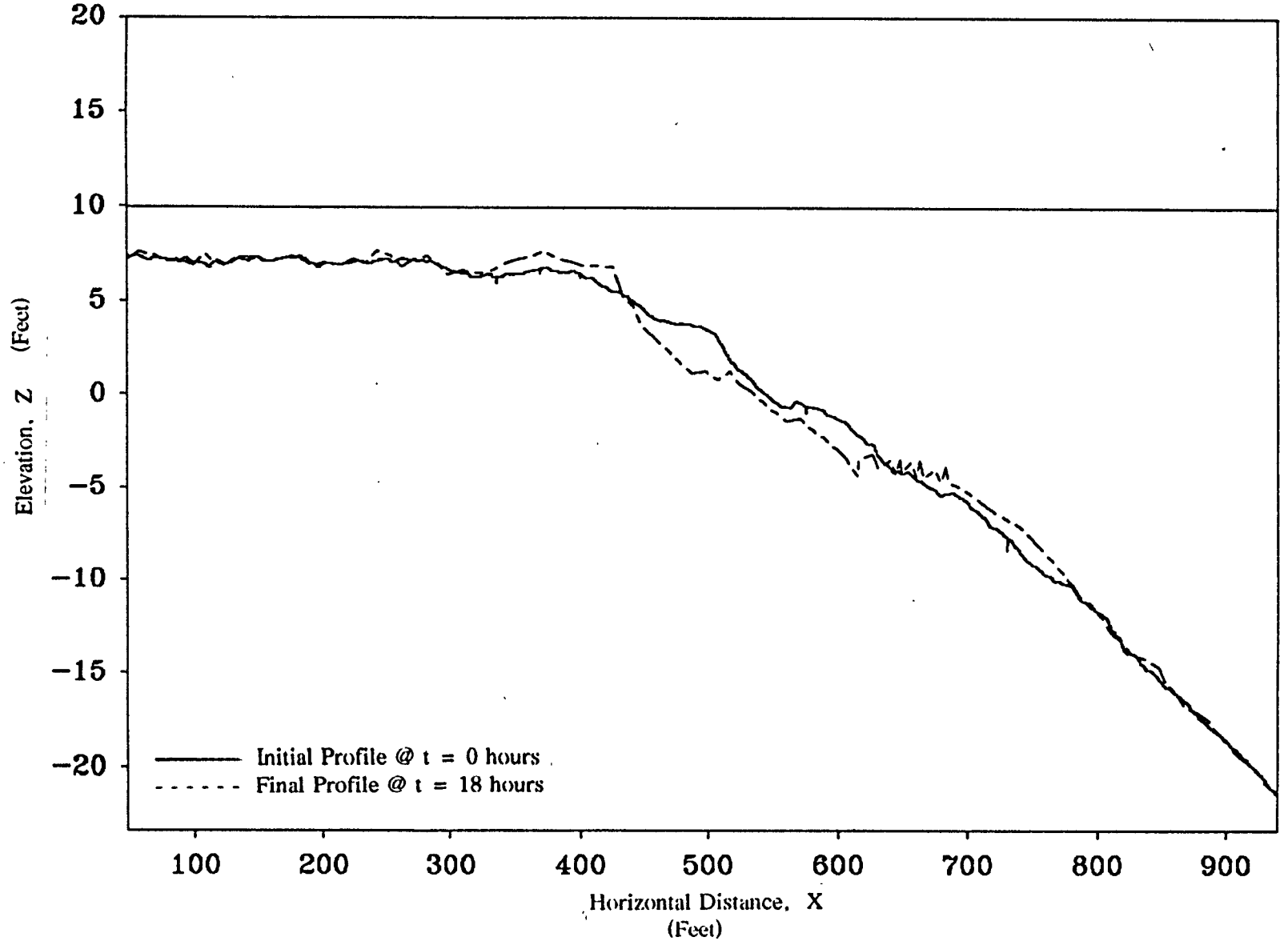

Figure 5.8 Measured Initial and Final Beach Profiles for Trial 1 (+10, 7.0, 8.0)

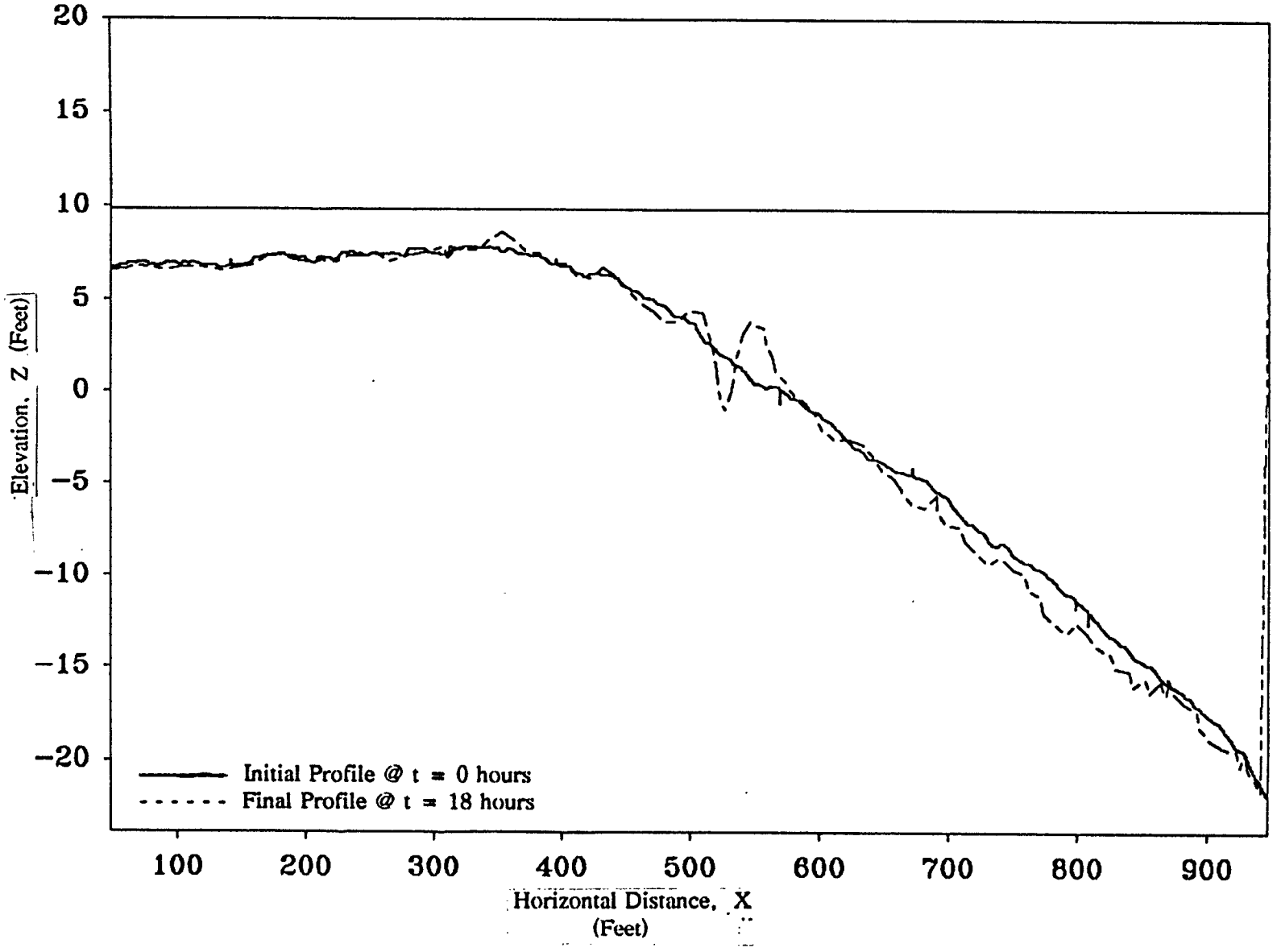

Figure 5.9 Measured Initial and Final Beach Profiles for Trial 2 (+10, 7.0, 10)

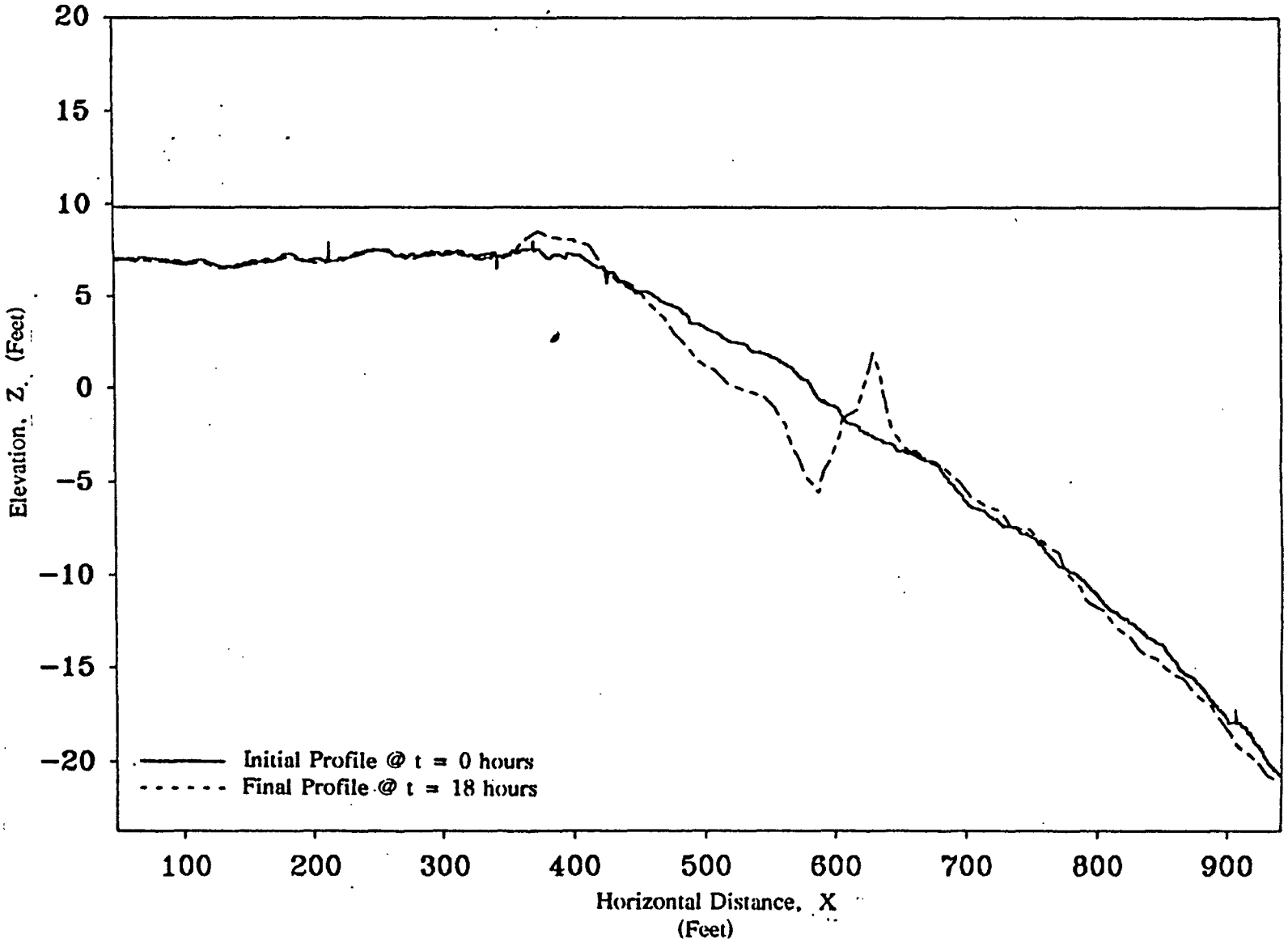

Figure 5.10 Measured Initial and Final Beach Profiles for Trial 3 (+10, 8.5, 8.0)

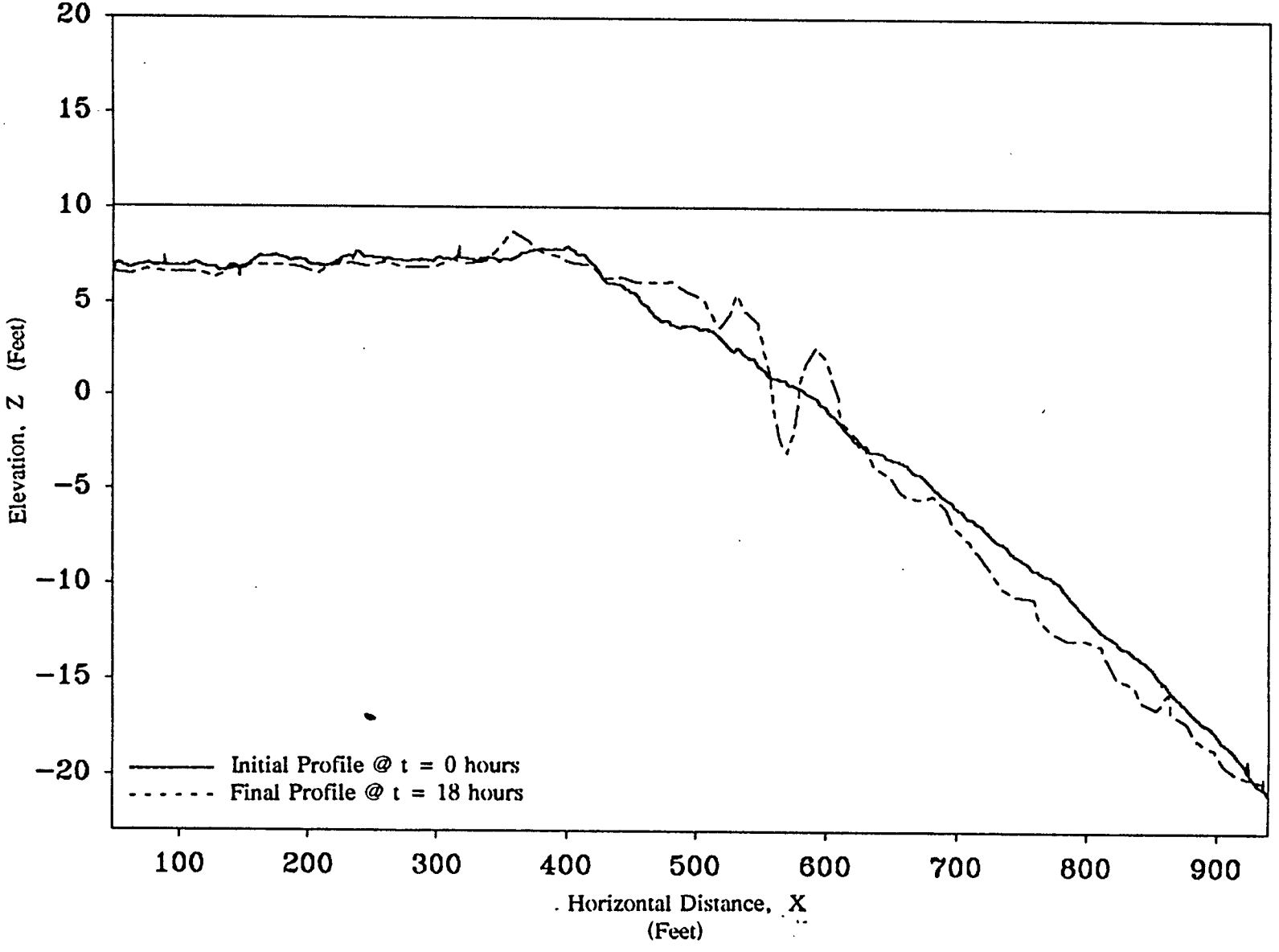

Figure 5.11 Measured Initial and Final Beach Profiles for Trial 4 (+10, 8.5, 10)

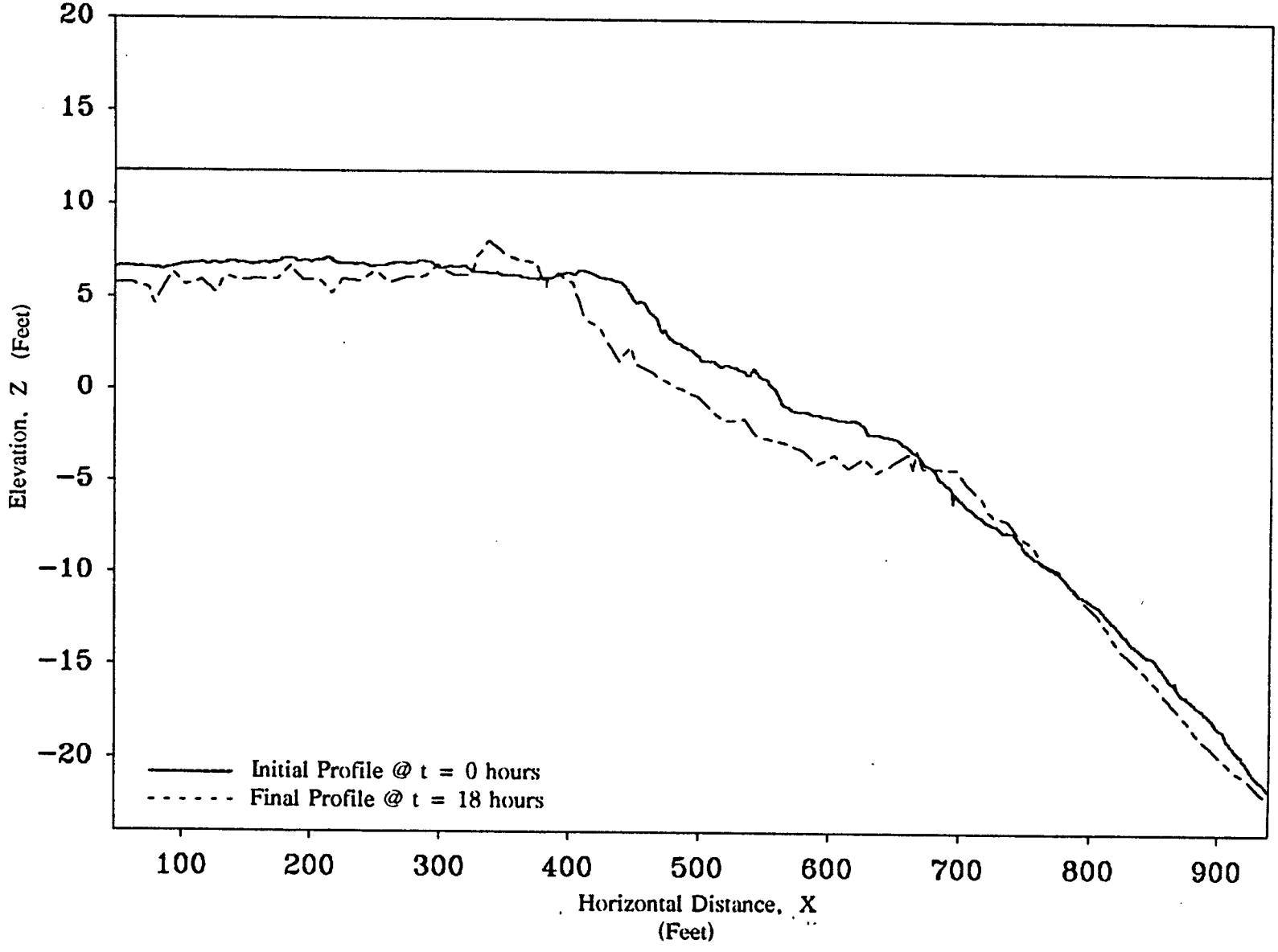

Figure 5.12 Measured Initial and Final Beach Profiles for Trial 5 (+11.5, 7.0, 8.0)

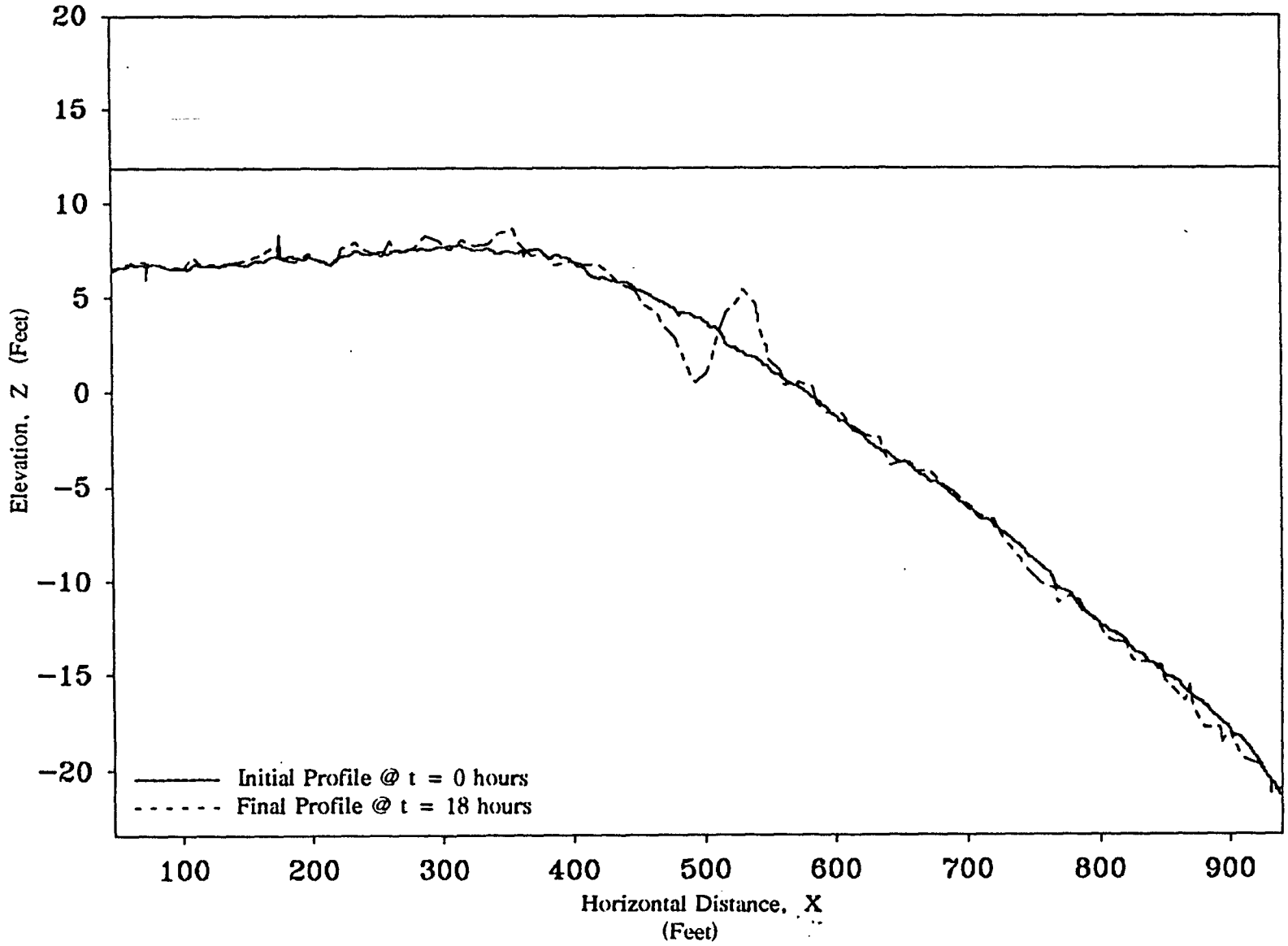

Figure 5.13 Measured Initial and Final Beach Profiles for Trial 6 (+11.5, 7.0, 10)

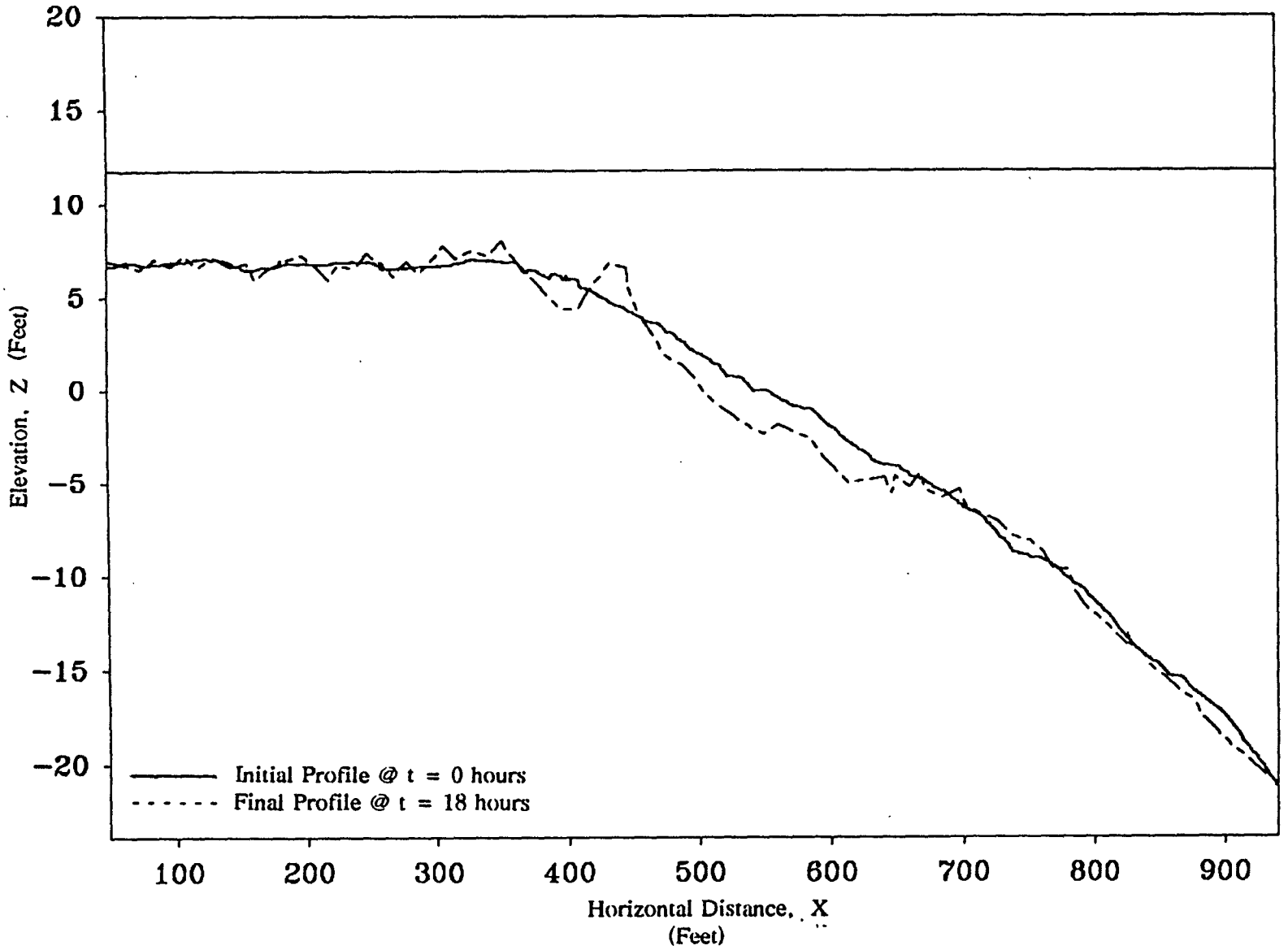

Figure 5.14 Measured Initial and Final Beach Profiles for Trial 7 (+11.5, 8.5, 8.0)

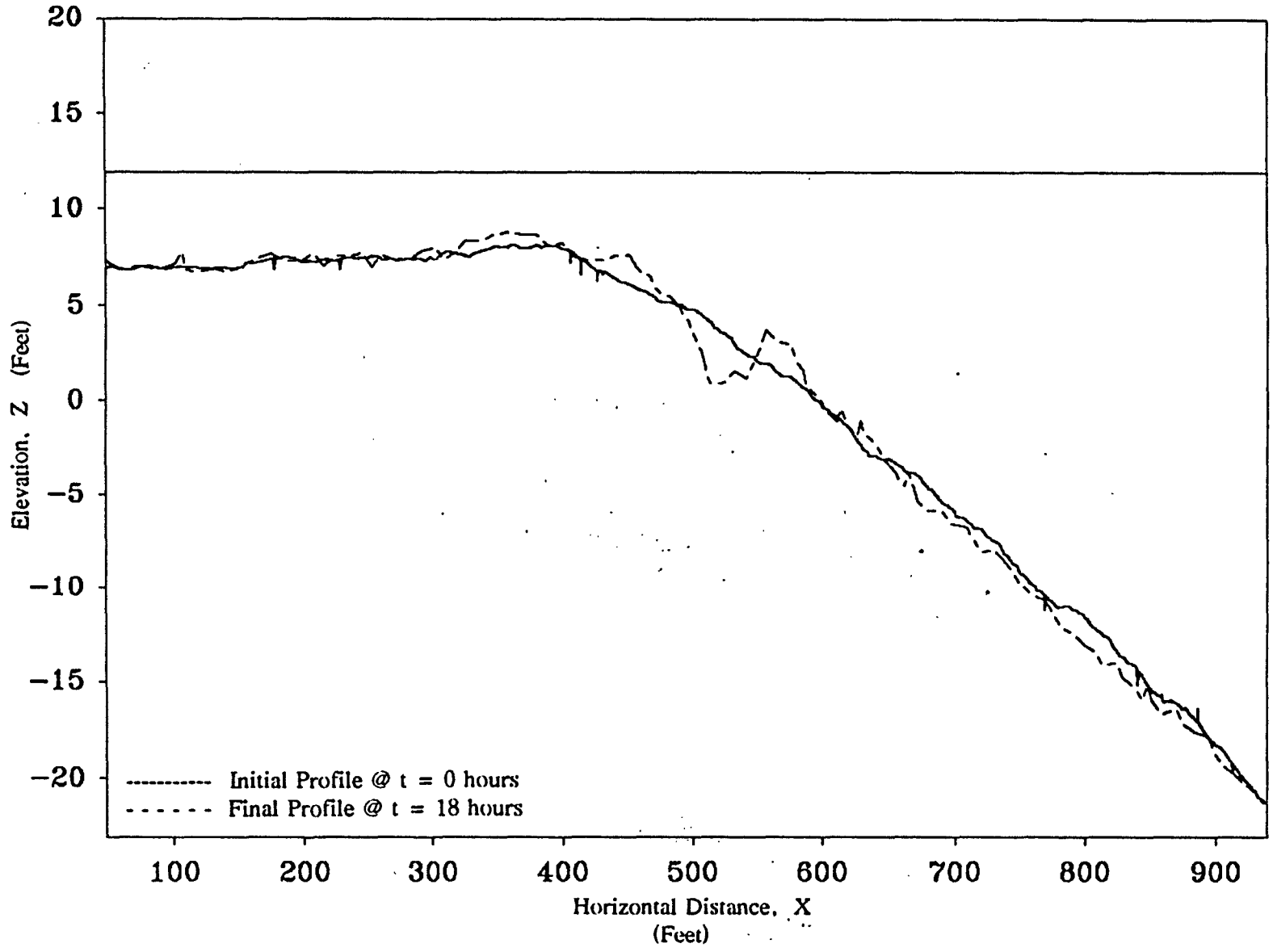

Figure 5.15 Measured Initial and Final Beach Profiles for Trial 8 (+11.5, 8.5, 10)

shoreward of this point distinguishes Trial 5 (+11.5, 7.0 ,8.0) (Figure 5.12). Except for bar formation, profile changes in Trial 6 (+11.5, 7.0. 10) (Figure 5.13) are minimal. Profile changes in Trial 7 (+11.5, 8.5, 8.0) (Figure 5.14) are limited to some erosion shoreward of the bar and deposition near the berm. The trial 8 (+11.5, 8.5, 10) bed profile (Figure 5.15) was characterized by a small bar and erosion seaward of the break point.

Trials 1 (+10, 7.0, 8.0), 5 (+11.5, 7.0, 8.0), and 7 (+11.5, 8.5, 8.0) did not have bar formation near the break point but did have substantial amounts of sand eroded shoreward of this point. This sand was then carried and deposited near the berm. The lack of bar formation in these three trials suggest that the combination of overwash depth and period can affect the strength of the return flow and perhaps bar formation. Trials 5 and 7 had the larger overwash depth but smaller period. If the period was increased in these two trials to ten seconds, bar formation was apparent. Trial 1 also supports this argument. This trial had the lower overwash depth and period but when the period was increased to ten seconds, a bar was created.

From the plots, it is evident that sand volumes over the island increased slightly. In most trials, there was a slight build up of sand near the entrance to the holding area and a decrease of sand near the berm. Small amounts of sand were captured in the containment area.

Water Surface Gradient Tests

Water surface gradients occur when there is an imbalance between the ocean and bay water levels. Their formation is caused by the incoming storm surge which creates "flood tides" that can sweep over the island. These gradients may be instrumental in transporting the sediment over the island during the overwash process. Therefore, four trials were performed to see the effects the gradient had on sediment transport over the island.

Four trials were completed. Due to inconsistent data measured by the wave gauge and current meter, trials 11 and 12 were subsequently discounted. Wave height and current readings

for the remaining two trials are listed in the following tables. Although the design deep water wave height for both trials was 8.5 Ft, the effects of the coflowing current where not accounted for when producing the desired deep water wave height in Trial 9. Thus this trial has a smaller breaking wave height.

Table 5.16: Trial 9 Wave Height Measurements for the Following Conditions: +10.0 Ft Overwash Depth, 8.5 Design Deep Water Wave Height, 8.0 Second Wave Period, and Full Pump Speed.

Category	Location (Ft)	Wave Height (Ft)
Deep Water	1072	7.42
Before Breaking	624	8.70
Break Point	528	9.63
Surf Zone	416	6.66
Over Island	320	3.98
Over Island	240	3.47
Over Island	112	2.87

Table 5.17: Trial 9 Current Measurements for the Following Conditions: +10.0 Ft Overwash Depth, 8.5 Design Deep Water Wave Height, 8.0 Second Wave Period, and Full Pump Speed.

Category	Location (Ft)	Current (Ft/Sec)	$Y_{.....}$ Depth (Ft)
Deep Water	1024	1.25	14.87
Before Breaking	576	1.02	12.04
After Breaking	480	1.68	6.35
Over Island	368	2.30	5.30
Over Island	272	3.96	5.01
Over Island	192	4.60	0.775
Over Island	64	4.96	1.73

Table 5.18: Trial 10 Wave Height Measurements for the Following Conditions: +10.0 Ft Overwash Depth, 8.5 Design Deep Water Wave Height, 8.0 Second Wave Period, and Half Pump Speed.

Category	Location (Ft)	Wave Height (Ft)
Deep Water	1120	7.28
Toe of Beach	944	8.65
Before Breaking	912	8.33
Before Breaking	880	7.08
Before Breaking	848	8.32
Before Breaking	816	9.23
Before Breaking	784	8.37
Before Breaking	752	7.62
Before Breaking	720	9.39
Before Breaking	688	8.26
Before Breaking	656	8.50
Before Breaking	624	10.07
Before Breaking	592	8.20
Before Breaking	560	9.50
Break Point	528	10.69
After Breaking	496	10.10
After Breaking	464	8.92
Surf Zone	432	8.05
Surf Zone	400	6.61
Over Island	368	5.74
Over Island	336	4.94
Over Island	304	4.16
Over Island	272	3.41
Over Island	240	3.23
Over Island	208	3.21
Over Island	176	3.07
Over Island	144	2.73
Over Island	112	2.12
Over Island	80	1.64
Over Island	48	2.13

Table 5.19: Trial 10 Current Measurements for the Following Conditions: +10.0 Ft Overwash Depth, 8.5 Design Deep Water Wave Height, 8.0 Second Wave Period, and Half Pump Speed.

Category	Location (Ft)	Current (Ft/Sec)	$Y_{measured}$ Depth (Ft)
Deep Water	1072	0.900	19.73
Before Breaking	896	1.12	20.00
Before Breaking	864	1.09	20.00
Before Breaking	832	0.876	20.00
Before Breaking	800	0.588	20.00
Before Breaking	768	0.604	20.00
Before Breaking	736	0.220	16.85
Before Breaking	704	0.600	13.70
Before Breaking	672	0.156	13.70
Before Breaking	640	0.376	13.70
Before Breaking	608	0.984	8.45
Before Breaking	576	0.904	8.45
Before Breaking	544	0.916	8.45
After Breaking	512	1.25	8.45
After Breaking	480	0.568	6.87
Surf Zone	448	2.47	3.20
Surf Zone	416	2.38	3.20
Over Island	384	2.95	3.20
Over Island	352	3.73	1.63
Over Island	334	4.12	1.63
Over Island	288	4.04	1.63
Over Island	256	4.08	1.63
Over Island	224	3.93	1.63
Over Island	192	4.76	1.10
Over Island	160	5.16	1.10
Over Island	128	5.32	1.10
Over Island	96	5.28	1.10
Over Island	64	5.76	1.10
Over Island	32	4.64	1.10
Bay Entrance	0	4.88	1.10

When a water surface gradient is formed, it produces a situation analogous to incoming waves atop a co-flowing current. When the current is produced, it alters the previous overwashing cases in four areas: 1) Break point location; 2) Wave decay; 3) Current profiles; 4) Beach profiles and bar formation.

Comparing trials 9 (+10, 8.5, 8.0, Full) and 10 (+10, 8.5, 8.0, Half) with those results from trial 3 (+10, 8.5, 8.0) in the overwash cases without a co-flowing current, it is evident that the break point has shifted shoreward for the case of an induced current. In trial 9, the break point is located at 528 feet when the pump is operating at full speed. The location does not change when the pump rate is reduced to half speed as seen in Trial 10. The previous location without the co-flowing current was 672 feet. The reason for the break point shift is due to the co-flowing assisting current reducing the shoaling rate of the wave, allowing it to break farther inshore.

Wave decay is also affected by the co-flowing current. In trials without the induced current, wave heights decayed gradually after breaking and remained nearly constant over the island. With the co-flowing current, wave decay is rapid after the break point then continues gradually over the entire island. Wave heights reach a constant value only on the latter part of the island.

The addition of the co-flowing current has also changed the velocity profiles across the surf zone and island. Previous velocity profiles showed marked negative velocities in deep water and the surf zone and positive velocities over the island. With the addition of the co-flowing current, the negative velocities in the surf zone have disappeared. Trial 9 (+10, 8.5, 8.0, Full) and trial 10 (+10, 8.5, 8.0, Half) velocity profiles shown in Figure 5.16 are now characterized by positive velocities throughout the beach profile and island. These positive velocities in the surf zone suggest that the return flow is nonexistent when the water surface gradient exists over

the island. Naturally, the velocities over the island have also increased with the occurrence of the shoreward surface gradient.

The positive values found throughout the velocity profiles are reflected in the beach profiles. With the absence of the return flow, presumably, strong breakpoint bar formation does not occur. As seen in Figures 5.17 and 5.18, bar formation is evident in not just one location but several areas. However, the bars are not as pronounced as they were in the trials without the co-flowing current. This multiple bar formation suggest that bar creation for these cases is not entirely dependent on the return flow but possibly on reflected waves. Finally, sediment volumes deposited on the island have shown a marked increase. The initial berm has shifted shoreward and there is an increased amount of sediment behind the new berm and over the rest of the island. Furthermore, large volumes of sand (a few hundred pounds compared to a few for the first eight trials) were captured in the containment area. Obviously, the sand in the containment area would have washed into the bay. This last event is important for landward growth of the barrier island.

5.2 Wave Transformation Modeling

Although data collection is the best means of understanding the overwash process, obtaining the necessary data can be difficult. An alternative to data collection is the use of computer modeling to simulate the overwash process. Deciding the type of model to use in simulating this process is based upon predominant forces at play. Since the overwash process is driven by the storm surge and the height of the incoming waves, wave transformation models have the potential to give a good understanding of the overwash condition. They can be used to simulate the breaking process and the associated decay across the surf zone and island. They can also predict the set-up and set-down during wave breaking and allow subsequent estimates of the mean velocity field.

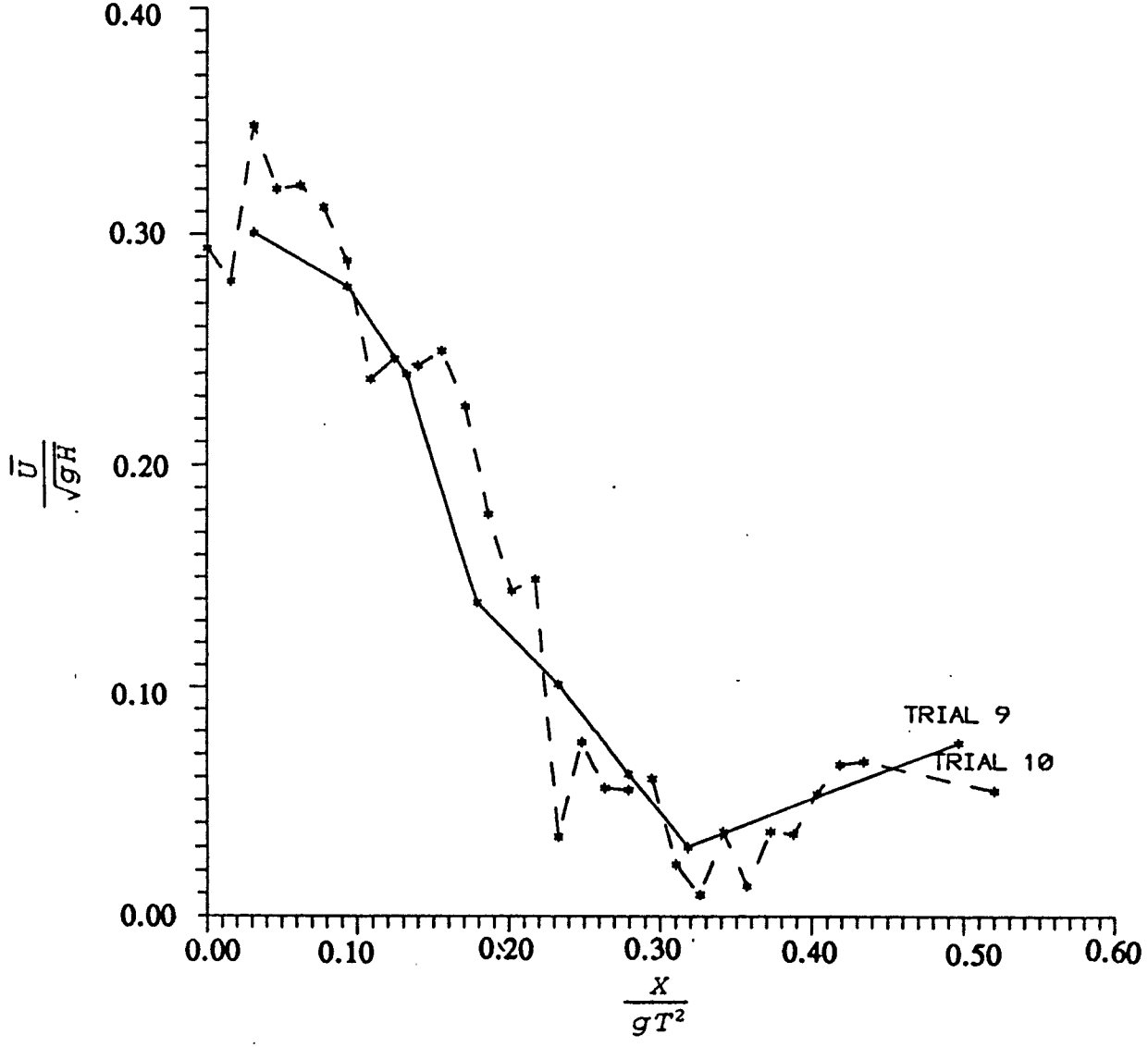

Figure 5.16 A Comparison of the Distribution of Non-Dimensional Mean Cross-Shore Velocity Between Trial 9 (+10, 8.5, 8.0, Half) and Trial 10 (+10, 8.5, 8.0, Full) (Measured at Mid-Depth)

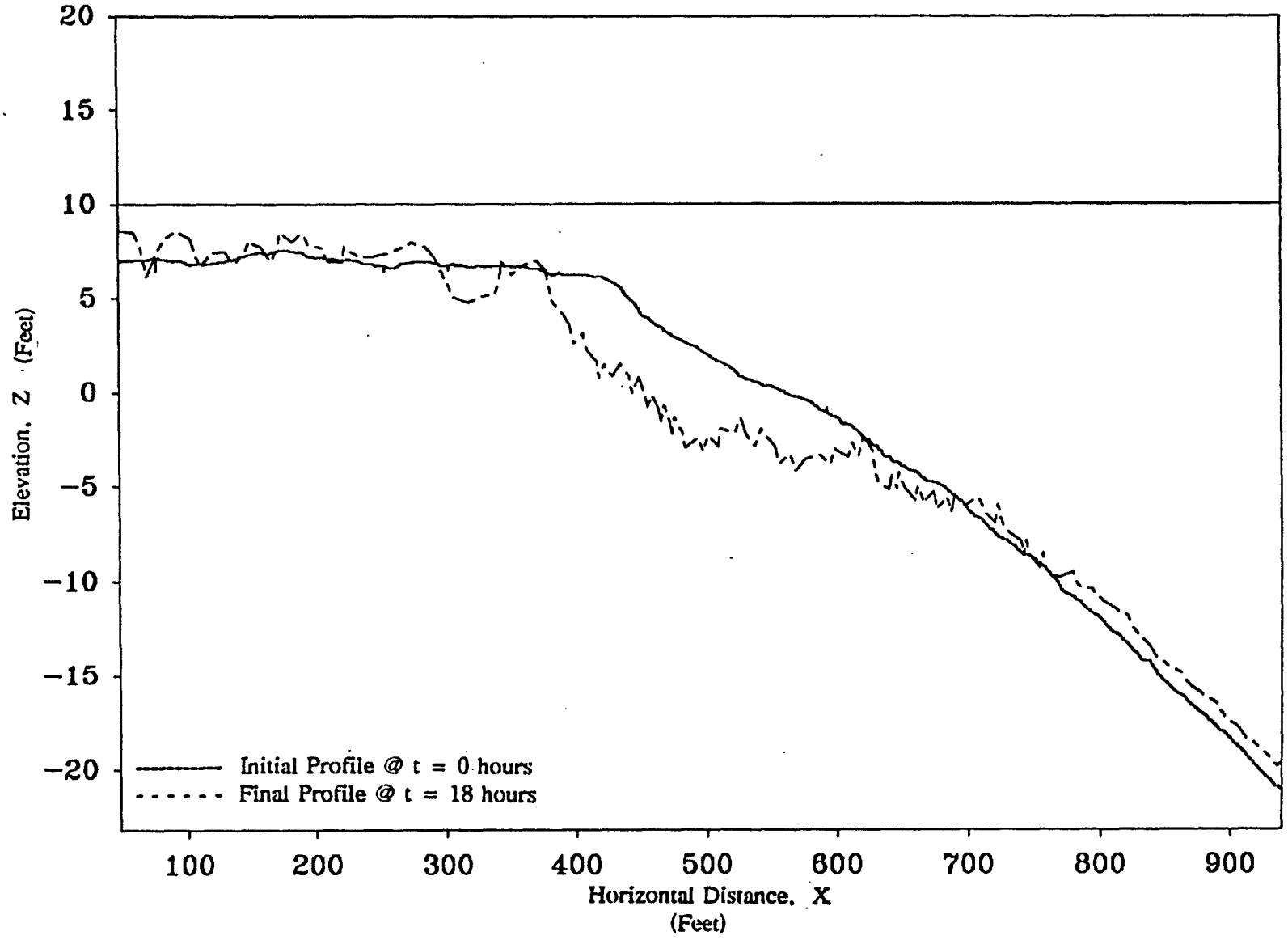

Figure 5.17 Measured Initial and Final Beach Profiles for Trial 9 (+10, 8.5, 8.0, Full)

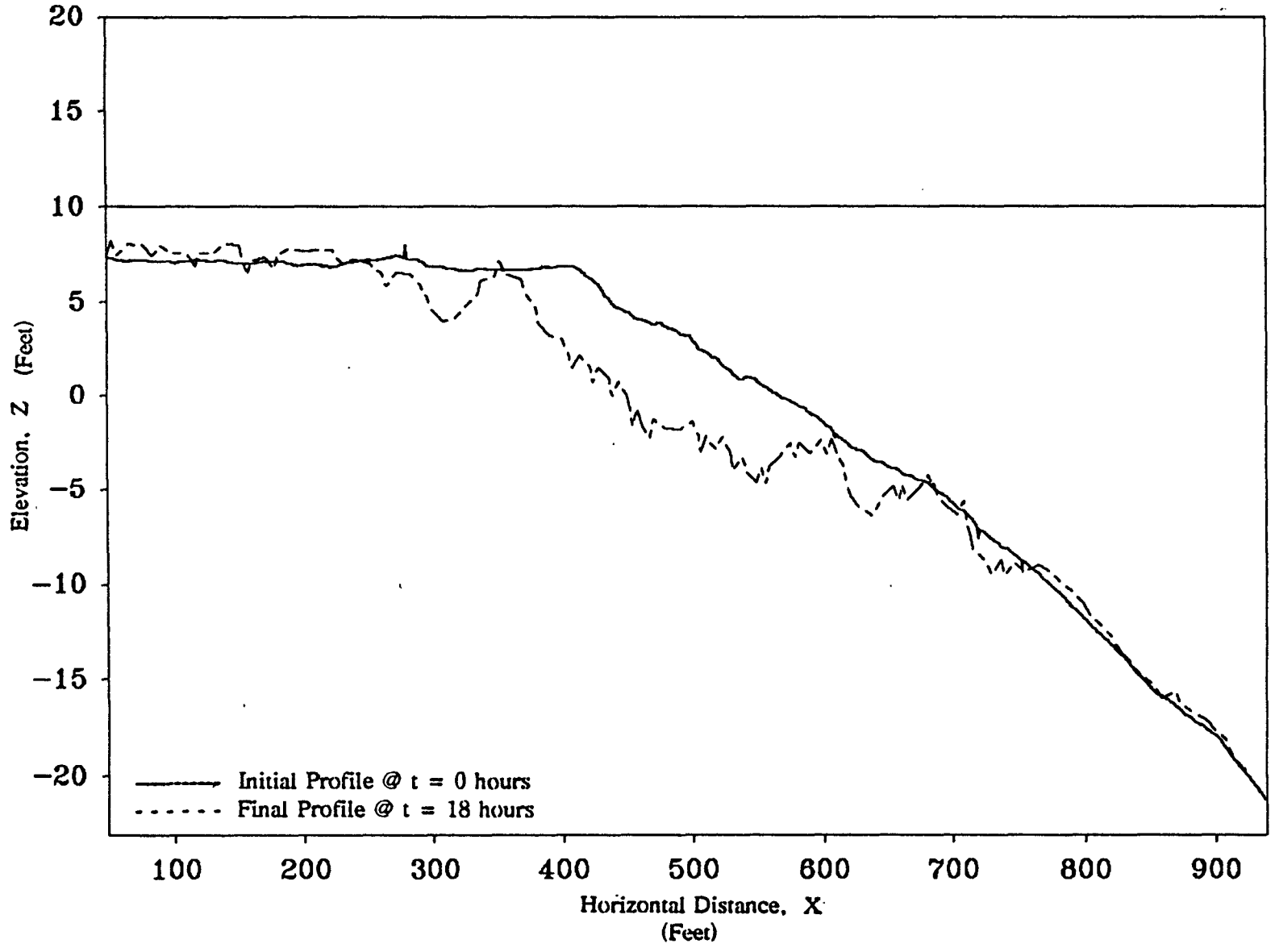

Figure 5.18 Measured Initial and Final Beach Profiles for Trial 10 (+10, 8.5, 8.0, Half)

There are several wave transformation models mentioned in the Chapter 2. The Dally, Dean and Dalrymple (1985) wave transformation model was selected for this application. This model takes into consideration wave transformation on a sloping and horizontal profile. Furthermore, this model allows for the decay rate constant, the beach profile, and the breaking height and breaker location to be specified. Since breaking wave dissipation is modelled relative to an empirically determined "stable wave" height, which is ideal for representing the change in dissipation characteristics over the island in this "open system", this model is suitable for this experiment. This model was used to predict the wave transformation across the surf zone and island for the eight trials listed in Chapter 4 and the two trials with the induced flows. The results are compared with those obtained from the laboratory experiment.

In order to eliminate as much variability between trials, values for the wave decay rate, K, and the wave stability factor, Γ, were common for all eight trials. Values of $K = 0.05$ and $\Gamma = 0.3$ were chosen because of the beach slope used and the fact that these values produced the best fit to the experimental data. Only the breaking height, location of the break point, and the beach profile changed for each trial. Since the wave heights for each trial were taken during different profiles as the experiment progressed, the beach profile at 6 hours prototype time was chosen as the input profile for all experiments. This value was chosen because the profile, at 6 hours, had reached an quasi-equilibrium for each trial. In addition, the value chosen to represent the break point location might not correspond to exactly the same position as the recorded break points in the trials. This is due to the lack of enough data points around the break point, making the exact location difficult to measure precisely.

In trial 1 (+10, 7.0, 8.0), the wave height to depth ratio at breaking (H_b/h_b) was 0.5. When the model was run, the results showed surprisingly good agreement with the data taken during the experiment. This can be misleading since there is a scarcity of data and there is no

way to predict exactly how the decay acts after breaking and over the island. Even with this lack of data, certain trends are evident in Figure 5.19. The decay rate is gradual from the breaking point to the berm. Waves continue to decay over the island until 100 feet where the wave height becomes relatively constant. In addition to wave transformation, the set-up and set-down were predicted. From the figure, it is evident that there is little set-down and that set-up remains constant over much of the island. However, set-up was not explicitly measured in the laboratory so no comparison can be made.

The overall lack of data in trial 2 (+10, 7.0, 10) (Figure 5.20) makes it difficult to determine if the model's prediction is correct. However, a few points can be made about the model's ability to predict wave decay across a bar-trough system. The predicted results show that the wave broke but to some extent reformed after it passed over the trough. This event is common in prototype bar-trough systems. It then can be assumed that the model is able to predict with some accuracy wave reformation over bar-trough systems, even with the addition of overwash. Another feature in this trial is that the set-up is larger than the wave heights over the island. This might be the result of the deeper water levels over the island, which will cause the wave heights to decrease.

The results from trial 3 (+10, 8.5, 8.0) are displayed in Figure 5.21. The wave heights decay gradually until the trough, where some reformation occurs. More reformation occurs after the waves pass over a small bar just outside of the berm. The wave height bayward of the berm is constant as is the set-up. The laboratory data shows a good fit with the model prediction except over the island. On the island, the model has underpredicted the one wave height that was measured.

The wave transformation for trial 4 (+10, 8.5, 10) is shown in Figure 5.22. The model is able to estimate the wave decay around the bar with accuracy. However, the model

overestimated the wave height just before the berm and under estimated it over the island. The extremely low wave height measured just before the berm is perhaps questionable.

Trial 5 (+11.5, 7.0, 8.0) results are presented in Figure 5.23. The model has represented the wave height decay with some precision except over the island, where it has slightly overpredicted. It should be noted that the model over estimated the wave height after breaking as well. The error might be due to the topography changes seen in this trial.

The results from trial 6 (+11.5, 7.0, 10) (Figure 5.24) closely parallel those seen in trial 2 (+10, 7.0, 10). Topography, the wave height to water depth ratio at breaking, and the test conditions for the two trials are nearly identical and the corresponding wave transformation is similar. The main difference between the two is that the decay rate over the island is more gradual. This is a result of the higher overwash depth seen in this trial.

The wave transformation prediction for trial 7 (+11.5, 8.5, 8.0) is shown in Figure 5.25. The predicted wave decay closely followed the results from the laboratory data. Only over the island did the results not agree. It is most probable that the model has estimated correctly the decay over the island. The wave heights measured at this location are indicating wave growth over the island and are somewhat suspicious.

In trial 8 (+11.5, 8.5, 10), the model has estimated the wave decay tolerably as seen in Figure 5.26. The wave transformation seen in this trial is similar to that of trial 4. Unlike trial 4 (+10, 8.5 ,10), the model was better able to predict the decay after the bar and trough system. The higher overwash depth in this trial accounts for the slower decay rate over the island as compared to trial 4.

Besides examining each trial individually, comparisons were done between trials of different overwash depths. Several conclusions can be drawn about the effects of overwash depth and the period on wave transformation modeling. Observing the wave height to water depth ratios

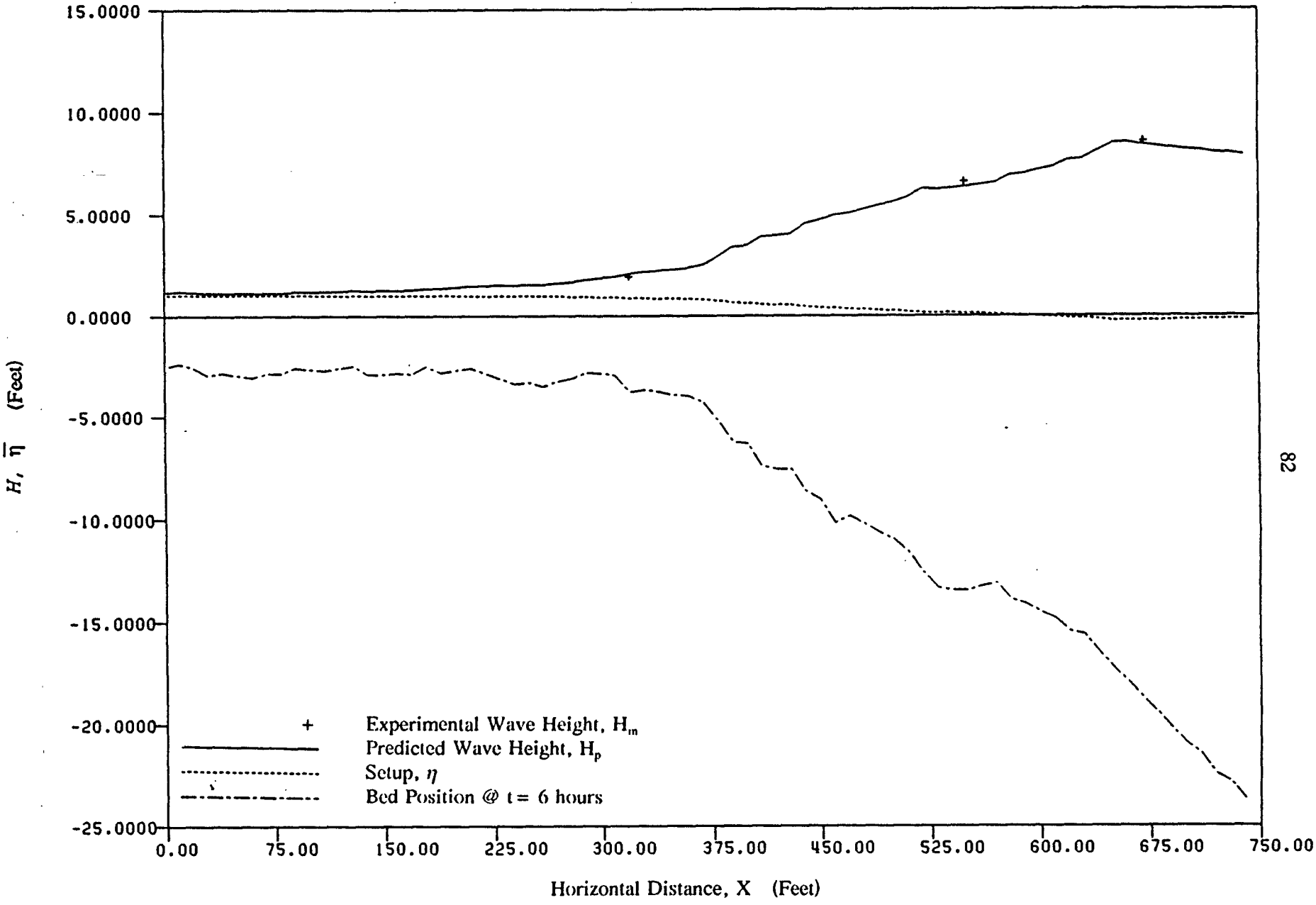

Figure 5.19 Computer Model Generated Wave Transformation and Setup Across the Surf Zone for Trial 1 (+10, 7.0, 8.0)

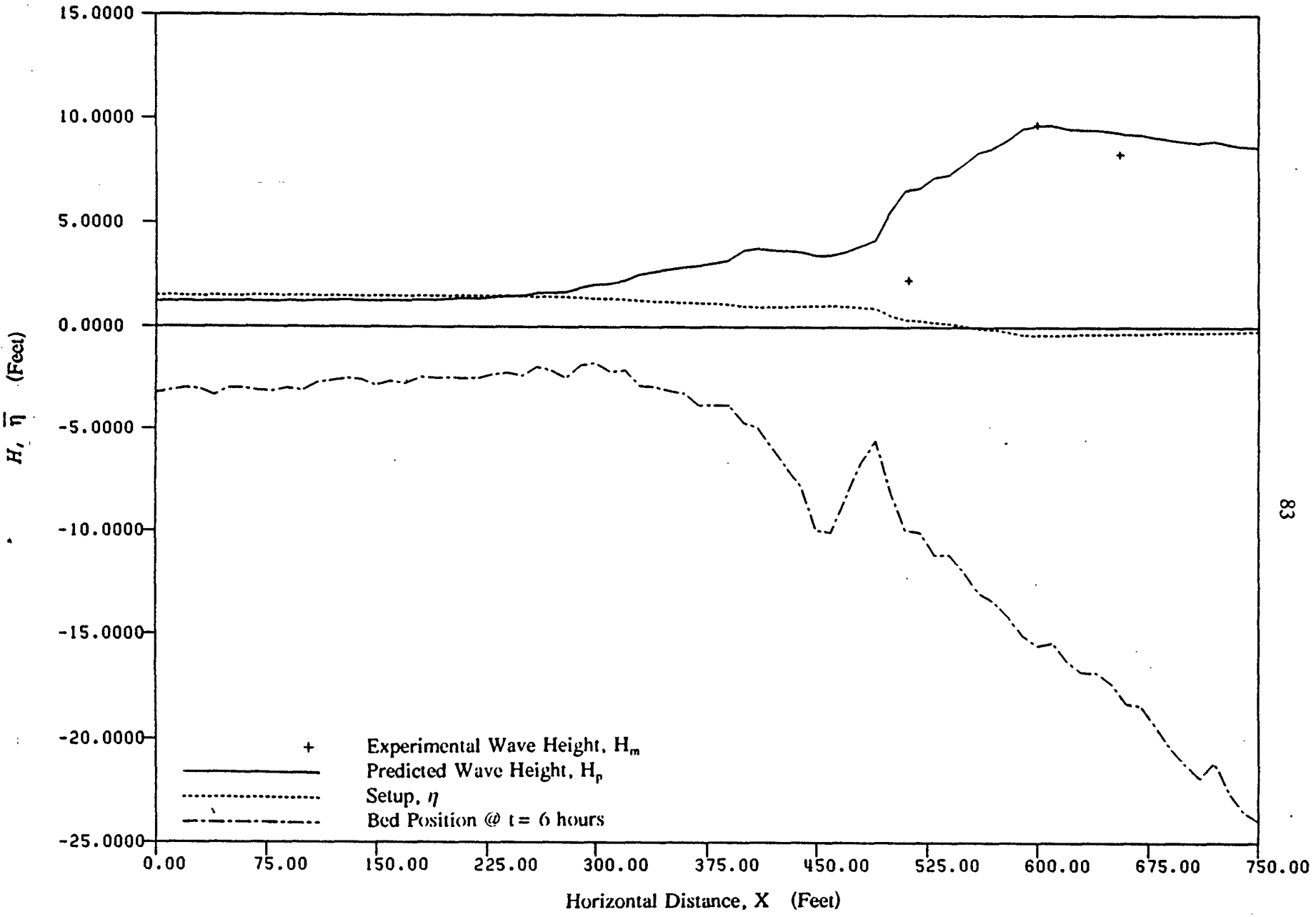

Figure 5.20 Computer Model Generated Wave Transformation and Setup Across the Surf Zone for Trial 2 (+10, 7.0, 10)

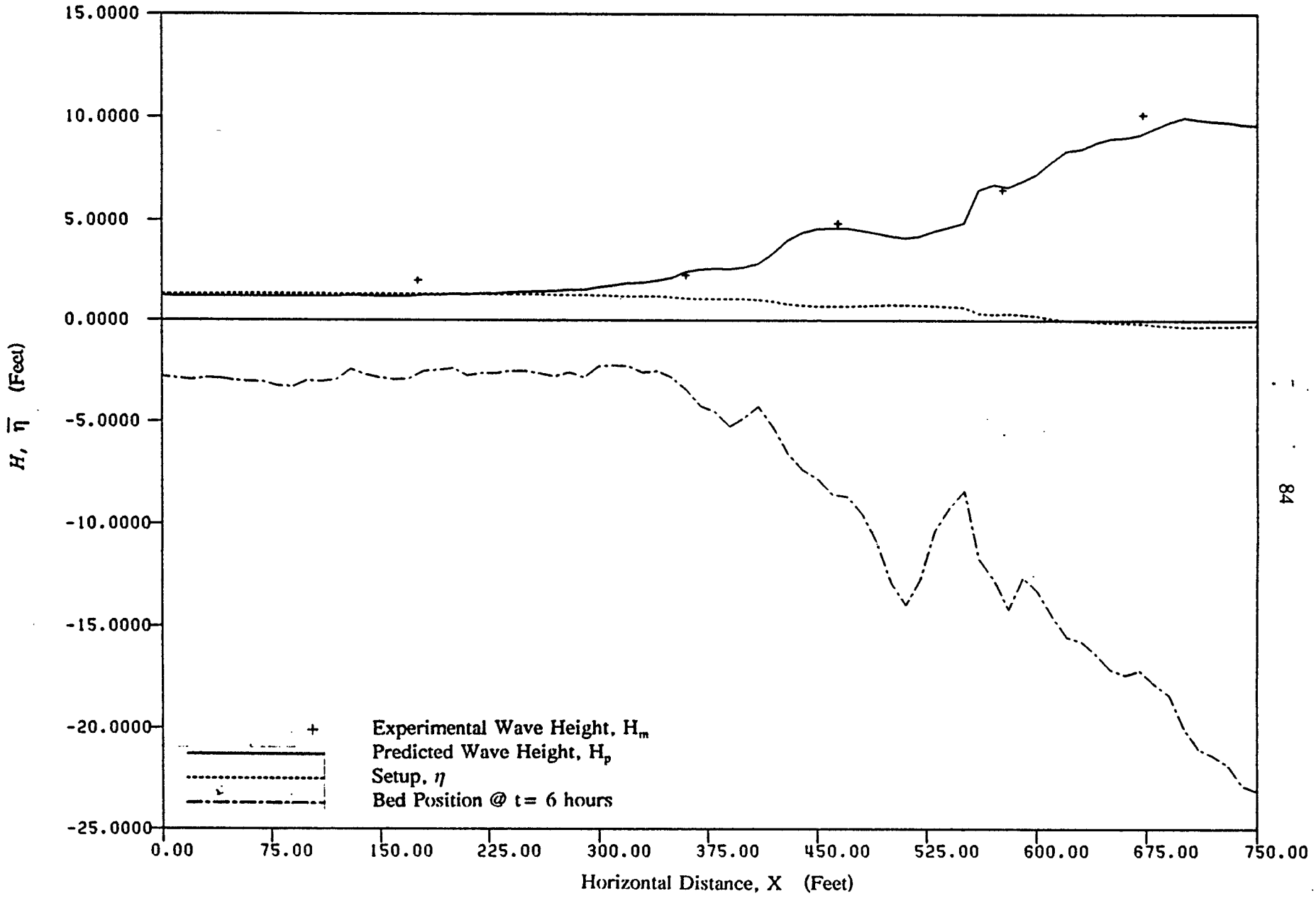

Figure 5.21 Computer Model Generated Wave Transformation and Setup Across the Surf Zone for Trial 3 (+10, 8.5, 8.0)

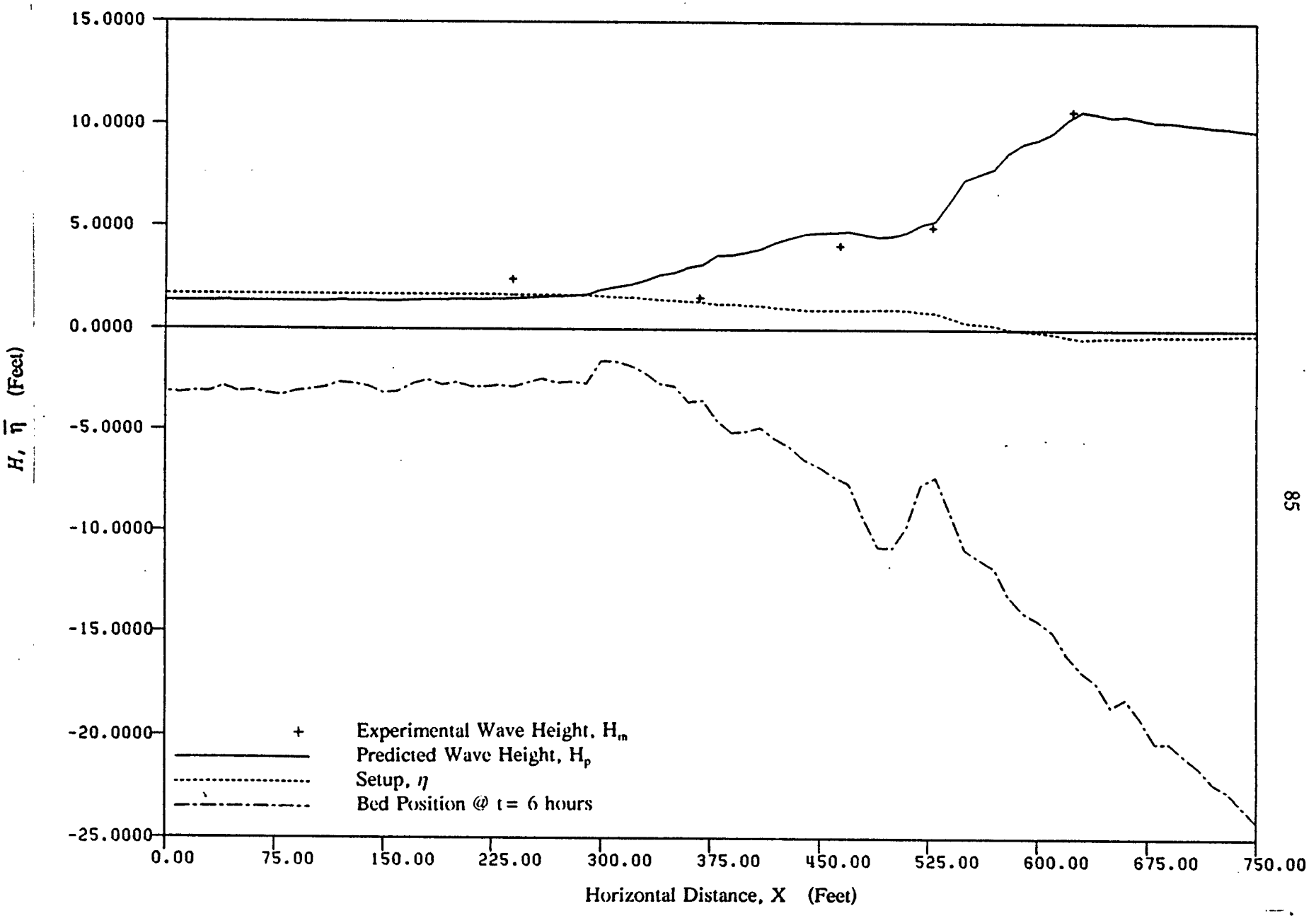

Figure 5.22 Computer Model Generated Wave Transformation and Setup Across the Surf Zone for Trial 4 (+10, 8.5, 10)

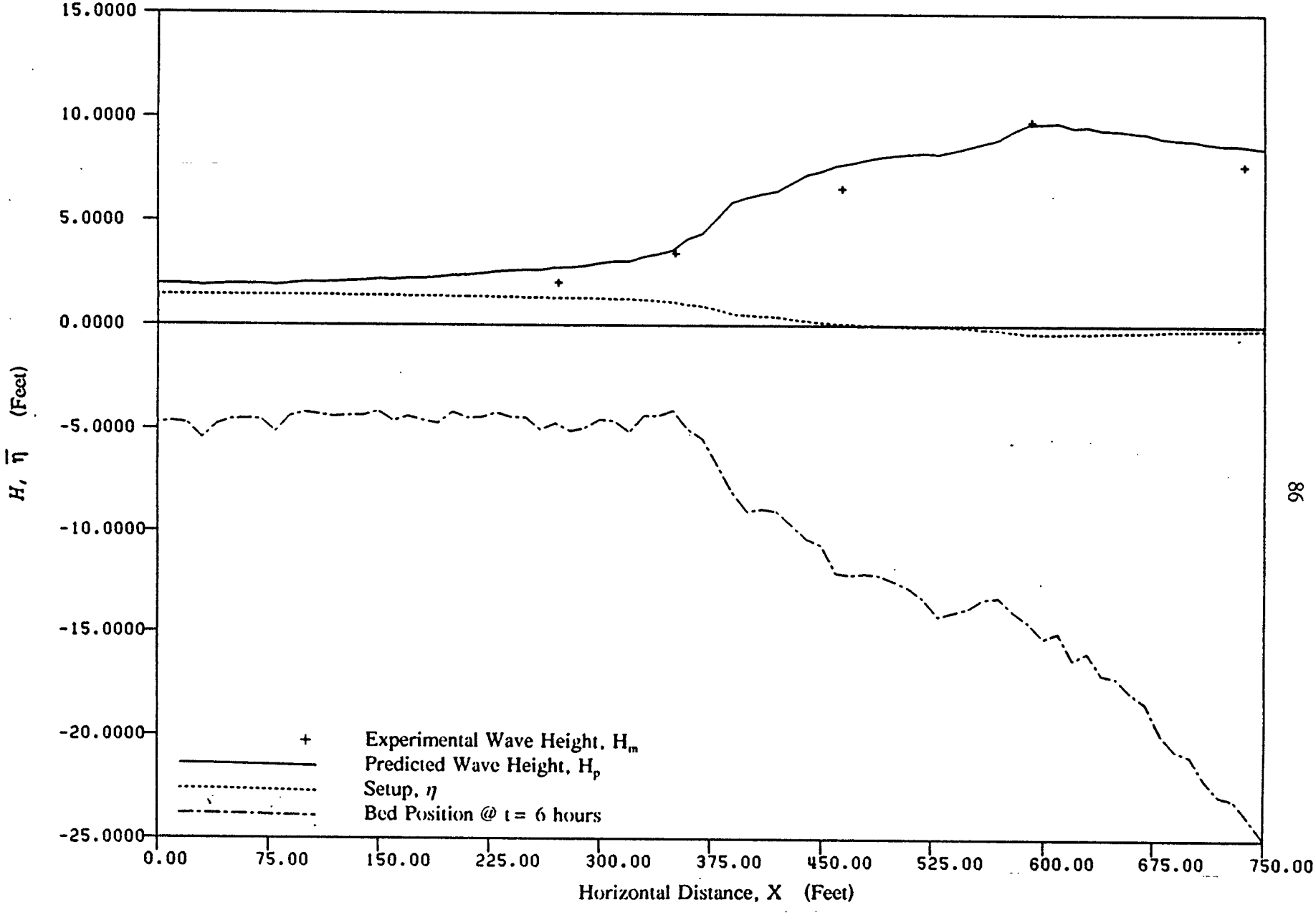

Figure 5.23 Computer Model Generated Wave Transformation and Setup Across the Surf Zone for Trial 5 (+11.5, 7.0, 8.0)

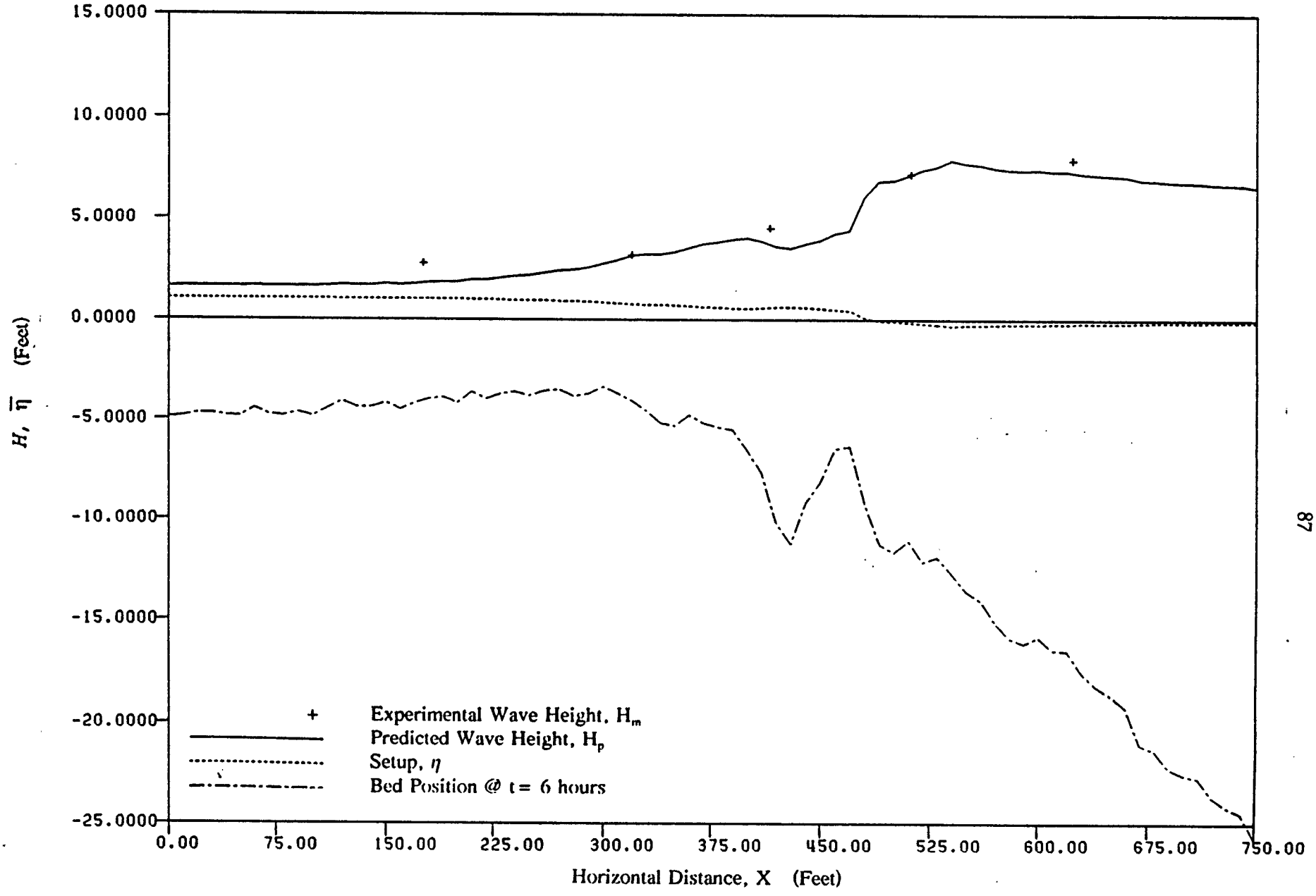

Figure 5.24 Computer Model Generated Wave Transformation and Setup Across the Surf Zone for Trial 6 (+11.5, 7.0, 10)

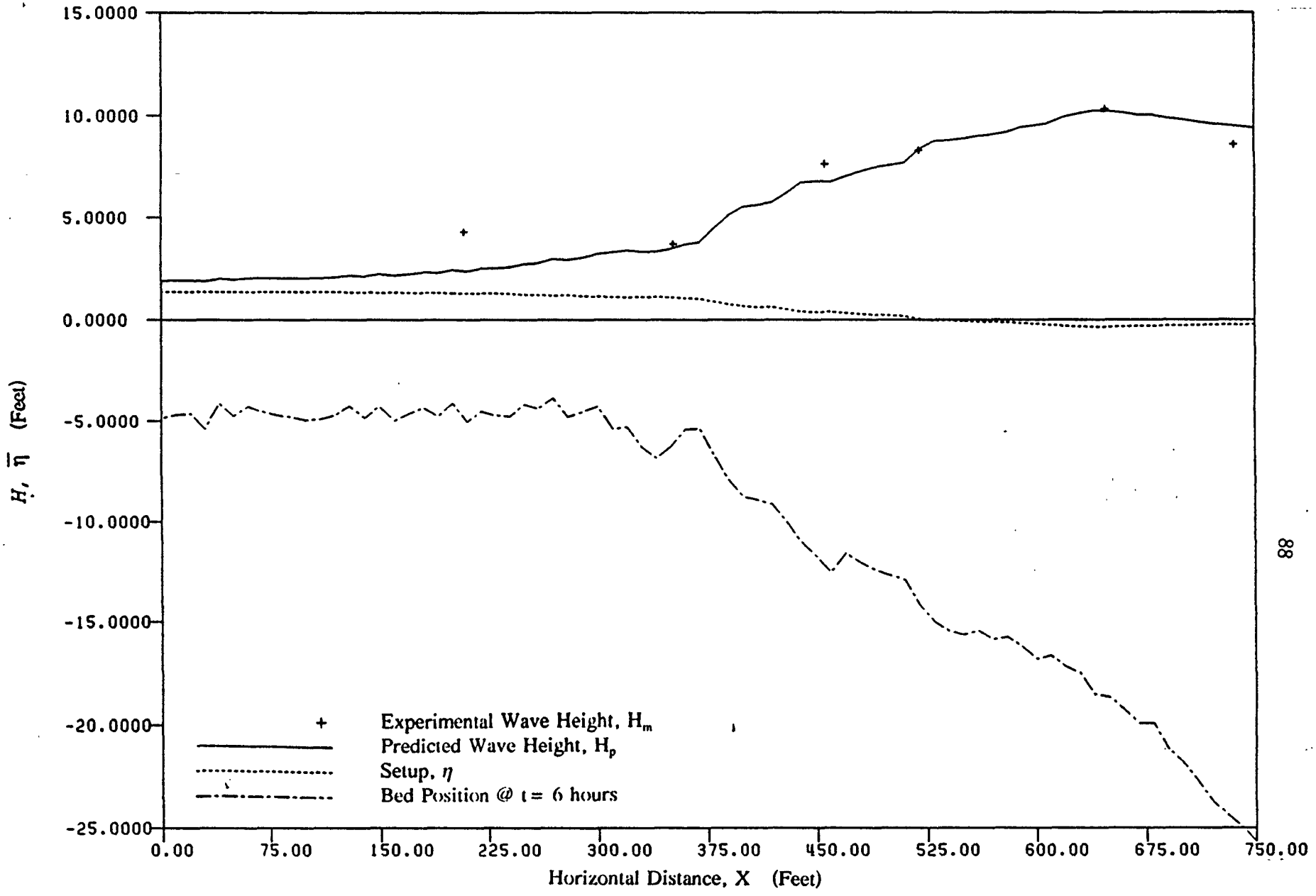

Figure 5.25 Computer Model Generated Wave Transformation and Setup Across the Surf Zone for Trial 7 (+11.5, 8.5, 8.0)

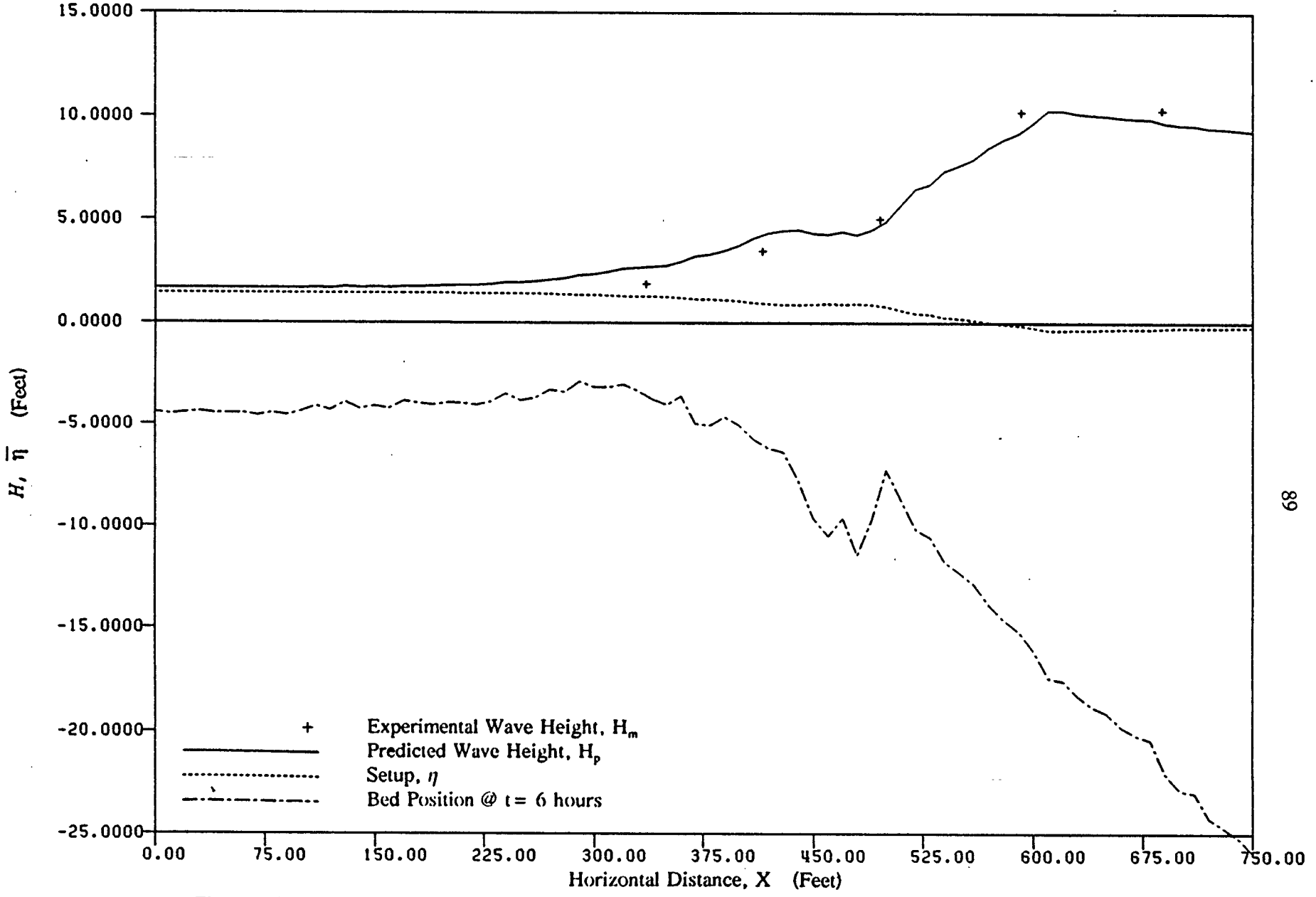

Figure 5.26 Computer Model Generated Wave Transformation and Setup Across the Surf Zone for Trial 8 (+11.5, 8.5, 10)

for all eight trials supports the earlier discussion of the effect of wave period on break point location. In the first four trials, trials 1 (+10, 7.0, 8.0) and 3 (+10, 8.5 ,8.0) have the smaller H_b/h_b and wave period. Their break points are farther offshore than those with the greater H_b/h_b and wave period. The same argument holds true for trials 5 through 8. In addition to wave period effects, the depth of overwashing seems to affect the decay rate of the wave, especially over the island. The decay rate for the larger overwash depths was gradual over the profile; not becoming relatively constant until the latter part of the island. This is the opposite of the lower overwash trials. Wave decay was faster until the beginning of the island, where it became constant.

Wave modeling was also performed for the two water surface gradient trials. Because of the co-flowing current, it was assumed that the waves would not decay as rapidly. Therefore, K was changed to 0.035 while Γ remained the same. In trial 9 (+10, 8.5 ,8.0, Full), the model was able to predict wave decay in the surf zone fairly well, including the wave decay near the bar. It failed, as shown in Figure 5.27, to estimate the wave decay over the island. In trial 10 (+10, 8.5, 8.0, Half), the model did not predict with great accuracy the wave height evolution over the multiple bar formation found throughout the surf zone. In Figure 5.28, the model failed to reproduce the behavior prior to breaking and under predicted the decay around the bar formation at 400 feet. But the model was able to approximate the decay rate over the island. Why is it that the model is able to predict the surf zone and not the island in one case and completely do the opposite in the other case? This answer lies with the water surface gradient. When the pump is at full speed, as in trial 9, the current has a greatest effect on the decay. Since the velocities over the island are the fastest of the entire profile, it is this area that the model will under predict. In trial 10, the pump is at half speed. Velocities over the island are not as large and thus the decay rate is not affected as much. However, the addition of the current in the surf

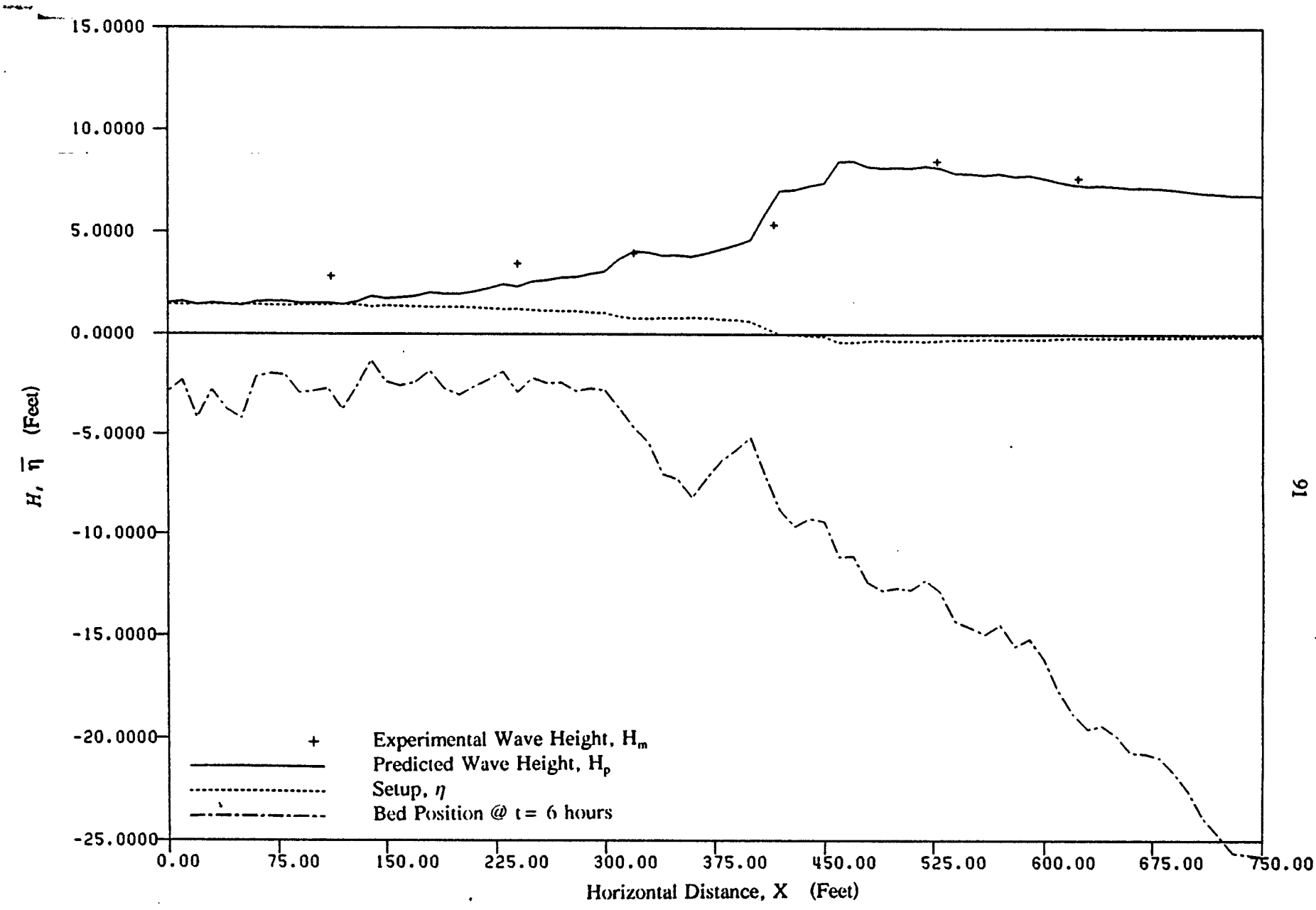

Figure 5.27 Computer Model Generated Wave Transformation and Setup Across the Surf Zone for Trial 9 (+10, 8.5, 8.0, Half)

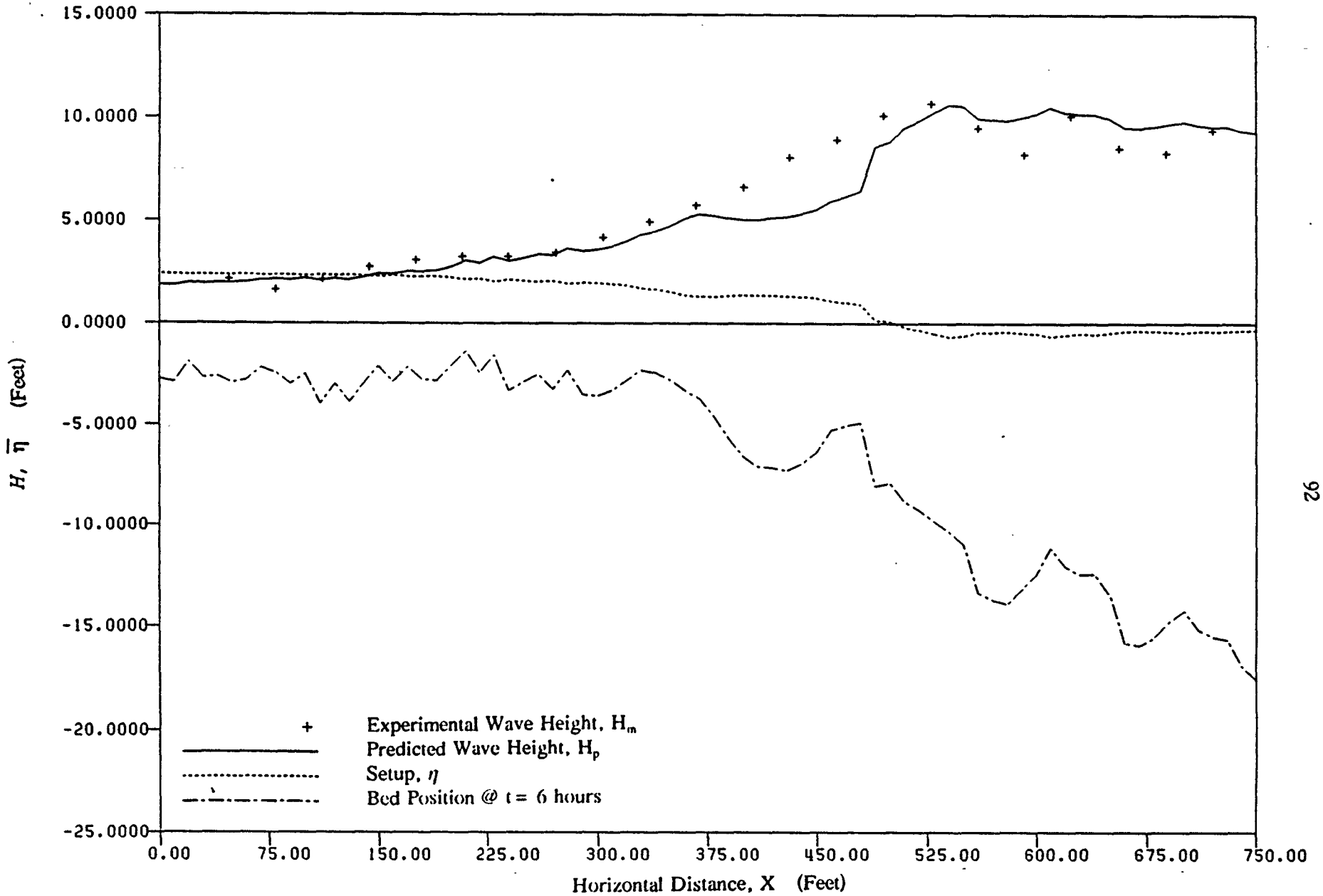

Figure 5.28 Computer Model Generated Wave Transformation and Setup Across the Surf Zone for Trial 10 (+10, 8.5, 8.0, Full)

zone does not allow the waves to decay fast enough, causing the model to over predict the decay over the bar. These results indicate that it is probably insufficient to simply lower the dissipation rate to account for the effect of the co-flowing current. It would perhaps be more appropriate to include the current directly in the momentum and energy equations utilized in the model.

Overall, it is apparent that wave transformation modeling is able, to some degree, to predict the wave height transformation across the surf zone. Figure 5.29 shows that in the cases of wave induced currents, agreement is quite good between the measured and predicted values. When a coflowing current exists, the model is less physically consistent and thus there is more scatter in Figure 5.30. In general, the model has a tendency to underpredict the wave heights. It would appear that this might be caused by the reduction in the breaking induced dissipation when the coflowing current is present.

5.3 Mean Current Prediction

Wave transformation modeling provides a detailed analysis of the wave and set-up processes during the overwashing event. Although these processes are important in causing sediment transport, they do not answer how the sediment is being transported and where. It is advantageous that the mean current distribution during the overwash process be examined so that more can be learned about direction and nature of flow.

There are several models that can simulate cross shore mean currents. Using measured wave height and set-up, the shoreward mass transport and return flow can be predicted. However, these models require detailed velocity data at various depths in the water column for proper comparison. Disagreement over the proper choice of boundary conditions for these models have been discussed, along with the need for some type of turbulence paramaterization (i.e. eddy viscosity). Note however that for the overwash case the zero net flux boundary condition is not applicable; in fact this boundary condition is unknown. Because of these reasons,

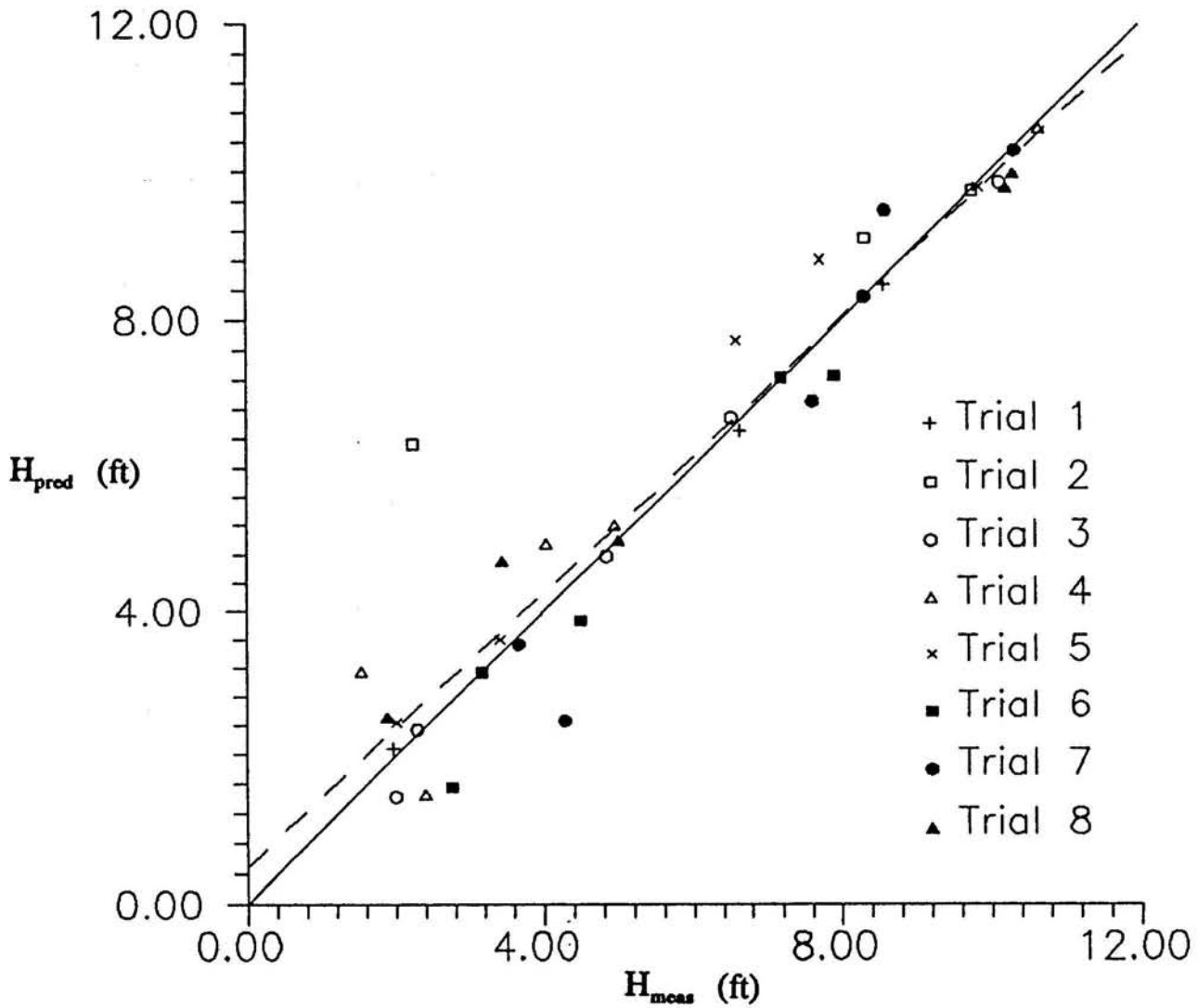

Figure 5.29 Predicted (H_{pred}) vs. Measured (H_{meas}) Wave Heights for Simple Cases (Trials 1-8) Using Model of Dally et al. (1985) with Coefficients (Gamma = 0.3, K = 0.05)
Note: Solid Line = Line of Equivalence
Dashed Line = Least-squares Best Fit to Data

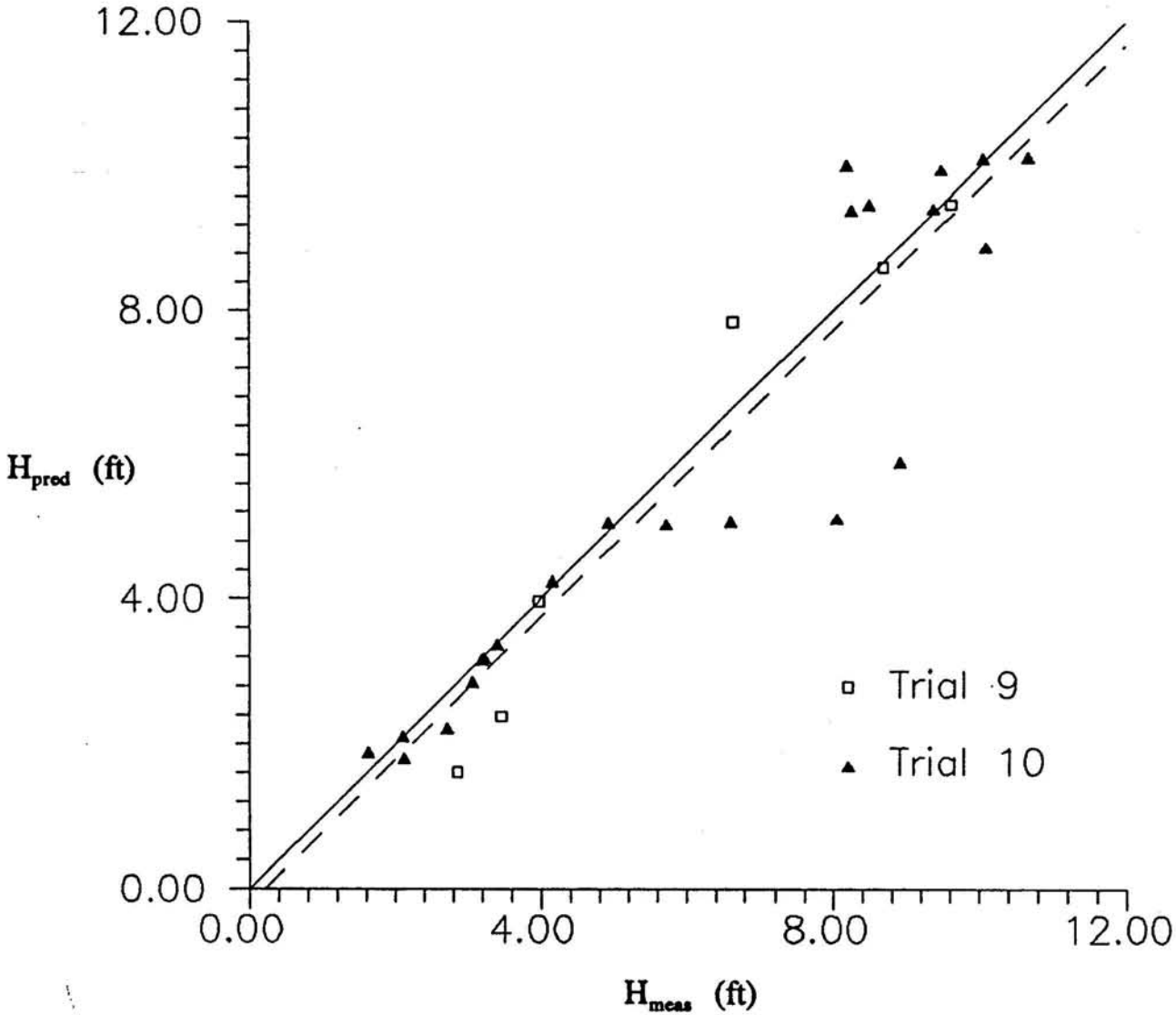

Figure 5.30 Predicted (H_{pred}) vs. Measured (H_{meas}) Wave Heights for Overwash Cases with a Coflowing Current (Trials 9-10) Using Model of Dally et al. (1985) with Coefficients (Gamma = 0.3, K = 0.035)
Note: Solid Line = Line of Equivalence
Dashed Line = Least-squares Best Fit to Data

and to avoid drawing attention away from the overall desire to find a rough estimate for the mean velocities, detailed "undertow" velocity profile models will not be used. However, simple calculations can still be done to give an estimation of the strength of mass transport and the return flow based on the amount of flow going over the island. This modeling effort is consistent with the level of laboratory current data collected.

Mass transport calculations for this experiment are based on linear wave theory and Svendsen's (1984b) mass flux equation for non-overwash conditions. In linear wave theory, mass transport per unit width is defined as:

$$M = \frac{E}{C} \tag{5.1}$$

where E is defined as the wave energy and C the wave celerity. It is considered a nonlinear quantity because the wave height is raised to the second power in the energy term. However, it is derived from linear wave theory. There are two approaches for determining mass transport in linear theory: Eulerian and Lagrangian. The Eulerian frame will be utilized since it is consistent with the Eulerian velocity data taken by the current meter during each trial.

Calculations of mass transport using linear wave theory will be performed at and prior to the break point. The nonlinearities and the additional mass flux in the breaking waves warrant a separate formulation. Values of mass transport in deep water do not have a significant bearing on the sediment transport processes and therefore will not be studied.

Using the measured wave heights, the mass transport for each of the six trials was calculated. Since there are no current measurements over the island for trials 2 and 6, these trials were not used. The mass transport values were then converted to volumetric units by multiplying these values with the width of the tank and then dividing them by the density of the water.

Svendsen's equation will be utilized in determining the mass transport values in the surf zone and over the island. His theory is based on the assumption that a breaking wave can be divided into two sections: the surface roller of the breaking wave and the water column below the roller. Accounting for the fact that the total mean volume flux is zero for non-overwashing cases, the total volume of water created by mass transport must be returned by a equal but opposite return flow volume. Using the notation from his roller assumptions, Svendsen's solved for the mass transport volume as shown in equation 5.2.

$$Q = C\frac{H^2}{h}\left(B_o + \frac{A}{H^2}\frac{h}{L}\right)\frac{d_{tr}}{h} \tag{5.2}$$

where

- C = speed of wave propagation.
- B_o = nondimensional time averaged energy flux.
- A = area of the roller and can be approximated as $A \sim 0.9 \cdot H^2$.
- d_{tr} = depth of the water from the bottom to the trough level.
- L = wave length
- h = water depth at the mean water line.

Several assumptions were made for the variables in Svendsen's equation. d_{tr} was approximated by taking the depth at the wave height measurement and subtracting the value of the wave height divided by two. B_o was determined by taking the average of the H_o/L_o values from all the measurements and finding the corresponding value from the graph in Svendsen (1984b). This value was estimated at $B_o = 0.07$.

Substituting in the values for the wave height and the variables above, the mass transport for the surf zone and island was calculated. In order to equate this mass transport with the mass transport solved using linear wave theory, the value was multiplied by the tank width.

Estimating values of shoreward mass transport involved solving the aforementioned two equations. A simplistic model was applied to obtain an estimation of the seaward return flow from the laboratory current measurements. This was accomplished by multiplying each current measurement by the width of the tank and the depth where the current reading was taken minus the value of H/2. The resulting calculation provides an estimation of the volume of water returned seaward. The calculated mass transport and estimated measured return flow calculations for the six trials are listed in the tables below. A positive value indicates shoreward flow; a negative value seaward flow.

Table 5.20: The Results of the Mass Transport and Return Flow Calculations for Trial 1.

Mass Transport (Ft^3/Sec) (Calcuated)	Location (Ft)	Return Flow (Ft^3/Sec) (Calculated)	Location (Ft)	$Y_{measured}$ Depth (Ft)
38.67	672	-14.93	624	11.47
21.60	548.8	-5.83	500.8	3.93
2.70	320	8.00 7.25	272	2.59 2.08

Table 5.21: The Results of the Mass Transport and Return Flow Calculations for Trial 3.

Mass Transport (Ft^3/Sec) (Calculated)	Location (Ft)	Return Flow (Ft^3/Sec) (Calculated)	Location (Ft)	$Y_{measured}$ Depth (Ft)
55.84	672	-42.30	624	9.50
6.98	576	-21.35	528	7.40
4.13	464	0.625 1.89	416	2.15 3.83
1.13	360	1.78	312	2.41
0.88	176	2.34	128	2.15

Table 5.22: The Results of the Mass Transport and Return Flow Calculations for Trial 4.

Mass Transport (Ft^3/Sec) (Calculated)	Location (Ft)	Return Flow (Ft^3/Sec) (Calculated)	Location (Ft)	$Y_{measured}$ Depth (Ft)
62.5	624	-44.95	576	9.50
3.83	528	-13.44	480	6.09
2.79	464	-4.03	416	3.99
0.56	368	1.05	320	2.94
1.09	240	3.15	192	2.68

Table 5.23: The Results of the Mass Transport and Return Flow Calculations for Trial 5.

Mass Transport (Ft^3/Sec) (Calculated)	Location (Ft)	Return Flow (Ft^3/Sec) (Calculated)	Location (Ft)	$Y_{measured}$ Depth (Ft)
56.87	592	-15.90	544	10.55
7.05	469	-8.92	416	4.25
2.07	352	5.07 1.19	304	1.89 4.67
0.94	272	6.39	224	3.83

Table 5.24: The Results of the Mass Transport and Return Flow Calculations for Trial 7.

Mass Transport (Ft^3/Sec) (Calculated)	Location (Ft)	Return Flow (Ft^3/Sec) (Calculated)	Location (Ft)	$Y_{measured}$ Depth (Ft)
56.1	648	-21.03	600	12.65
31.23	520	6.94 -6.62	472	3.99 8.19
8.93	456	3.96 -10.82	408	3.10 5.67
2.56	352	2.23	304	3.86
3.03	208	7.31	160	4.93

Table 5.25: The Results of the Mass Transport and Return Flow Calculations for Trial 8.

Mass Transport (Ft^3/Sec) (Calculated)	Location (Ft)	Return Flow (Ft^3/Sec) (Calculated)	Location (Ft)	$Y_{measured}$ Depth (Ft)
50.43	688	-19.60	640	13.96
13.07	592	-12.83	544	10.55
3.87	496	-4.56 -11.26	448	2.52 5.20
2.13	416	4.96 1.41	368	1.63 3.73
0.78	336	3.44	288	1.36

From the tables, it is apparent that the mass transport values and the return values at each location do not equal each other. The overwash event is the direct cause of this inequality. In a non-overwash case, it is necessary that the total mean volume flux be zero. In other words, the shoreward mass flux should be negated by the seaward return flow (Equation 5.3).

$$\int_{-h}^{\eta} u\,dz = Q = 0 \tag{5.3}$$

When overwash occurs, a percentage of the total volume of water travels over the island. The portion that flows over the island is now equal to the sum of the mass transport minus the return flow, or, there is a net positive volume flux at any section (Equation 5.4).

$$\int_{-h}^{\eta} u\,dz = Q \tag{5.4}$$

Since there is a lack of detailed velocity data at any one location, there is not enough evidence to assure that the return flow calculated is an exact representation of the true velocity field. Thus, the sum of the mass transport minus the return flow does not equal that net volume flux (ie. Q) found over the island for these experiments. However, the data from each trial does gives credence to equation 5.4 in general.

The data also suggests that there are some trends regarding bar formation and sediment transport. For example, it is evident that the greatest flows over the island occur during the deeper overwashing depths. The only exception is trial 1 (+10, 7.0 ,8.0), which has a lower overwash depth. Regardless of trial 1, the higher overwash depths allows a greater potential for volume flux over the island. This explanation is confirmed by the lack of bar formation in these trials. The return flow is not as strong thus offshore sediment transport is curtailed. The exception to this rule is trial 8. Bar formation is evident at this higher overwash depth but it is possible that the larger wave period factors into bar formation.

As seen in the velocity profiles, trials 3 (+10, 8.5, 8.0) and 4 (+10, 8.5 ,10) have the greatest percentage of return flow and the largest bar formation. It is evident that the small flows over the island do not significantly affect the strength of the return flow. Finally, the data do not allow any conclusions to be drawn concerning which overwash depth transports more sediment over the island. In all trials, changes in sediment volumes were small regardless of the volume of water flowing over the island. This result suggests that wave-induced currents are not strong enough to move large amounts of material over the island.

In addition to the eight trials, mass transport and return flow calculations were completed for the two induced flow trials. Tables 5.26 and Tables 5.27 list the results for the two trials.

Table 5.26: The Results of the Mass Transport and Return Flow Calculations for Trial 9.

Mass Transport (Ft^3/Sec) (Calculated)	Location (Ft)	Return Flow (Ft^3/Sec) (Calculated)	Location (Ft)	$Y_{measured}$ Depth (Ft)
57.42	568	38.112	480	6.35
20.13	416	26.64	368	5.30
8.01	328	5.44	272	5.01
5.04	240	13.84	192	0.775
4.11	112	10.45	64	1.73

The water surface gradient results verify earlier velocity profile findings. It is evident in both trials that the return flow is nonexistent. The results indicate that the incoming volume of water must all flow over the island. However, the volume flow rates over the island in both trials do not provide complete closure to substantiate this claim. It can be assumed that a return flow might exist close to the bottom part of the water column. Due to a lack of data, there is no way to confirm if this assumption is correct.

Table 5.27: The Results of the Mass Transport and Return Flow Calculations for Trial 10.

Mass Transport (Ft^3/Sec) (Calculated)	Location (Ft)	Return Flow (Ft^3/Sec) (Calculated)	Location (Ft)	$Y_{measured}$ Depth (Ft)
80.23	528	8.38	480	6.87
27.68	496	10.04	448	3.20
10.26	464	19.73	416	3.20
22.41	432	5.12	384	3.20
17.34	400	31.04	352	1.63
7.11	368	35.08	320	1.63
0.45	336	12.29	288	1.63
6.93	304	5.31	256	1.63
5.58	272	8.53	224	1.63
5.28	240	17.80	192	1.10
13.89	208	19.86	160	1.10
4.38	176	36.67	128	1.10
4.11	144	17.80	96	1.10
3.06	112	30.04	64	1.10
1.95	80	25.50	32	1.10
6.27	48	24.48	0	1.10

The difference in flow rates over the island in both trials also suggests that wave height might influence the volume of water traveling over the island. In trial 9 (+10, 8.5, 8.0, Full), the pump rate was at full speed. It could be assumed that the flow rate would be largest in this

trial. This, however, is not the case. Trial 10, which is run at half pump speed, has the greater flow rate. This peculiarity may result from the fact that the breaking wave height for trial 9 was smaller than trial 10. When the trial was begun, the amplitude on the wave generator was not adjusted to account for the coflowing current. Therefore, the deep water wave height was not the designed 8.5 foot height and thus breaking wave height was smaller. This error was corrected in trial 10 and a larger breaking wave height occurred.

Earlier it was stated that the overwash cases without the water surface gradient did not appreciably change the sand volumes over the island, and that there was minimal deposition in the containment area (a few pounds). Except for trial 5 (+11.5, 7.0, 8.0), the sand was shifted inside the bed profile itself and only a small quantity of sand was moved into the containment area. This is not the case for these two trials with the water surface gradient over the island. From visual observation of the profile and containment area, a large amount of sand (a few hundred pounds) was eroded from the sloping profile and moved over the island and into the containment area. Due to sand leakage in the containment area, the total volume between the two trials could not be determined, but visually the two volumes appeared similar. From these results, it can be inferred that the water surface gradient is the primary mechanism for producing "significant" overwashing of sediment over the island.

CHAPTER 6
CONCLUSIONS AND RECOMMENDATIONS

6.1 Summary of Investigation

The recent attention being focussed on barrier islands warrants further investigation of the wave and current mechanics of the overwash process to determine how overwash affects the barrier island's long term stability. A laboratory test was carried out to measure the wave and current forcing during complete inundation of the barrier island. Various combinations of wave heights, wave periods, and overwash depths were utilized in eight trials. In addition, two trials were performed to include the effects of an imposed water surface gradient over the island. Wave height, current, and bed profiles were measured for all ten trials. The data were analyzed and then compared against results from predictions based on wave height transformation modeling and simple calculations of the mean currents in the surf zone.

6.2 Important Findings

The results of the laboratory experiments and the predictions from the model and calculations provide some interesting evidence in understanding and predicting the effects of the overwash process. Implications of these results will be discussed in five general areas: 1) mechanisms for "significant" overwash; 2) general mechanisms for bar formation; 3) wave height modeling during the overwash process; 4) return flow modeling; and 5) overwash process and long term stability.

Mechanism for "Significant" Overwash

The variations in sand volumes transported across the island in the ten trials suggest that certain mechanisms of the overwash process are responsible for determining the amount of sediment transport over the island. The first eight trials suggest that wave-induced currents by themselves do not produce any "significant" overwash. In these trials, only a few pounds were deposited in the containment area. It is apparent that the wave-induced currents generated were not of sufficient strength to cause substantial sediment transport rates over the island. In most instances, sediment was transported just shoreward of the berm. The results from these trials support Leatherman's explanation that small overwashing events acts as sediment suppliers to eroded areas of the beach and foredunes.

From trials 9 and 10, it is evident that the water surface gradient (and the resulting steady current) has the greatest impact in producing "significant" overwash events. From visual observations, the sand volumes in the containment area were estimated to be between two and three hundred pounds, compared to the few pounds for the first eight trials. From the data, the addition of the co-flowing current causes greater net shoreward flow rates in the surf zone and over the island. This increased strength is apparent if the velocity profiles and mean current predictions are compared between trials 9 and 10 and trial 3. The difference between the two water surface gradients and Trial 3 is large. It is probable that the large increase in velocity caused the large change in sediment transport volumes. However, it is also possible that the shape of the velocity profile plays a part in the large scale sediment transport. In cases without a water surface gradient, the wave-induced velocity profile typically decays rapidly with depth; the current is faster in the upper part of the water column than near the bottom. When a co-flowing current exists, the shape of the velocity profile is more constant through the water column. Therefore, the faster current near the bed is able to transport more sediment. In

summary, the results of these two trials suggest that the water surface gradient is the driving force behind large scale sediment transport during the overwash process.

Although the water surface gradient is singularly the most important factor is producing "significant" overwashing, another factor that deserves mention is the overwash depth. It may appear logical to assume that larger overwash depths would allow more sediment to be carried farther over the island. This, however, might not be the case. The deeper overwash depth did not affect the amount of sediment transported in the trials where wave-induced currents were the only driving force. And it is unknown if a greater overwash depth would have made a difference when the water surface gradient was included. The measured overwash velocities do not exhibit a firm dependence on the overwash depth. From Figure 6.1, it is evident that the overwash velocities depend more on the wave steepness than on the overwash depth. A possible explanation for this occurrence might be that there is some intermediate overwash depth (and wave steepnes) for which the over-island velocities are maximized producing the greatest sediment transport. Since the values in this experiment where within 1.5 feet of each other, both values might have been too high or low to show any significant difference. If the effect of the overwash depth is to be singled out, a wide range of overwashing depths should be studied.

Mechanisms for Bar Formation

Another finding that was noted in the analyzed lab data is the formation of bars in the offshore region. Except for Trials 1, 5, and 7, bar formation is evident in all trials. The forces leading to evolution of bars have been the subject of considerable debate. A prevalent theory behind bar formation is that the return flow transports sand shoreward where it is deposited near the break point. The results from the laboratory experiment show that this theory has merit. From Figure 6.2, it is apparent that there is a tendency for bar formation in the cases where there is stronger return flows. In trials 3 and 4, the return flow is the largest and so is the bar

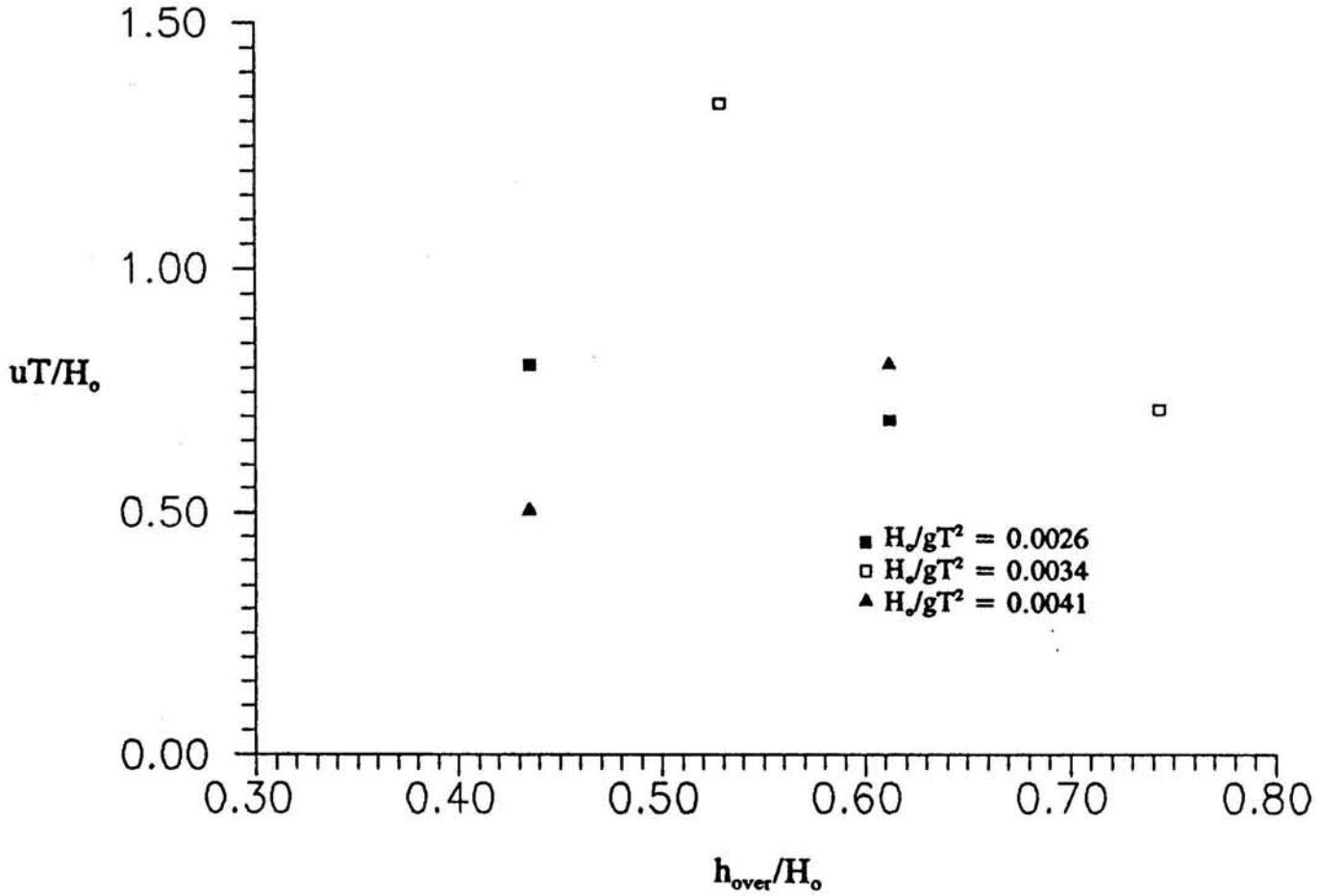

Figure 6.1 Nondimensional Mean Cross-shore Velocity Over the Barrier Island vs. Dimensionless Overwash Depth Over the Berm, for Various Values of Wave Steepness

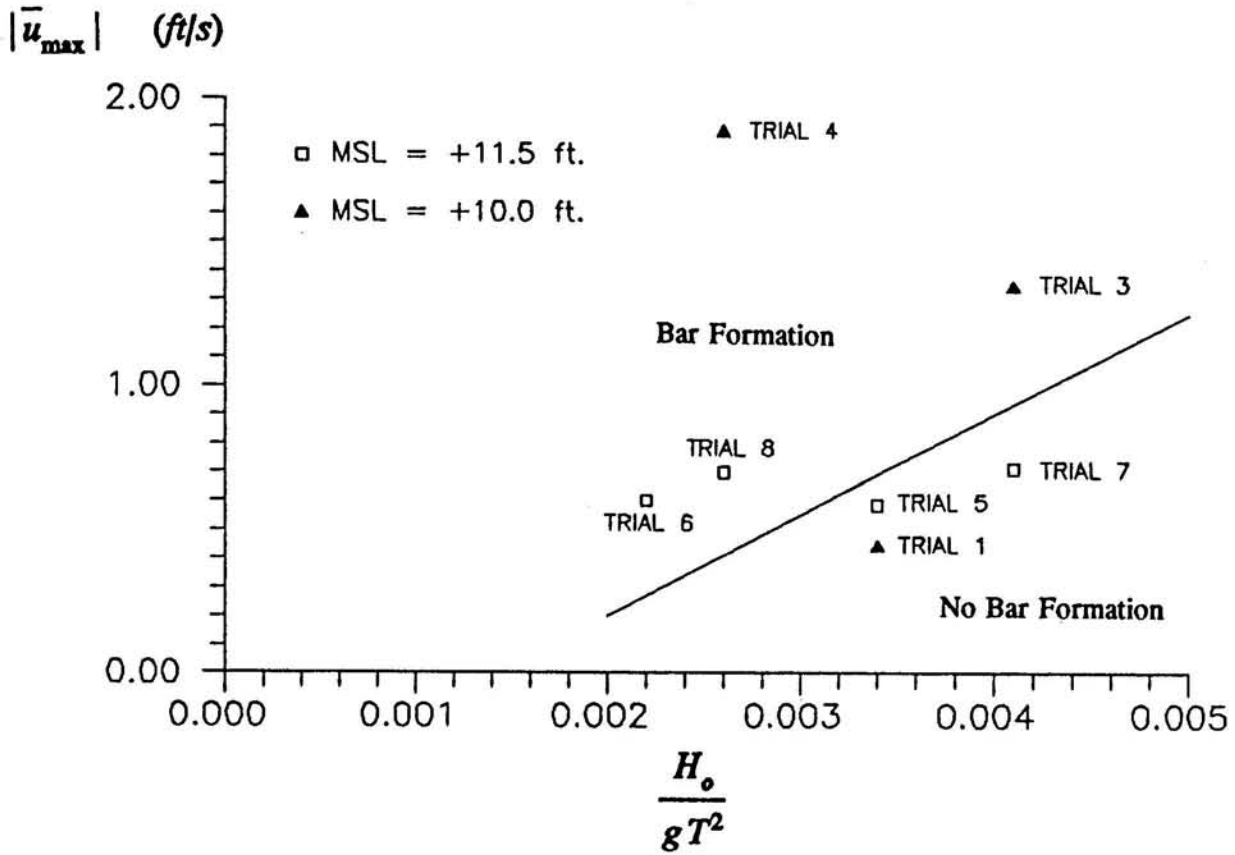

Figure 6.2 Maximum Mean Cross-shore Return Flow (Absolute Value) vs. Wave Steepness. Solid Line Marks Approximate Separation of Conditions of Bar Formation and No Bar Formation

formation. When there is an increase in overwash depth, two of the pairs (4, 8 and 3, 7) show a significant reduction in return flow and bar formation (which is not seen in pair 1, 5). Note that in the case of trial 7, the reduction in return flow seems to be enough to inhibit bar formation. However for the cases with an overwash depth of +11.5 ft., the return flow velocities are all similar, and the occurrence of bar formation is associated with waves of decreasing wave steepness (which is contrary to typical observations on non-overwashed beaches). Although the results from the first eight trials somewhat substantiate this reasoning, the results from the last two trials do not. Since a measurable return flow is not apparent when there is a water surface gradient, this cannot explain the multiple bar formation observed in these two cases. However, these bars are not nearly as prominent as those associated with the cases of strong return flows. The formation of other bars farther offshore may be caused by the reflection of waves from the beach. The distance between these successive bars is roughly one half of a wave length, which suggests this as a possible cause. However, the reflection data determined from deep water wave heights, seen in Table 6.1, for the ten trials does not substantiate this reasoning. It is possible that the weakening of the return flow in these two cases may cause the reflection to have a more prominent effect on the bed profile.

Wave Height Modeling

Predicting the wave height transformation can help to understand the impact that overwashing has on the barrier island. Modeling the transformation can provide a basis for predicting mean velocity distribution over the island and thus can be used to describe the direction of sediment transport. A wave transformation model formulated by Dally, Dean, and Dalrymple (1985) was utilized. Although this model was not expressly written to model the overwash process, the model was nevertheless able to predict certain aspects of wave transformation. In most instances, the model accounted for the presence of a bar by allowing the wave to "reform"

Table 6.1 Deep Water Wave Height Reflection Coefficient for all Trials.

Trial Number	Location (Ft)	Reflection Coefficient
1	1040	0.0216
2	1024	0.0157
3	1024	0.0515
4	1024	0.0345
5	1024	0.0360
6	1024	0.0435
7	1024	0.0235
8	1024	0.0311
9	1024	0.0300
10	1120	0.0299

after breaking commenced. Furthermore, it was able to predict, with consistency, wave shoaling before breaking (although this is expected since the breaking position and height are specified). The prediction of wave transformation after breaking varied between trials. The model was able to predict the breaking with some success for all trials except trial 2 where inconsistencies arose between the data and model results. The model could not, however, consistently predict the wave height decay over the island. The wave heights were underestimated in all trials with the exception of trial 4, which was overestimated. The discrepancy between the model and actual data is most likely due to fact that the model was not written with the overwash condition considered, so that the net mass flux "through the system" and the reduced wave height decay over the island are not accounted for, producing small but persistent deviations.

In the trials where the water surface gradient is present, the model results show some variability. In trial 10, the model under estimated the wave height decay near the bar but was

able to predict the decay over the island. In trial 9, the wave height decay over the bar was predicted correctly but under predicted over the island. The confused results for these two trials suggest that it is inappropriate to use the model for predicting wave height decay when co-flowing current exists by simply reducing the dissipation. If the model is to predict this condition correctly, the governing equations must be modified to incorporate terms reflecting the impact of the coexsiting current.

Return Flow Modeling

The results from the mass transport and return flow calculations confirm several conclusions in terms of bar formation and "significant" overwash. It is evident from the bed profiles and velocity distributions that the return flow is directly related to bar formation. In terms of the overwash process, it was apparent from the net flow rates that the mass transport in the upper part of the water column is able to sustain and transport suspended sediment shoreward. However, the simplistic approach taken in calculating these two flows does not correctly predict their strength. There are several probable contributing factors to this disagreement. In many cases, mass transport calculations from linear wave theory are over estimations since surf zone waves are not completely sinusoidal. This is somewhat accommodated by Svendsen (1984b) theory. He bases his mass transport equation in terms of a "surface roller" which is a simple empirical representation of a complex wave motion. The return flows computed are compared with velocity measurements that are approximately taken at mid-depth. Since the return flow in reality varies with depth, the calculated values may not necessarily correspond exactly with the measurements. A more thorough series of tests measuring wave height, set-up, and velocity profiles would permit the use of a return flow model for predicting the exact nature of the mean currents in the surf zone.

Overwash Process and Long Term Stability

Several conclusions can be drawn from the laboratory and model results about the overwash process and its impact on the long and short term stability of the barrier island. The outcome of the laboratory trials suggest that "significant" overwash is most likely driven by a water surface gradient formed by a differential storm surge elevation on th ocean and bay sides of the island. The resulting steady flow causes sand to be transported over the island and deposited in the barrier flats and bays, thereby allowing the island to counter the effects of the rising sea level. Therefore, it is apparent that only large overwash events affect the long term stability of the barrier island. The results also show that the overwash process can affect the short term stability of the island. In trials where the only driving force was the wave induced flow, sand was deposited near the berm of the island. This sand acts as a reservoir supplying eroded areas of the beach and foredunes. These mechanisms are consistent with the observations of several earlier geologic and engineering studies.

6.3 Future Investigations

If future laboratory studies of the overwash process are to be performed using this study as a baseline, it is recommended that several changes be instituted. Wave height and current measurements should be taken at the same location and at closer intervals. Furthermore, current readings should be taken at several depths in the water column so a complete velocity profile can be formed. This would be helpful for future wave transformation and return flow modeling. In terms of future wave transformation modeling, some modifications, such as the appropriate mean flow terms in the governing equations, are needed to predict wave heights during the overwash process with and without a water surface gradient.

Besides the results gathered in this study, there are several areas of the overwash process that need additional examination. More information is needed about the interaction of mass

transport and return flow in transporting sand shoreward. This area was only briefly touched upon here. In addition, a study is needed pertaining to the effects of dune and vegetation on the sediment transport characteristics. Dune and vegetation tend to trap sand during overwash causing a certain degree of build-up to occur. Another area that needs further examination is the relationship between overwash deposits and subsequent aeolian transport. Pertinent field data in terms of wave height, current, and surge level measurement would be ideal for supplementing laboratory and model results. However, the harsh conditions which prevail during overwash events tend to make such data scarce and difficult to obtain. Nevertheless such information would be extremely valuable to focus laboratory and modelling efforts on other aspects (such as wind and three dimensional effects) of the very complex overwash process.

REFERENCES

Andrews, P.B., "Facies and Genesis of a Hurricane Washover Fan, St. Joseph Island, Central Texas Coast," Report of Investigation No. 67, Bureau of Economic Geology, University of Texas, Austin, TX., 1970.

Coastal Engineering Research Center, U.S. Army Corps of Engineers, Coastal Hydraulic Models, Special Report No. 5, May 1979, Chapter V.

Dally, W.R., R. G. Dean, and R.A. Dalrymple, "Wave Height Variation Across Beaches of Arbitrary Profile," Journal of Geophysical Research, 90.C6, 1985, pp. 11917-11927.

Dalrymple, R.A. and W.W. Thompson, "Study of Equilibrium Beach Profiles," Proceedings from the 15th Coastal Engineering Conference, Vol. 2, 1976, pp. 1277-1302.

Davis, R.A., "Barrier Island Dynamics: We Should Let Nature Take Its Course," Proceedings from Conference on Beach Preservation Technology, Florida Shore and Beach Preservation Inc., Tallahassee, Florida, 1981, pp 22-40.

Dean, R.G., "Heuristic Models of Sand Transport in the Surf Zone," Conference on Engineering Dynamics in the Surf Zone, 1973, pp. 208-215.

Dean, R.G., Littoral Processes Class Notes, Coastal and Oceanographic Engineering Department, University of Florida, 1991.

Dillon, W.P., "Submergence Effects on a Rhode Island Barrier and Lagoon and Inferences on Migration of Barriers," Overwash Processes, Stephen Leatherman, ed, Hutchinson Ross Publishing Company, New York, N.Y., 1981, pp. 225-228.

Divoky, D., B. LeMehaute, and A. Lin, "Creating Waves on Gentle Slopes," Journal of Geophysical Research, Vol. 73, March 1970, pp. 1681-1692.

Dolan, R., "Barrier Islands: Natural and Controlled," Coastal Geomorphology, State University of New York, Binghamton, New York, 1972, pp. 263-278.

Dyhr-Nielsen, M. and T. Sorensen, "Some Sand Transport Phenomena on Coasts with Bars," Proceedings from the 12th Coastal Engineering Conference, New York, N.Y., 1970, pp. 855-865.

Fisher, J.S., S.P. Leatherman, and Capt. F.C. Perry, "Overwash Processes on Assateague Island," Proceedings from the 14th Coastal Engineering Conference, Vol. 2, 1974, pp. 1194-1211.

Fisher, J.S. and D.K. Stauble, "Washover and Dune Interaction on a Barrier Island," Proceedings from the Coastal Zone 78 Symposium, ASCE, 1978, pp. 1611-1617.

Godfrey, P.J., "Oceanic Overwash and Its Ecological Implications on the Outer Banks of North Carolina," U.S. Department of Interior, National Park Service, Office of Natural Science Studies, Washington, D.C., 1970.

Graff, J.V., "Dune Erosion During a Storm Surge," Coastal Engineering, Vol. 1, No. 2, August 1977, pp. 99-133.

Hayes, M.O., "Hurricanes as Geological Agents, South Texas Coast," Overwash Processes, Stephen Leatherman, ed., Hutchinson Ross Publishing Company, New York, N.Y., 1981, pp.189-194.

Hayes, M.O. and T.W. Kana, "Nature of Erosional/Depositional Trends on Barrier Islands," Proceedings from Conference on Beach Preservation Technology, Florida Shore and Beach Preservation Association Inc., Tallahassee, Florida, 1980, pp. 41-55.

Horikawa, K. and C. Kuo, "A Study of Wave Transportation Inside the Surf Zone," Proceedings from the 10th Coastal Engineering Conference, Vol. 1, 1966, pp. 217-233.

Leatherman, S.P., "Barrier Island Dynamics: Overwash Processes and Aeolian Transport," Proceedings of the 15th Coastal Engineering Conference, Honolulu, HI, 1976, pp. 1958-1974.

Leatherman, S.P., "Overwash Hydraulics and Sediment Transport," Proceedings of Coastal Sediments 77 Symposium, ASCE, Charleston, S.C., 1977, pp. 135-148.

Leatherman, S.P., "Barrier Island Handbook," National Park Service, Cooperative Research Unit, The Environmental Institute, University of Massachusetts at Amherst, 1979.

LeMehaute, B., "On Non-Saturated Breakers and the Wave Runup," Proceedings from the 8th Coastal Engineering Conference, 1962, pp. 77-92.

Lobeck, A.K., Geomorphology- An Introduction to the Study of Landscapes, McGraw-Hill Book Company, New York, N.Y., 1939.

Noda, K.E., "Equilibrium Beach Profile Scale Model Relationship," Proceedings of the Journal of Ports, Harbors, and Waterways, Vol. 98, November 1972, pp. 511-528.

Parchure, T., R.G. Dean, and R. Srinivas, "Laboratory Study of Overwash on Barrier Islands," UFL/COEL-91/006, Coastal and Oceanographic Engineering Department, University of Florida, March, 1991.

Price, W.A., "Equilibrium of Form and Forces in Tidal Basins of the Coast of Texas and Louisiana," Bullentin of American Association of Petroleum Geology, Vol. 31, 1947, pp. 1619-1663.

Price, W.A., "Environment and Formation of the Chenier Plain," Quarternaria, Vol. 2, 1955, pp. 35-86.

Saville, T., "Wave Runup on Composite Slopes," Proceedings from the 6th Coastal Engineering Conference, 1957, pp. 691-699.

Schwartz, R.K., "Nature and Genesis of Some Storm Washover Deposits," Overwash Processes, Stephen Leatherman, ed., Hutchinson Ross Publishing Company, New York, N.Y., 1981, pp. 229-260.

Stive, M.J.F. and H.G. Wind, "Cross-Shore Mean Flow in the Surf Zone," Coastal Engineering, Vol. 10, 1986, pp. 325-340.

Svendsen, I.A., "Wave Heights and Set-Up in a Surf Zone," Coastal Engineering, Vol. 8, 1984a, pp. 303-329.

Svendsen, I.A., "Mass Flux and Undertow in the Surf Zone," Coastal Engineering, Vol. 8, 1984b, pp. 347-365.

Svendsen, I.A. and J.B. Hansen, "The Interaction of Waves and Currents over a Longshore Bar," Proceedings from the 20th Coastal Engineering Conference, Vol. 2, 1986, pp. 1580-1594.

Svendsen, I.A. and J.B. Hansen, "Cross Shore Currents in Surf-Zone Modelling," Coastal Engineering, Vol. 12, 1988, pp. 23-42.

Vellinga, P., "Movable Bed Model Tests on Dune Erosion," Proceedings from the 16th Coastal Engineering Conference, Hamburg, Germany, 1978, pp. 2020-2039.

Wilby, F.B., G.R. Young, C.H. Cunningham, A.C. Lieber, Jr., R.K. Hale, T. Saville, and M.P. O'Brien, "Inspection of Beaches in Path of the Hurricane of September 21, 1938," Overwash Processes, Stephen Leatherman, ed., Hutchinson Ross Publishing Company, New York, N.Y., 1981, pp. 19-23.

Williams, Peter J., "Laboratory Development of a Predictive Relationship for Washover Volume on Barrier Island Coastlines," Master's Thesis, University of Delaware, 1978.

The World Almanac and Book of Facts, Time and Warner, Inc., publisher, New York, N.Y., 1992, pp. 1123.